

THE GROUNDWATER TRANSPORT OF CHLOROPHENOLICS THROUGH
A HIGHLY FRACTURED SOIL AT ALKALI LAKE, OREGON

Richard Lee Johnson Jr.
B.S., University of Washington, 1973
M.S., Oregon Graduate Center, 1981

A dissertation presented to the faculty
of the Oregon Graduate Center
in partial fulfillment of the
requirements for the degree of
Doctor of Philosophy
in
Environmental Science

November, 1984

The dissertation "The Groundwater Transport of Chlorophenolics Through a Highly Fractured Soil at Alkali Lake, Oregon" by Richard L. Johnson, Jr., has been examined and approved by the following Examination Committee:

~~James~~ F. Pankow, Thesis Advisor
Associate Professor

~~James~~ J. Huntzicker
Associate Professor

M. A. K. Khalil
Professor

~~Joann~~ Sanders-Loehr
Professor

~~John~~ A. Cherry
Professor
University of Waterloo

DEDICATION

This dissertation is dedicated to Shirley O'Brien whose
love and support have helped me reach this goal.

ACKNOWLEDGEMENTS

This dissertation represents the efforts of many people. Foremost among these is James F. Pankow without whose support this work would not have been completed. The timely advice of John A. Cherry has also been crucial to the success of this dissertation. To my co-workers who spent long, often harsh days at Alkali Lake I would like to extend my deepest appreciation. The efforts of Susan Brillante, Jim Houck, Rick DeCesar, Jim Bryan, Jerry Bryan, Lorne Isabelle, Shirley O'Brien, Mike Zimmerman, Jim Pankow, Kathy Pankow, Joe Brillante, and others made the field work both easier and more enjoyable. The assistance of Bill Asher in the laser induced fluorescence analysis and Lorne Isabelle in keeping the mass spectrometer running were important to the success of this work. The support of the Oregon Department of Environmental Quality and people like Richard Reiter and Richard Gates is appreciated. The financial support of the United States Environmental Protection Agency (Grant number 808272) under the management of Louis Swaby is also thankfully acknowledged. Finally, to The Group of people I call friends, thank you for helping me to keep things in perspective.

CONTENTS

Approval	ii
Dedication	iii
Acknowledgements	iv
List of Tables	viii
List of Figures	ix
Abstract	xxii
I. INTRODUCTION	1
I.A. Background	3
I.B. Mathematical Statement of the Problem	9
II. SITE CHARACTERIZATION	14
II.A. Site Description	14
II.B. Water Sampling Devices	16
II.C. Groundwater Characterization	26
II.C.1. Water Table Measurements	26
II.C.1.a. Conductance/ Water Table Measurement Probes	28
II.C.2. Specific Conductance Measurements	35
II.D. SOIL CHARACTERIZATION	38
II.D.1. Mineralogical Analysis	38
II.D.2. Porosity and Bulk Density Determinations	40
II.D.3. Soil Organic Carbon (SOC) Determinations	42

II.E.	Hydraulic Conductivity Determinations Using Slug Tests	43
II.E.1.	Experimental	43
II.E.2.	Results	45
II.F.	Pumping Drawdown Tests	48
III.	CONTAMINANT DISTRIBUTIONS AT THE ALKALI LAKE CHEMICAL DISPOSAL SITE (CDS)	57
III.A.	Introduction	57
III.B.	The Waste Materials	57
III.C.	Chemical Analysis	62
III.C.1.	Sample Collection	63
III.C.2.	Sample Preparation and Analysis	64
III.D.	Contaminant Distributions	70
III.E.	Partition Coefficient Determinations	83
III.E.1.	Experimental	83
III.E.2.	Results	84
IV.	TRACER TESTS	86
IV.A.	The Natural Gradient Tracer Test	87
IV.A.1.	Experimental	87
IV.A.2.	Results	91
IV.A.3.	Simulation of the Natural Gradient Tracer Test	96
IV.B.	Two-Well Pumping Tracer Tests	97
IV.B.1.	Experimental	97
IV.B.2.	Results	102

IV.C. One-Well "Push-Pull" Tests	109
IV.C.1. Experimental	109
IV.C.2. Results	115
IV.C.3. Modeling of the "Push-Pull" Tests	132
V. CONTAMINANT TRANSPORT AT THE ALKALI LAKE CDS	151
V.A. Introduction	151
V.B. Retardation In Porous Fractured Media	152
V.C. The Equivalent Porous Medium Approach	155
V.D. Observed Retardation of the Chlorophenolics	161
V.E. Possible Explanations of the Contaminant Distributions	167
IV. CONCLUSIONS	185
Appendix A. The Referenced Paper Pankow et al., 1984	189
Appendix B. The Referenced Paper Johnson et al., 1985	200
Appendix C. "Slug Test" Data	217
Appendix D. Selected Ion Chromatogram and Mass Spectra of the Standard Sample WW08820914	232
Appendix E. Listing of the Fortran Computer Program "PUSHPULL"	242
References	248
Vita	251

LIST OF TABLES

II.C.1.	Groundwater Quality Data	37
II.E.1.	Hydraulic Conductivity (K_H) Data	46
III.D.1.	Transport Distances of the Chloro-phenolics	82
III.E.1	Partition Coefficient (K_P) Data for the Chlorophenolics	85
IV.C.1.	HPLC Conditions for the Iodide Analyses	114
IV.C.2.	Fracture Parameters From the "Push-Pull" Tests	135
V.D.1.	Relative Retardation Factor Data	162
V.D.2.	Simulated Transport Distances for the 2%, 25% and 50% Concentration Fronts	164
V.D.3.	Relative Retardation Factors Calculated from the Data of Table V.D.2.	165
V.D.4.	Estimations of Error Introduced by Using 2% and 25% Relative Retardation Factors (Based on the Data of Table V.D.3.)	166

LIST OF FIGURES

I.A.1	Topographic map of Alkali Lake playa and surrounding area. Major contours are at 200 foot intervals. (Prepared on the basis of maps obtained from the Defense Mapping Agency Topographic Center, Washington, D.C.)(Taken from Pankow et al., 1984)	4
I.A.2	Topographic map of the site vicinity. (Prepared with the assistance of U.S.EPA (1983) data.)	5
I.A.3	Chemical structures of four phenoxy acid herbicides. (2,4-D and MCPA are found at the Alkali Lake CDS.)	6
I.A.4	Map showing the location of the "ODEQ-type" wells used for water sampling and water table measurements.	8
I.A.5	Schematic drawings of advective-diffusive transport in fractured media for: a) a non-porous medium; b) a porous medium; and c) a sorbing compound in a porous medium. (After Freeze and Cherry, 1979).	11
II.A.1	Individual precipitation event values plotted versus day of the year, together with monthly averages. (Based on 1972-1984 data, NOAA (1984).)	17
II.A.2	(Precipitation x frequency) versus precipitation (cm) histogram and average cumulative annual precipitation versus precipitation (cm) curve. (Based on 1972-1984 data, NOAA (1984).)	18
II.B.1	Map showing the locations of the points sampled by the stainless steel probes (P-series) (marked with an X). Positions of the "ODEQ-type" wells are included as dots on the map for reference.	20

List of Figures (continued)

II.B.2	Map showing the locations of the S-series samplers used for water sampling, water table measurement and slug tests.	22
II.B.3	Schematic drawing of the multi-level devices (J- and L-series) showing: a) cut-away detail of the screened intervals; b) removable inner tube used for single-level "slug tests"; and c) removable devices for single-level water sampling and water table measurements.	24
II.B.4	Schematic drawing of single-discrete-level sampler.	25
II.C.1	Water table at "ODEQ" Wells 2 and 8 as a function of time over the period 1977-1984. The data are relative to the datum: top of Well 2 casing = 1000 cm.	27
II.C.2	Hydraulic gradient between "ODEQ" Wells 2 and 8 as a function of time over the period 1977-1984.	29
II.C.3	Water table as a function of month of the year over the period 1977-1984. The data are relative to the datum: top of Well 2 casing = 1000 cm.	30
II.C.4	Hydraulic gradient between "ODEQ" Wells 2 and 8 as a function of month of the year.	31
II.C.5	Water table maps in centimeters obtained during November 1981, and February, May and September 1982. The data are relative to the datum: top of Well 2 casing = 1000 cm.	32
II.C.6	Water table map in centimeters obtained during April 1984 using the S-series samplers. The data are relative to the datum: top of Well 2 casing = 200 cm.	33

List of Figures (continued)

II.C.7	0.64 cm O.D. probes used to monitor specific conductance of the groundwater and the water table.	34
II.C.8	Calibration curve for the 0.64 cm O.D. conductance probes versus the YSI probe.	36
II.C.9	Specific conductance isopleths (April 1983), micromhos/cm x 10 ⁻² .	39
II.D.1	Percent of soil material below a given grain size versus grain size for two samples taken near Well 34 at 1.2 and 2.4 m below ground level.	41
II.E.1	Water reservoir used for the "slug tests".	44
II.E.2	Map showing locations of the "slug tests" used to determine K _H values.	47
II.F.1	Piezometer layout for pumping drawdown test T7P. (Located near wells 33 and 25, Figure I.D.4.)	50
II.F.2	Drawdown (cm) versus time for pumping test T7P (Located near wells 33 and 25, Figure I.D.4.) for piezometers open at approximately 1 m below the water table at 0,1,3,5,10 and 20 m from the pumping well.	51
II.F.3	Drawdown (cm) versus time for pumping test T7P (Located near wells 33 and 25, Figure I.D.4.) for piezometers open at approximately 1 and 2.3 m below the water table at 1 m from the pumping well.	52
II.F.4	Drawdown (cm) versus time for pumping test T7P (Located near wells 33 and 25, Figure I.D.4.) for piezometers open at approximately 1 and 2.3 m below the water table at 3 m from the pumping well.	53

List of Figures (continued)

II.F.5	Drawdown (cm) versus time for pumping test T7P (Located near wells 33 and 25, Figure I.D.4.) for piezometers open at approximately 1 and 2.3 m below the water table at 5 m from the pumping well.	54
II.F.6	Drawdown (cm) versus time for pumping test T7P (Located near wells 33 and 25, Figure I.D.4.) for piezometers open at approximately 1 m below the water table at 5,8 and 10 m from the pumping well (piezometers C, D and E, respectively, Figure II.F.1).	55
II.F.7	Drawdown (cm) versus time for pumping test T7P for piezometers open from approximately 1 to 3 m below the water table at 10 and 25 m from the pumping well (Wells 33 and 25, respectively, Figure I.D.4).	56
III.B.1	Reaction scheme for the production of 2,4-D from phenol showing the major waste products which result from side reactions.	59
III.B.2	Structures of the chlorophenols found in the materials disposed of at Alkali Lake.	60
III.B.3	Polymerization of 2,4-DCP molecules to form CPP.	61
III.C.1	Apparatus used for the separation and concentration of the chlorophenolics in the groundwater from Alkali Lake.	65
III.D.1	Concentration contours for 2,4-DCP (in ppm) in the vicinity of the Alkali Lake CDS as of April 1984.	71
III.D.2	Concentration contours for 2,6-DCP (in ppm) in the vicinity of the Alkali Lake CDS as of April 1984.	72
III.D.3	Concentration contours for 2,4,6-TCP (in ppm) in the vicinity of the Alkali Lake CDS as of April 1984.	73

List of Figures (continued)

III.D.4	Concentration contours for TeCP (in ppb) in the vicinity of the Alkali Lake CDS as of April 1984.	74
III.D.5	Concentration contours for PCP (in ppb) in the vicinity of the Alkali Lake CDS as of April 1984.	75
III.D.6	Concentration contours for CL2D2 (in ppb) in the vicinity of the Alkali Lake CDS as of April 1984.	76
III.D.7	Concentration contours for CL3D3 (in ppb) in the vicinity of the Alkali Lake CDS as of April 1984.	77
III.D.8	Concentration contours for CL4D2 (in ppb) in the vicinity of the Alkali Lake CDS as of April 1984.	78
IV.A.1	Map showing the locations of the source well and sampling points for the natural gradient tracer test.	89
IV.A.2	Block diagram of the laser induced fluorescence system used for fluorescein detection.	90
IV.A.3	Typical calibration curve for the LIF procedure used for the fluorescein analyses.	92
IV.A.4	Tracer distribution for the natural gradient tracer test during April 1984 (at approximately 1 year). Concentrations are in nM.	94
IV.A.5	Integrated transects of fluorescein concentration constructed from Figure IV.A.2 plotted versus distance from the source well.	95

List of Figures (continued)

IV.A.6	"Best fit" one-dimensional EPM simulation of the natural gradient test data (Figure IV.A.5) plotted with the observed integrated transects versus distance from the source well.	98
IV.A.7	Sensitivity of EPM simulation of the natural gradient tracer test to velocity. Simulations have been plotted along with observed integrated transects versus distance from the source well. (1 year after injection, April 1984.)	99
IV.A.8	Sensitivity of EPM simulation of the natural gradient tracer test to longitudinal dispersion. Simulations have been plotted along with observed integrated transects versus distance from the source well. (1 year after injection, April 1984.)	100
IV.B.1	Breakthrough (recovery) curve for fluorescein in the 3-meter pumping tracer test. (Near Wells 33 and 25, Figure I.D.4.)	103
IV.B.2	Conceptual drawing of the imaginary hemispherical volume element used in estimating total fracture porosity for the pumping tracer tests.	105
IV.B.3	Conceptual drawing of the imaginary cylindrical volume element used in estimating total fracture porosity for the pumping tracer tests.	106
IV.B.4	Breakthrough (recovery) curve for fluorescein in the 6-meter pumping tracer test. (Near Wells 33 and 25, Figure I.D.4.)	108
IV.C.1	Schematic drawing of the apparatus used for the "push-pull" tracer tests.	111

List of Figures (continued)

IV.C.2	Fraction of mass recovered during pumping versus residence time of the tracer in the ground prior to beginning of pumping for the "push-pull" tests using fluorescein.	116
IV.C.3	Fluorescein recovery curve for the "push-pull" test H0.8404.F with residence time = 0 hours. (Piezometer H, Figure II.E.2.)	117
IV.C.4	Fluorescein recovery curve for the "push-pull" test G0.8404.F with residence time = 0 hours. (Piezometer G, Figure II.E.2.)	118
IV.C.5	Fluorescein recovery curve for the "push-pull" test A25.8404.F with residence time = 0.25 hours. (Piezometer A, Figure II.E.2.)	119
IV.C.6	Fluorescein recovery curve for the "push-pull" test E5.8404.F with residence time = 0.5 hours. (Piezometer E, Figure II.E.2.)	120
IV.C.7	Fluorescein recovery curve for the "push-pull" test F1.8404.F with residence time = 1.0 hour. (Piezometer F, Figure II.E.2.)	121
IV.C.8	Fluorescein recovery curve for the "push-pull" test G2.8404.F with residence time = 2.0 hours. (Piezometer G, Figure II.E.2.)	122
IV.C.9	Fluorescein recovery curve for the "push-pull" test H4.8404.F with residence time = 4.0 hours. (Piezometer H, Figure II.E.2.)	123
IV.C.10	Iodide recovery curve for the "push-pull" test H0.8404.I with residence time = 0 hours. (Piezometer H, Figure II.E.2.)	124

List of Figures (continued)

IV.C.11	Iodide recovery curve for the "push-pull" test A25.8404.I with residence time = 0.25 hours. (Piezometer A, Figure II.E.2.)	125
IV.C.12	Iodide recovery curve for the "push-pull" test B25.8404.I with residence time = 0.25 hours. (Piezometer B, Figure II.E.2.)	126
IV.C.13	Iodide recovery curve for the "push-pull" test E5.8404.I with residence time = 0.5 hours. (Piezometer E, Figure II.E.2.)	127
IV.C.14	Iodide recovery curve for the "push-pull" test C1.8404.I with residence time = 1.0 hour. (Piezometer C, Figure II.E.2.)	128
IV.C.15	Iodide recovery curve for the "push-pull" test F1.8404.I with residence time = 1.0 hour. (Piezometer F, Figure II.E.2.)	129
IV.C.16	Iodide recovery curve for the "push-pull" test G2.8404.I with residence time = 2.0 hours. (Piezometer G, Figure II.E.2.)	130
IV.C.17	Iodide recovery curve for the "push-pull" test H4.8404.I with residence time = 4.0 hours. (Piezometer H, Figure II.E.2.)	131
IV.C.18	Fluorescein recovery curve and simulation results for the "push-pull" test H0.8408.F. (Piezometer H, Figure II.E.2.)	136
IV.C.19	Fluorescein recovery curve and simulation results for the "push-pull" test A25.8408.F. (Piezometer A, Figure II.E.2.)	137

List of Figures (continued)

IV.C.20	Fluorescein recovery curve and simulation results for the "push-pull" test E5.8408.F. (Piezometer E, Figure II.E.2.)	138
IV.C.21	Fluorescein recovery curve and simulation results for the "push-pull" test F1.8408.F. (Piezometer F, Figure II.E.2.)	139
IV.C.22	Fluorescein recovery curve and simulation results for the "push-pull" test G2.8408.F. (Piezometer G, Figure II.E.2.)	140
IV.C.23	Fluorescein recovery curve and simulation results for the "push-pull" test H4.8408.F. (Piezometer H, Figure II.E.2.)	141
IV.C.24	Sensitivity of the shape of the "push-pull" tracer recovery curve to residence time in the ground before pumping was initiated.	142
IV.C.25	Sensitivity of the shape of the "push-pull" tracer recovery curve to dispersion caused by mixing in the fractures during recovery (called "residual" in the model).	143
IV.C.26	Sensitivity of the shape of the "push-pull" tracer recovery curve to the matrix diffusion coefficient.	144
IV.C.27	Sensitivity of the shape of the "push-pull" tracer recovery curve to fracture aperture.	145
IV.C.28	Sensitivity of the shape of the "push-pull" tracer recovery curve to fracture spacing.	146

List of Figures (continued)

IV.C.29	Sensitivity of the shape of the "push-pull" tracer recovery curve to matrix porosity.	147
IV.C.30	Mass of tracer remaining in the fractures versus residence time. Data are based on computer simulation of the "push-pull" tests.	149
V.D.1	Normalized concentration down the approximate contaminant plume center versus distance from the site for 2,4-DCP, 2,6-DCP and 2,4,6-TCP.	168
V.D.2	Normalized concentration down the approximate contaminant plume center versus distance from the site for 2,6-TCP, TeCP, CL3D3, CL2D2, and CL4D2.	169
V.D.3	Normalized concentration down the approximate contaminant plume center and one-dimensional EPM simulation of the contaminant distribution versus distance from the site for 2,6-DCP.	170
V.D.4	Normalized concentration down the approximate contaminant plume center and one-dimensional EPM simulation of the contaminant distribution versus distance from the site for TeCP.	171
V.D.5	Normalized concentration down the approximate contaminant plume center and one-dimensional EPM simulation of the contaminant distribution versus distance from the site for CL3D3.	172
V.D.6	Normalized concentration down the approximate contaminant plume center and one-dimensional EPM simulation of the contaminant distribution versus distance from the site for CL4D2.	173
V.E.1	Normalized integrated transects versus distance from the site for 2,4-DCP, 2,6-DCP and 2,4,6-TCP.	177

List of Figures (continued)

V.E.2	Normalized integrated transects versus distance from the site for TeCP, CL2D2, CL3D3 and CL4D2.	178
V.E.3	Normalized concentration and normalized integrated transect versus distance from the site for 2,6-DCP.	179
V.E.4	Normalized concentration and normalized integrated transect versus distance from the site for TeCP.	180
V.E.5	Normalized concentration and normalized integrated transect versus distance from the site for CL3D3.	181
V.E.6	Normalized concentration and normalized integrated transect versus distance from the site for CL4D2.	182
App.C.1	Graphical estimation of T_0 for the slug test at piezometer A.	219
App.C.2	Graphical estimation of T_0 for the slug test at piezometer B.	220
App.C.3	Graphical estimation of T_0 for the slug test at piezometer C.	221
App.C.4	Graphical estimation of T_0 for the slug test at piezometer D.	222
App.C.5	Graphical estimation of T_0 for the slug test at piezometer G.	223
App.C.6	Graphical estimation of T_0 for the slug test at piezometer H.	224
App.C.7	Graphical estimation of T_0 for the slug tests at piezometer J1. Tests were conducted at depth ranges below ground surface of 2-3 m (3), 3-4 m (4) and 4-5 m (5).	225

List of Figures (continued)

App.C.8	Graphical estimation of T_o for the slug tests at piezometer J2. Tests were conducted at depth ranges below ground surface of 2-3 m (3), 3-4 m (4) and 4-5 m (5).	226
App.C.9	Graphical estimation of T_o for the slug tests at piezometer J3. Tests were conducted at depth ranges below ground surface of 2-3 m (3), 3-4 m (4) and 4-5 m (5).	227
App.C.10	Graphical estimation of T_o for the slug tests at piezometer J4. Tests were conducted at depth ranges below ground surface of 2-3 m (3), 3-4 m (4), 4-5 m (5) and 5-6 m (6).	228
App.C.11	Graphical estimation of T_o for the slug tests at piezometer J5. Tests were conducted at depth ranges below ground surface of 2-3 m (3), 3-4 m (4), 4-5 m (5) and 5-6 m (6).	229
App.C.12	Graphical estimation of T_o for the slug tests at piezometer L4. Tests were conducted at depth ranges below ground surface of 2-3 m (3), 3-4 m (4), 4-5 m (5) and 5-6 m (6).	230
App.C.13	Graphical estimation of T_o for the slug tests at piezometer L10. Tests were conducted at depth ranges below ground surface of 2-3 m (3), 3-4 m (4) and 4-5 m (5).	231
App.D.1.	Part 1 of the selected ion chromatogram of standard sample WW08820914.	233
App.D.2.	Part 2 of the selected ion chromatogram of standard sample WW08820914.	234
App.D.3.	Mass spectrum of TeCP.	235
App.D.4.	Mass spectrum of PCP.	236
App.D.5.	Mass spectrum of CL2D2.	237

List of Figures (continued)

App.D.6.	Mass spectrum of Fluoranthene.	238
App.D.7.	Mass spectrum of CL3D3.	239
App.D.8.	Mass spectrum of CL4D2.	240
App.D.9.	Mass spectrum of Chrysene.	241

ABSTRACT

The Groundwater Transport of Chlorophenolics Through A Highly Fractured Soil at Alkali Lake, OR

Richard Lee Johnson Jr., Ph.D.
Oregon Graduate Center, 1984

Supervising Professor: James F. Pankow

This study explores the groundwater transport of a series of chlorophenols and chlorophenoxyphenols from the chemical disposal site at Alakli Lake, Oregon. Since burial in 1976, the contaminants have moved up to 600 m in the shallow water table aquifer beneath the site. Groundwater movement in the area is controlled by a series of springs to the east of the site which maintains a west-ward hydraulic gradient around and through the site towards West Alkali Lake.

Transport of the contaminants is facilitated by the presence of a very large number of fractures in the soil. These fractures probably had their origins as bedding planes in the lacustrine sediments of the playa on which the site is situated. The bedding planes may have been opened by the processes of dehydration and rehydration and/or by dissolution of carbonates. Groundwater velocities in the fractures may exceed 1 m/day, even under the moderate hydraulic gradient (0.001) present at the site. Solute transport is much slower than 1 m/day, however, because of the retarding effect of matrix diffusion. The average

velocity of a non-sorbed tracer downgradient of the site is probably 0.1 m/day or less.

The roles of the fractures and of matrix diffusion in transport have been successfully characterized by a series of field tracer tests. These tests provided direct evidence that the groundwater is flowing primarily through fractures and that matrix diffusion is important in retarding contaminant transport. The tests also made possible a quantitative evaluation of the average properties of the fracture system (fracture aperture and spacing, matrix diffusion coefficient, etc.) and the effective velocity and dispersion of the contaminants at the site.

The current distributions of contaminants downgradient of the site indicate that sorption has been important in retarding the movement of some of the compounds. Because both sorbing and non-sorbing compounds were buried at the site, the movement of the sorbed compounds relative to the non-sorbed compounds could be used to investigate the processes which have led to the observed distributions. Retardation has also been predicted from laboratory measurements of batch equilibrium partitioning, bulk soil density and porosity. The retardation factors estimated from the observed contaminant distributions were much smaller than those predicted from the laboratory data. The primary reason for this is the local groundwater flow pattern which results in:

1) non-uniform flow through the site; 2) decreasing velocity with distance from the site; and 3) spreading of the contaminant plume beyond 150+/-50 m west of the site.

Groundwater flow is not uniform through the CDS. Data suggest that the primary pathway of water movement is through the southern portion of the site, with a secondary pathway along the northern edge of the site. Groundwater flow through the center of the site may be reduced due to a decrease in hydraulic conductivity within the site as a result of the burial process. This flow pattern has a large impact on the shape of the contaminant distributions, causing concentrations to drop with distance from the CDS more rapidly than predicted by a one-dimensional model of the site. The effect of the slowing and spreading of the groundwater as it moves away from the site is to allow the sorbed compounds to "catch up" with the non-sorbed compounds, resulting in an apparent decrease in relative retardation of the sorbed compounds.

The ultimate destination of the contaminants from the site is probably West Alkali Lake. There is a high probability that contaminants will reach ground surface in that area. There is also the possibility that seasonal fluctuations in the water table will bring contaminants to the surface at distances of from 200 to 400 m west of the CDS, a region where levels of contamination are currently quite high.

I. INTRODUCTION

The goal of the research presented here has been to understand the physical processes which control the groundwater transport of chlorophenolic wastes in and around the chemical disposal site (CDS) at Alkali Lake, Oregon. These processes include advection, molecular diffusion, dispersion and sorption. The processes of volatilization, biodegradation and plant uptake may also affect transport, but are believed to be of secondary importance. The Alkali Lake site (hereafter referred to simply as "the site" or "the CDS") is appealing as a study site because of the chemical nature of the wastes buried there. Contained in the wastes is a series of chemically similar compounds whose water solubilities and soil/water partition coefficients vary in a regular manner. Use has been made of the differences in sorption of these compounds in an attempt to understand both the processes involved in transport and the history of contaminant migration from the site.

The hydrology of the site also presents some excellent research opportunities. The soil in the vicinity of the site is a clay-like silt whose hydraulic conductivity is dramatically

increased due to a very large number of fractures in the saturated soil. As a result, it has been necessary to understand not only the roles of sorption, dispersion and advection in transport, but also the role of matrix diffusion and its effect on sorption and dispersion. To date, relatively few field investigations of such fractured porous systems have been carried out.

The work presented in this dissertation falls into three broad categories: 1) characterization of the important transport processes; 2) measurement of the spatial distribution of the contaminants at Alkali Lake; and 3) conceptual and mathematical modeling of the aquifer. This document has been divided into six sections: 1) background information and a description of the site; 2) hydrological investigations, including most of the field and laboratory measurements of the physical properties of the soil/water/contaminant system; 3) description of the current contaminant distributions at the site (including information pertaining to the quantitative analysis of the chlorophenolic materials); 4) field tracer studies designed to investigate the effects of diffusion and sorption during transport through the fractured soil; 5) evaluation of the laboratory and field data and integration of that data into a conceptual and a mathematical model; and 6) conclusions.

I.A BACKGROUND

The history of the Alkali Lake CDS has been reviewed by Pankow et al. (1984)(in Appendix A). Early interest in the Alkali Lake playa was mining oriented. Claims were first filed by an Oregon firm in the late 1800's. These claims changed ownership several times and were purchased by Chem Waste, Inc. (Portland, OR) in 1967 for the purpose of establishing a 4 ha chemical disposal site (CDS). The CDS was located on the playa near its south-west edge (Figures I.A.1-2) in an area not covered by the intermittent playa lake. The CDS was licensed by the Oregon Department of Agriculture (ODA) in 1968 as a pesticide waste storage site. Storage of wastes at the CDS began in 1969. The feasibility of using land application to degrade the wastes was investigated in 1970 at several sites near the CDS (Goulding, 1973).

By late 1971, a total of 25,049 206 L (55 gal) drums of manufacturing waste from the production of 2,4-D (2,4-dichlorophenoxyacetic acid), and MCPA (4-methyl-2-chlorophenoxyacetic acid) (Figure I.A.3) had been stockpiled on pallets at the CDS. The wastes represented primarily the distillation residues ("still-bottoms") which resulted during the separation of the desired chlorophenols from a phenol

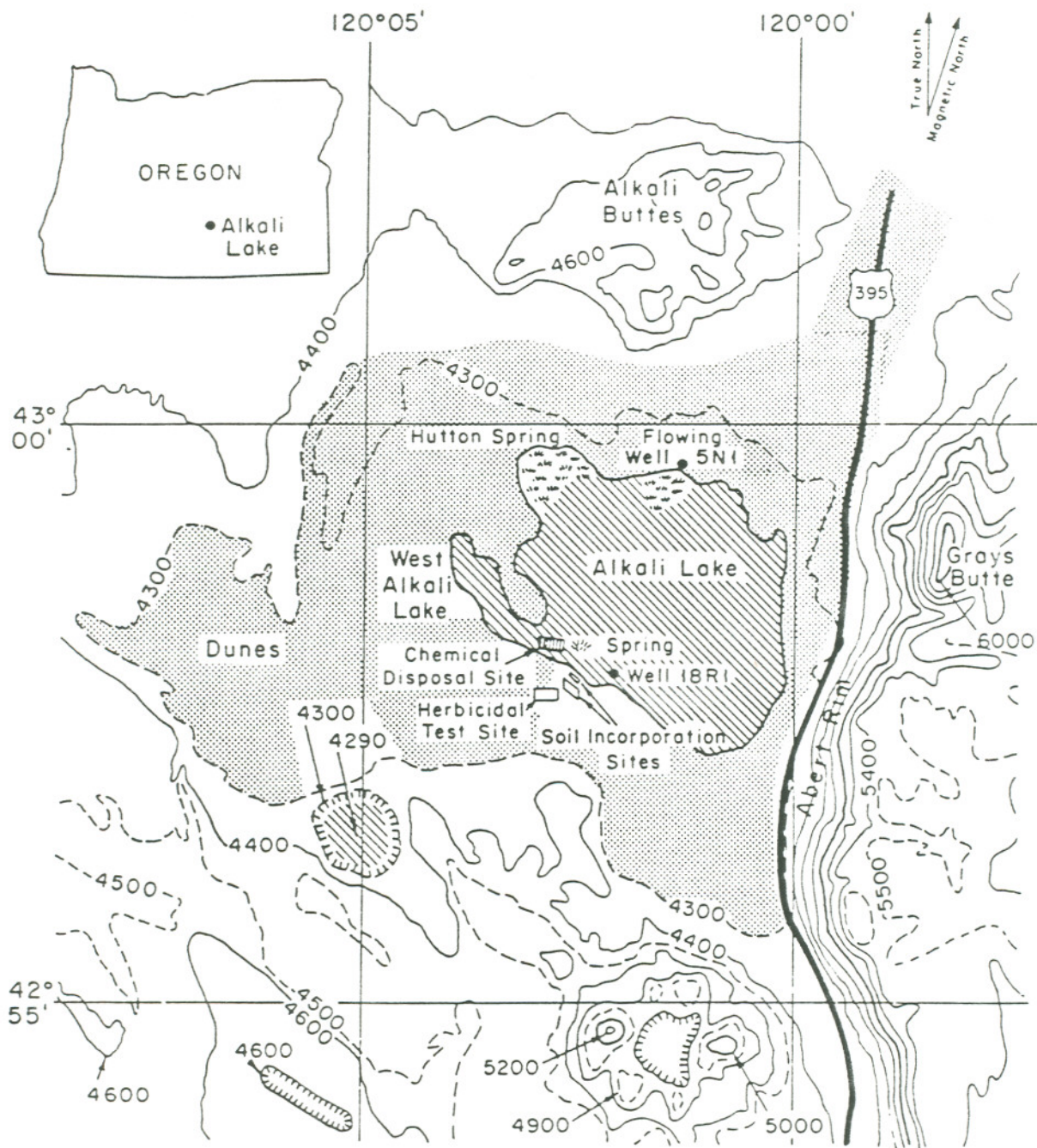
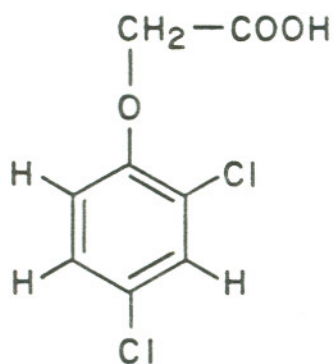
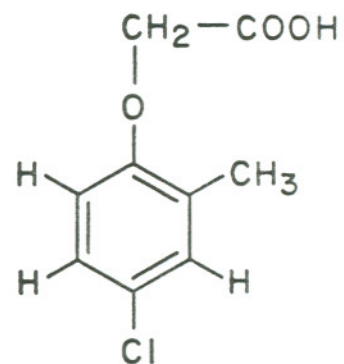


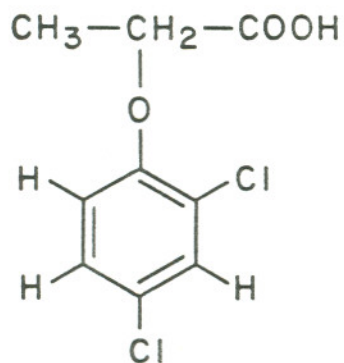
Figure I.A.1 Topographic map of Alkali Lake playa and surrounding area. Major contours are at 200 foot intervals. (Prepared on the basis of maps obtained from the Defense Mapping Agency Topographic Center, Washington, D.C.)(Taken from Pankow et al., 1984)



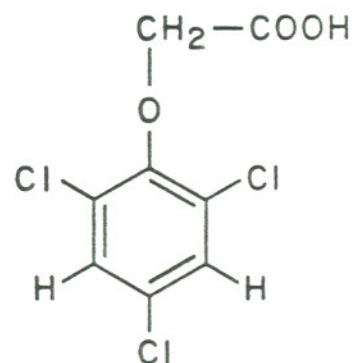
2,4-D
(2,4-Dichloro-
phenoxyacetic acid)



MCPA
(4-Chloro-2-Methyl-
phenoxyacetic acid)



2,4-DP
(2,4-Dichlorophenoxy-
propionic acid)



2,4,5-T
(2,4,5-Trichloro-
phenoxyacetic acid)

Figure I.A.3 Chemical structures of four phenoxy acid herbicides. (2,4-D and MCPA are found at the Alkali Lake CDS.)

chlorination mixture. Included in the still-bottoms were various chlorophenols and a large variety of polymeric chlorophenoxyphenols (CPP) (Pankow et al., 1981). Due to the general corrosiveness of the waste (the chlorophenols, CPP and phenoxy herbicides are all acids), by this point in time, many of the drums had begun to leak (Pankow et al., 1984). In November 1976, under contract from ODEQ, the drums were crushed and buried in 12 shallow (0.6-0.8 m deep), unlined trenches 130 m long and 20 m apart (EPA, 1976; ODEQ, 1977a). It was hoped that the location of the site inside of the closed Alkali Lake basin would limit the movement of the contaminants in the groundwater.

During the period November 1976-September 1981 the ODEQ installed a series of monitoring wells to define the movement of contaminants from the site in the groundwater. These wells were numbered 1-21 (Figure I.A.4). The concentrations of total phenols and 2,4-D as well as water table levels were routinely measured at each of the wells (ODEQ, 1977a, 1977b, 1978, 1979, 1981, 1982). These data indicate that the plume was moving west-northwest towards West Alkali Lake under the influence of a consistent east to west hydraulic gradient.

The Oregon Graduate Center became involved at the site in 1981 when it received a grant from EPA to study the fates of the wastes buried at the site. In addition to the work reported

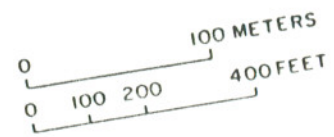
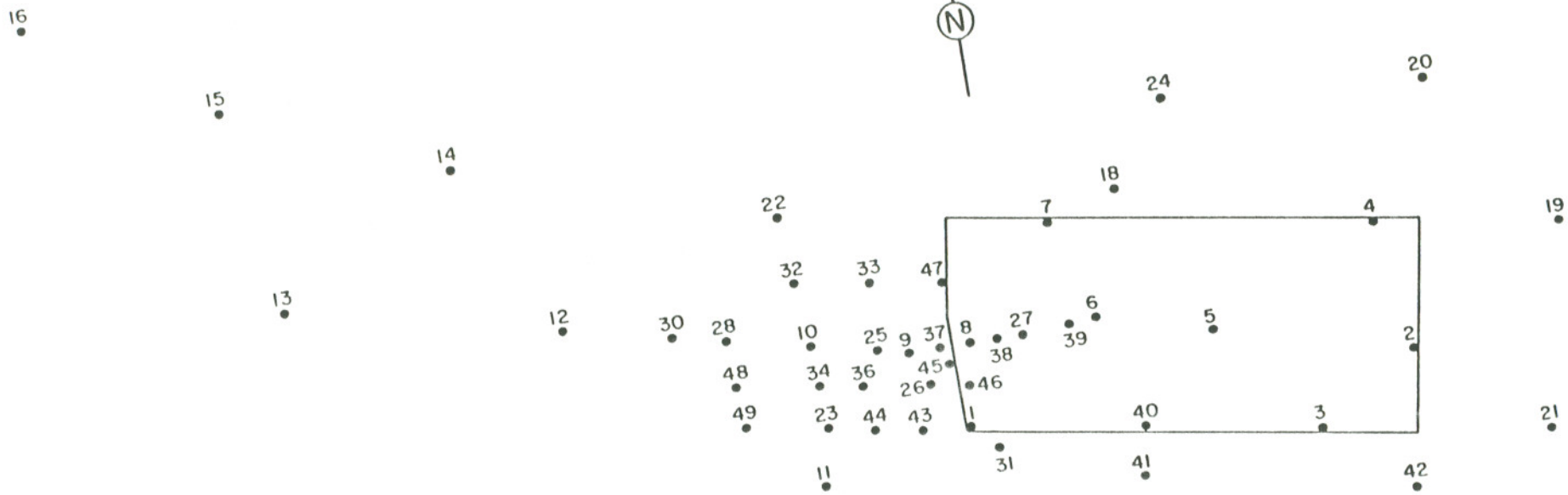


Figure I.A.4 Map showing the location of the "ODEQ-type" wells used for water sampling and water table measurements.

here, investigations of the volatilization and degradation of the chlorophenols as well as mapping of the areal profiles of pH, temperature and specific conductance of the groundwater and the level of the water table are currently being conducted.

I.B MATHEMATICAL STATEMENT OF THE PROBLEM

The mathematical modeling of solute transport at Alkali Lake was treated in a deterministic manner. That is, specific physical parameters were estimated for the aquifer system. The parameters estimated were those which appear in the differential equation selected to describe the aquifer. Values for each parameter were either measured in the field or laboratory, or estimated from literature values. Modeling was then carried out using these values.

For the aquifer underlying the site at Alkali Lake, there are a number of pieces of physical evidence which indicate that groundwater flow through the aquifer system is highly non-uniform. The data to be presented here suggests that advective flow actually occurs through only a few percent of the total soil volume. Observation confirms that the saturated playa appears to be highly fractured in both horizontal and vertical directions. Contaminant distributions measured downgradient from

the site suggest that horizontal transport is much more important in spreading the contaminants than is vertical transport. (The primary reason for this is probably the consistent decrease in hydraulic conductivity with depth observed at the site.) This has led to the conceptualization of the system as one of idealized, parallel, horizontal fractures. The fractures are assumed to be equally spaced and of equal aperture, thus only one fracture-matrix pair need be modeled. If transverse dispersion is small, or if the contaminant concentration is integrated transversely across the plume, the model can be reduced to one dimension. Mathematically this leads to a partial differential equation of the form:

$$V \frac{\partial c}{\partial z} - D \frac{\partial^2 c}{\partial z^2} + \frac{\partial c}{\partial t} + \frac{F(x)}{b} = 0 \quad (I.1)$$

where V = velocity in the fracture,

D = dispersion coefficient in the fracture,

b = fracture halfwidth, and

$F(x)$ = flux of solute from the fractures into the
matrix.

This process is depicted in Figure I.A.5. It is assumed that the fractures are longitudinally extensive. The flux term represents Fickian diffusion into the matrix from a reservoir (the fracture) of limited volume.

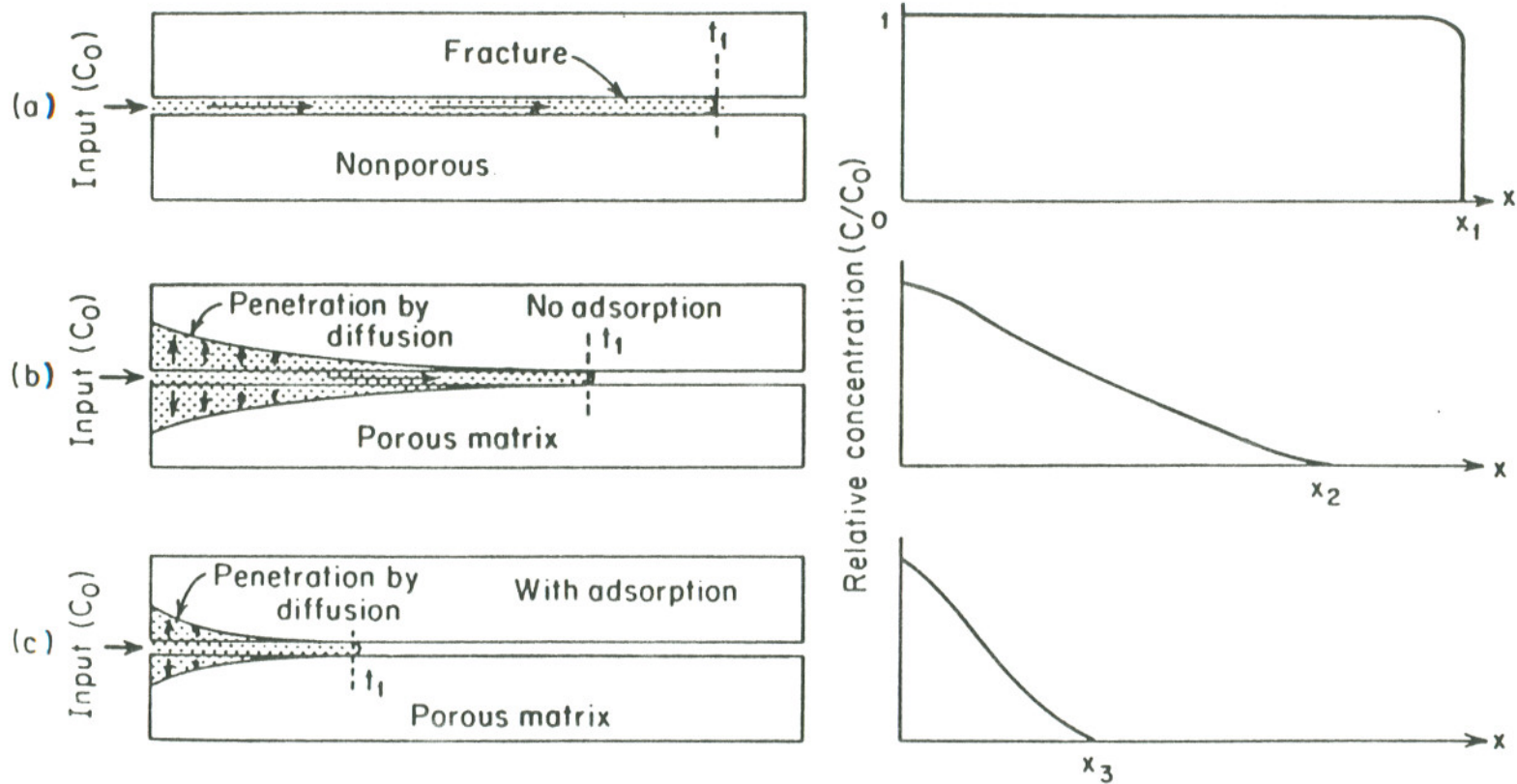


Figure I.A.5 Schematic drawings of advective-diffusive transport in fractured media for: a) a non-porous medium; b) a porous medium; and c) a sorbing compound in a porous medium. (After Freeze and Cherry, 1979).

$$F(x) = -nD' \frac{\partial c'}{\partial x} \quad (\text{I.2})$$

where n = the matrix porosity, and

D' = diffusion coefficient of the solute in the soil matrix.

c' = concentration in the soil matrix

The time derivative of the concentration of solute within the matrix is described by Fick's second law:

$$\frac{\partial c'}{\partial t} = D' \frac{\partial^2 c'}{\partial x^2} \quad (\text{I.3})$$

If there is sorption of the solute by the matrix, the net flux into the matrix is increased and the concentrations in both the fracture and matrix water are reduced. If sorption is assumed linear with concentration, Equation I.3 may be expressed as:

$$\frac{\partial c'}{\partial t} = \frac{D'}{R'} \frac{\partial^2 c'}{\partial x^2} \quad (\text{I.4})$$

where R' is the retardation factor due to sorption in the matrix.

$$R' = 1 + \frac{P_m K_p}{n} \quad (\text{I.5})$$

where ρ_m = the bulk density of the matrix, and

K_p = the partition coefficient of the solute to the
matrix.

Modeling of the entire site as a system of discrete fractures has not been possible because of the large difference in scale between the apertures of the fractures and the transport distance (150 μm vs. 400 m). (The discrete fracture approach has, however, been used in analyzing data from the "push-pull" tracer tests in Section IV.) As a result, an alternate model which treats the system as an equivalent porous medium (EPM) has been employed. In one dimension, the representative differential equation takes the form:

$$\frac{\partial c}{\partial t} = \frac{D_{L-EPM}}{R} \frac{\partial^2 c}{\partial x^2} - \frac{V_{EPM}}{R} \frac{\partial c}{\partial x} \quad (I.6)$$

where V_{EPM} and D_{L-EPM} are the effective velocity and longitudinal dispersion coefficient, respectively. These values can either be estimated by field tracer study, or calculated from the properties of the fracture system. R is the retardation factor due to sorption similar to Equation I.5. Application of the EPM approach requires an underlying knowledge of the fracture system to ensure that the assumptions inherent in treating the fractured porous system as an EPM are met. This will be discussed further in Section V.

II. SITE CHARACTERIZATION

This section and Section IV are concerned with the determination of the physical parameters which are important for the characterization of contaminant transport in the groundwater at the site. Section II is divided into six parts. The first will involve a general description of the site. The second will discuss the specifics of the sampling devices used at the site. The third will discuss the general hydraulics of the area as they relate to the site. The remaining parts will cover the laboratory and field experiments used to determine the physical constants characterizing the aquifer system (e.g. hydraulic conductivity, porosity, etc.).

II.A. SITE DESCRIPTION

Alkali Lake is located on the northwestern edge of the Basin and Range Physiographic Province (Fenneman, 1931). As previously discussed by Pankow, et al. (1984), this section of the Province is characterized by a large graben which contains a number of closed lake basins (bolsons). The Alkali Lake playa, covering approximately 20 square kilometers, is located in one of

those bolsons. The playa is partially covered with water during most of the year and becomes the wettest in the late winter-early spring. Evapotranspiration in the playa area substantially exceeds precipitation. The water deficit is made up by surface and groundwater flow towards the playa. The site is located on the southwest edge of the playa in a topographically low arm which appears in Recent times to have connected Alkali Lake with West Alkali Lake, another intermittent playa lake. This arm has been partially filled with either eolian or lacustrine deposits (which are less consolidated than the surrounding playa surface) and appears to provide a conduit for groundwater flow towards West Alkali Lake.

The geology of the immediate Alkali Lake area has been discussed by Mundorff (1947), Newton and Baggs (1971), and with specific regard to the CDS by Pankow et al. (1984). Soil in the vicinity of Alkali Lake consists primarily of Recent and Pleistocene eolian and lacustrine beds of gravel, sand, silt, and clay-sized particles. In the area of the CDS these beds are believed to be in excess of 30 m thick (Newton and Baggs, 1971). Soil cores taken in the zone of contamination show evidence of a large number of horizontal and vertical fractures. The horizontal fractures are regularly spaced. Originally, they were probably bedding planes in the lacustrine sediments which later opened to form fractures. The fractures appear to be spatially extensive.

Both the vertical and horizontal fractures may have been created by the processes of dehydration and rehydration, or by the dissolution of carbonates.

The topography in the vicinity of the CDS is flat to the north and east, gently sloping up to the south and down to the west. The elevation of the site is approximately 1300 m above sea level (EPA, 1983). The CDS is approximately 1 m above the level of Alkali Lake, and 2 m above West Alkali Lake.

The climate is typical of a high altitude western North American desert. Basic meteorological measurements have been made at a site 4.8 km from the CDS since 1961 (NOAA, 1983). During the years 1972-1984, the annual precipitation averaged 17.5 cm. The period of lowest precipitation occurs during the winter months of November-February (Figure II.A.1). High precipitation events (greater than 2 cm/day) occur primarily between May and September. The precipitation-weighted frequency plot (Figure II.A.2) for data from 1972-1984 indicates that greater than 80% of the precipitation falls in events of less than 1.5 cm.

II.B WATER SAMPLING DEVICES

Between October 1981 and the present, 28 piezometer/sample

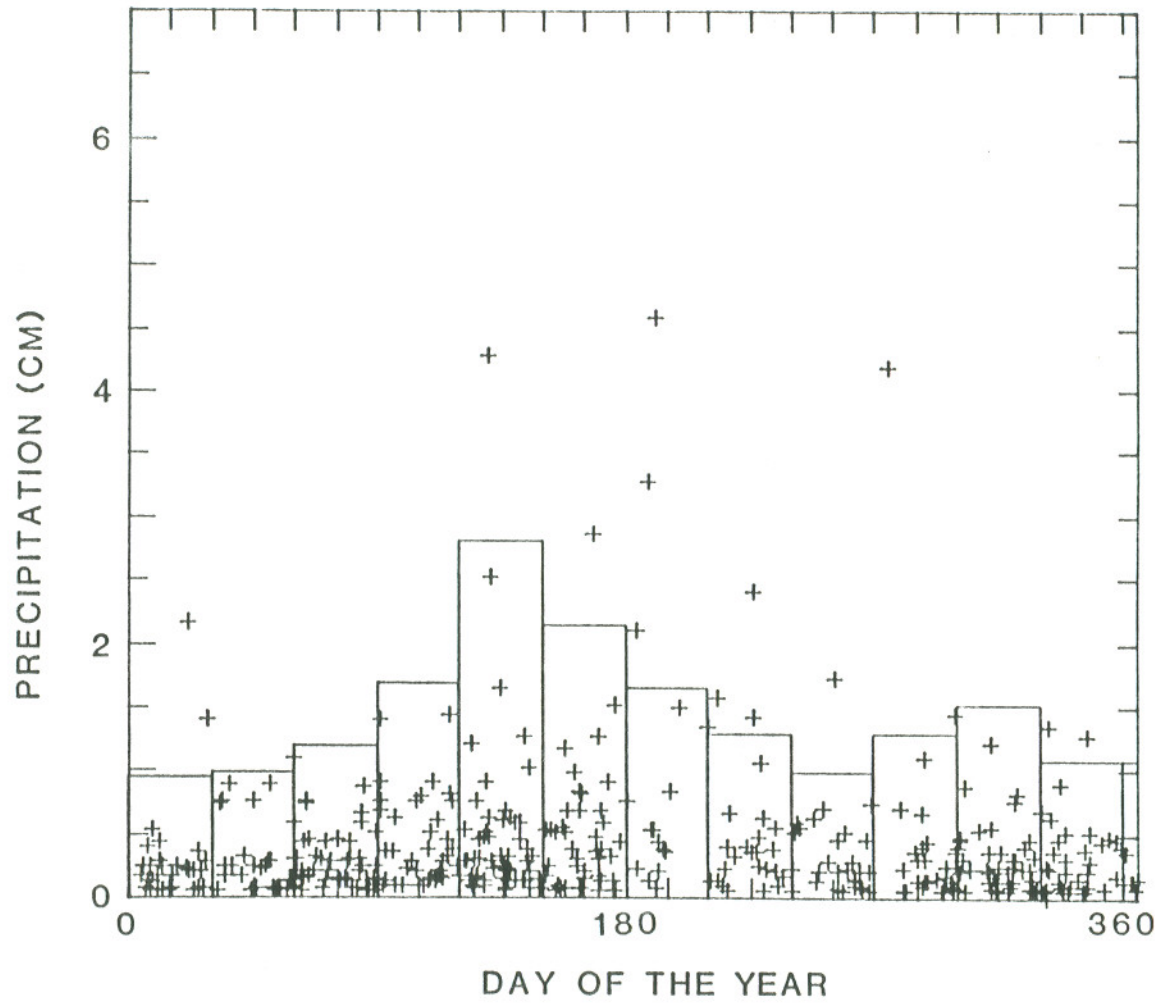


Figure II.A.1 Individual precipitation event values plotted versus day of the year, together with monthly averages. (Based on 1972-1984 data, NOAA (1984).)

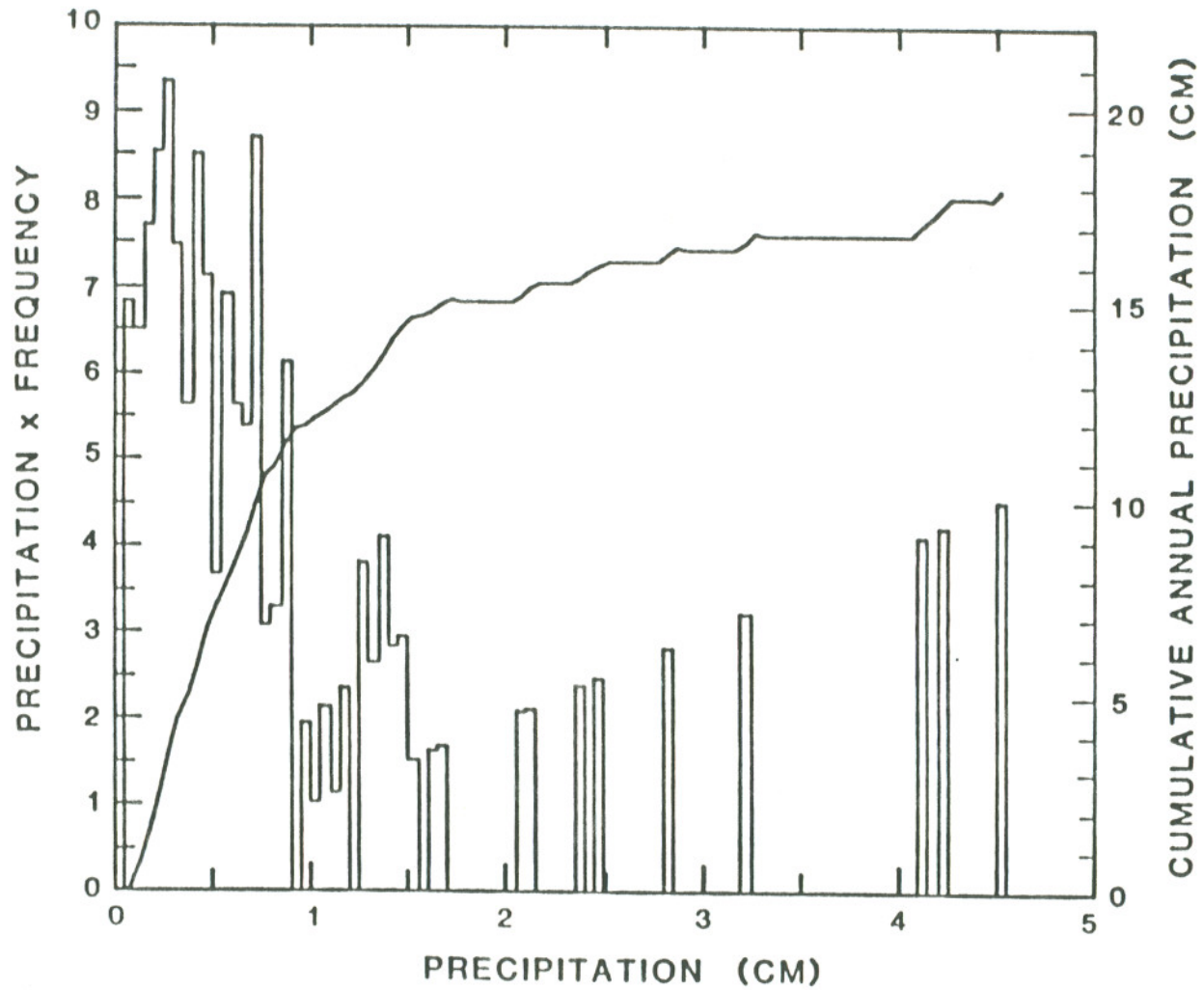


Figure II.A.2 (Precipitation x frequency) versus precipitation (cm) histogram and average cumulative annual precipitation versus precipitation (cm) curve. (Based on 1972-1984 data, NOAA (1984).)

wells were added by OGC to expand the sampling network of 21 such wells already installed at the site by ODEQ. The new devices were 4 m long, 7.5 cm I.D., open-bottomed, and constructed from PVC, as were the "ODEQ-type" wells. They were slotted from above the water table (approximately 1 m below ground-surface) to the bottom of the tube (3.5 m below ground). No contamination or loss problems with the PVC casings are expected at this site. Each tube was slotted so as to be 9% open below a depth of 1.0 m. They were designated "Wells 22-49" (Figure I.D.4), and were installed at the site by hand augering a 9 cm diameter hole and dropping in the tube. No caving problems were experienced during augering. As with the "ODEQ-type" wells, each tube was fitted with a removable PVC cap.

In order to obtain more spatial resolution in the measurement of the contaminant distributions, water table and specific conductance, two additional networks were installed. Approximately 90 points (Figure II.B.1) were sampled in April 1983 using 1.8-2.5 m long, 0.64 cm O.D., 0.46 cm I.D. type 316 stainless steel (SS) tubes. After placing a 0.45 cm O.D. rod inside the open-bottomed, unslotted tubes, they were pushed 1.3-2.3 m into the ground by hand. The inner rod was retracted leaving a open sampling tube. A hand vacuum pump (Nalge, Inc., Rochester, NY or Cole-Parmer, Chicago, IL) was attached to the steel tube via FEP Teflon tubing, and 100 mL of groundwater were

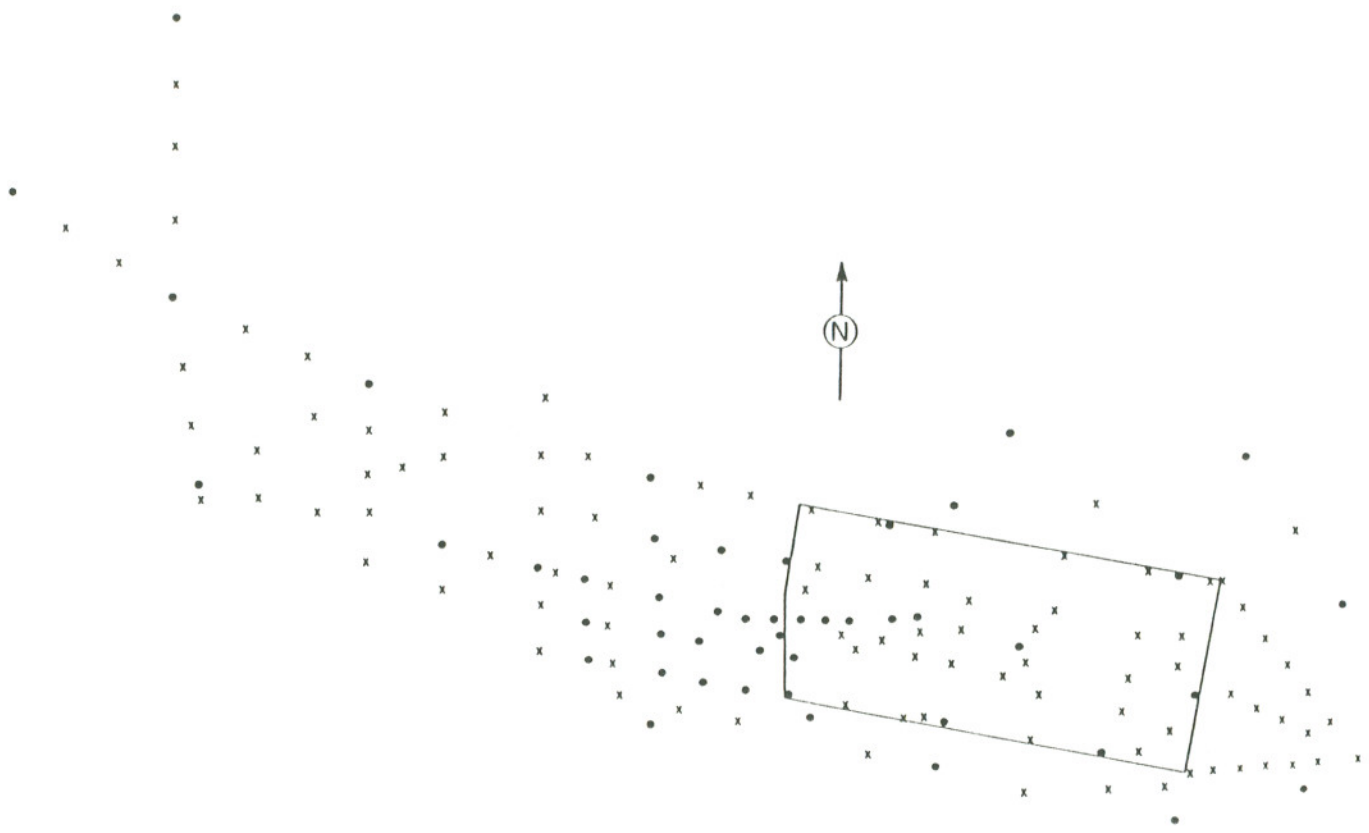


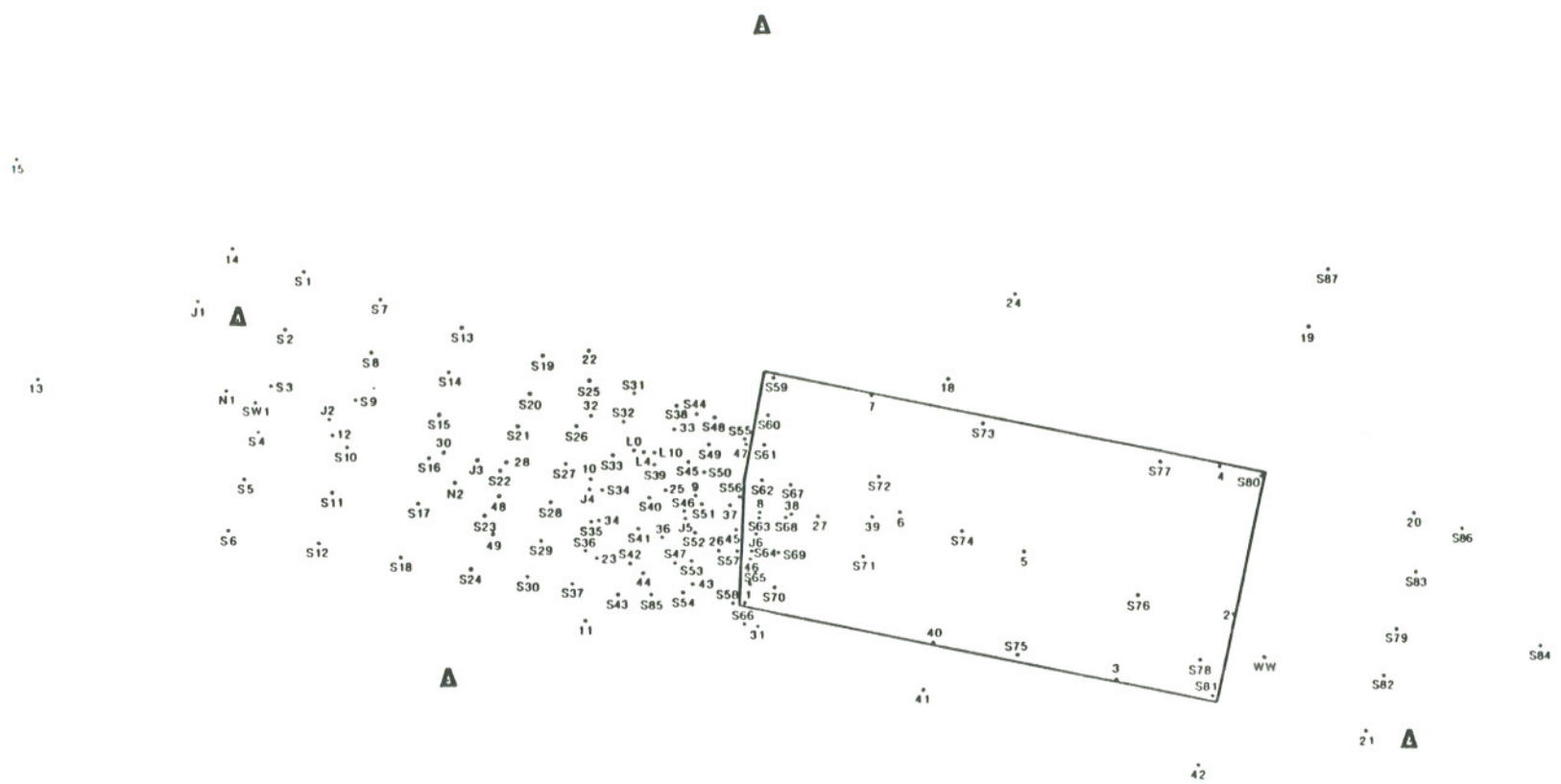
Figure II.B.1 Map showing the locations of the points sampled by the stainless steel probes (P-series) (marked with an X). Positions of the "ODEQ-type" wells are included as dots on the map for reference.

0 100 METERS
 0 100 200 400 FEET

withdrawn and placed in a 125 mL vial. After sample collection the SS tubes were removed and reused.

A second sampling network, consisting of 1.4 cm O.D., 0.9 cm I.D. PVC (1/4" Schedule 40) tubes, was installed in April 1984 at locations indicated in Figure II.B.2. These tubes, designated the "S-series", were approximately 3 m long and were slotted over the bottom two meters of their length (slots were .06 cm wide on 0.6 cm centers, two slots at each depth on opposite sides of the tube). The tubes were installed by first forcing a 1.6 cm O.D. stainless steel rod into the ground to a depth of 3.0 m. Next a 0.9 cm O.D. SS rod was placed inside the PVC tube to provide rigidity and the tube was forced into the hole created by the 1.6 cm O.D. rod. The SS insert was then removed and installation was complete. As with the "ODEQ-type" wells, these were designed to provide a sample whose concentration was integrated over the top 2 m of the water table.

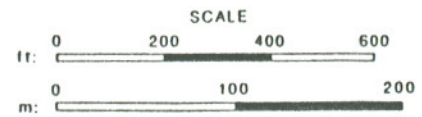
For sampling and aquifer testing at specific depths, two types of piezometers were installed at the site. The first, a series of multi-level devices which extended to 6 m below groundlevel (designated the J- and L- series), were designed to sample over 5 depth ranges (0-2, 2-3, 3-4, 4-5 and 5-6 m). As seen in Figure II.B.3 these piezometers were constructed of PVC with an overall diameter of 8.6 cm. 85 cm sections of slotted



DECLINATION 18° 10' E
 KLAMATH FALLS SECTIONAL AERONAUTICAL CHART (1983)

Figure II.B.2

Map showing the locations of the S-series samplers used for water sampling, water table measurement and slug tests.



(0.06 cm slots on 0.32 cm centers) 8.6 cm O.D. PVC (Hydrophillic Industries, Puyallup, WA) were mounted on a continuous piece of 6.3 cm O.D. PVC tubing on 100 cm centers. A glued ring of PVC provided a water-tight seal between the inner and outer tubes at the top and bottom of each slotted section. 3.0 cm holes were drilled in the 6.3 cm tube in the regions covered by the larger slotted tubes. Outside the 6.3 cm tube, between the sections of 8.6 cm tube, rings of pressed Wyoming bentonite were positioned to act as seals between the levels when installed. The bentonite was retained between the slotted sections by PVC sealing rings at the top and bottom of each slotted section. Several different devices were designed to be inserted inside the 6.3 cm tubes. Figure II.B.3 shows devices for discrete level "slug tests" and discrete level sampling.

A second type of specific level sampler was constructed of 2.1 and 2.8 cm O.D. PVC tube (Figure II.B.4). This device incorporated a 23 cm length of slotted 2.8 cm O.D. tubing as the screened interval. A 2.1 cm O.D. PVC tube connected to the slotted section and extended to the ground surface upon installation. A neoprene gasket, slightly larger than the diameter of the borehole, was placed on top of the slotted section of pipe to provide a seal and Bentonite was packed above the gasket. These have been used for water table measurement, sampling, slug tests (Section II.E) and "push-pull"

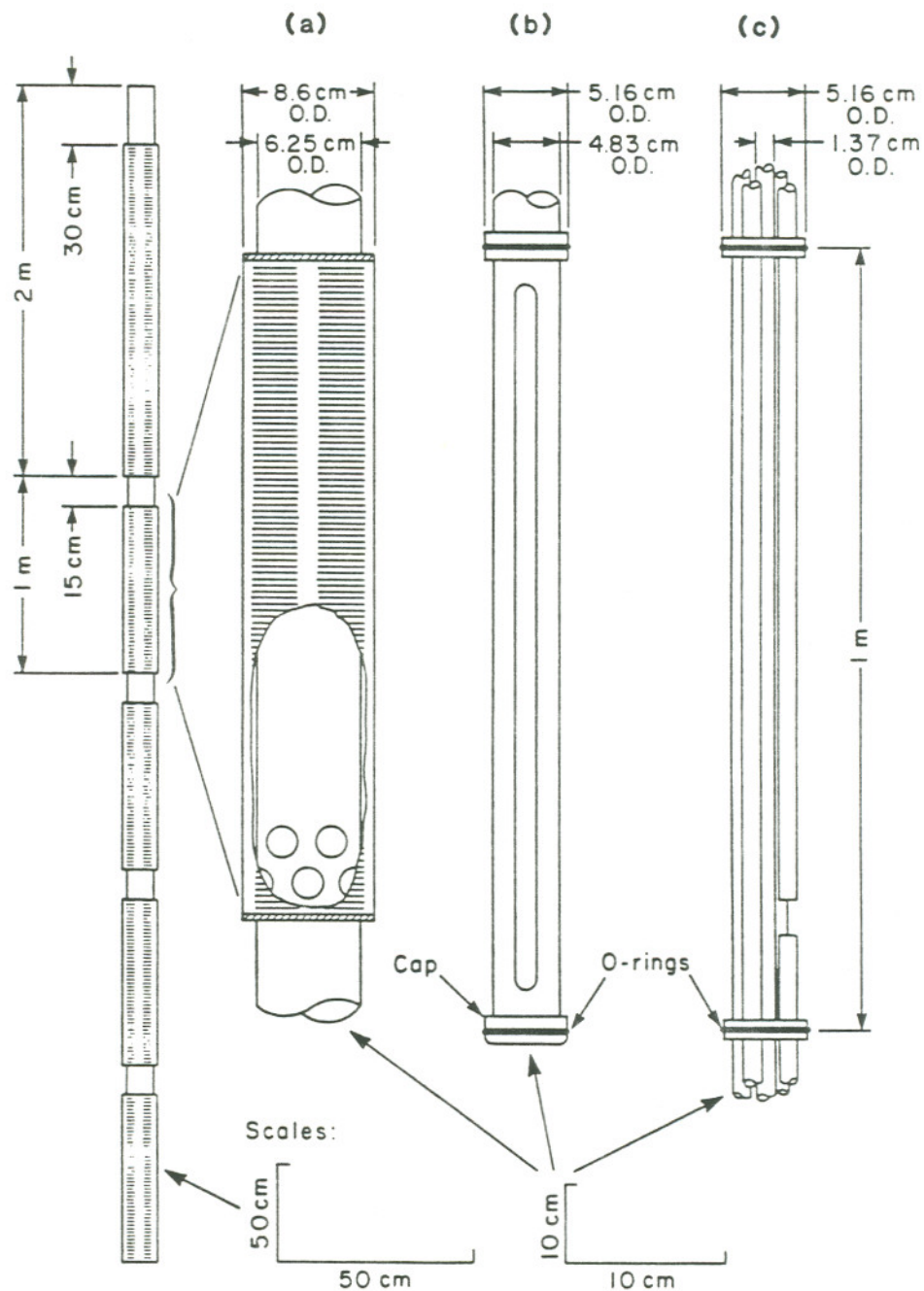


Figure II.B.3 Schematic drawing of the multi-level devices (J- and L-series) showing: a) cut-away detail of the screened intervals; b) removable inner tube used for single-level "slug tests"; and c) removable devices for single-level water sampling and water table measurements.

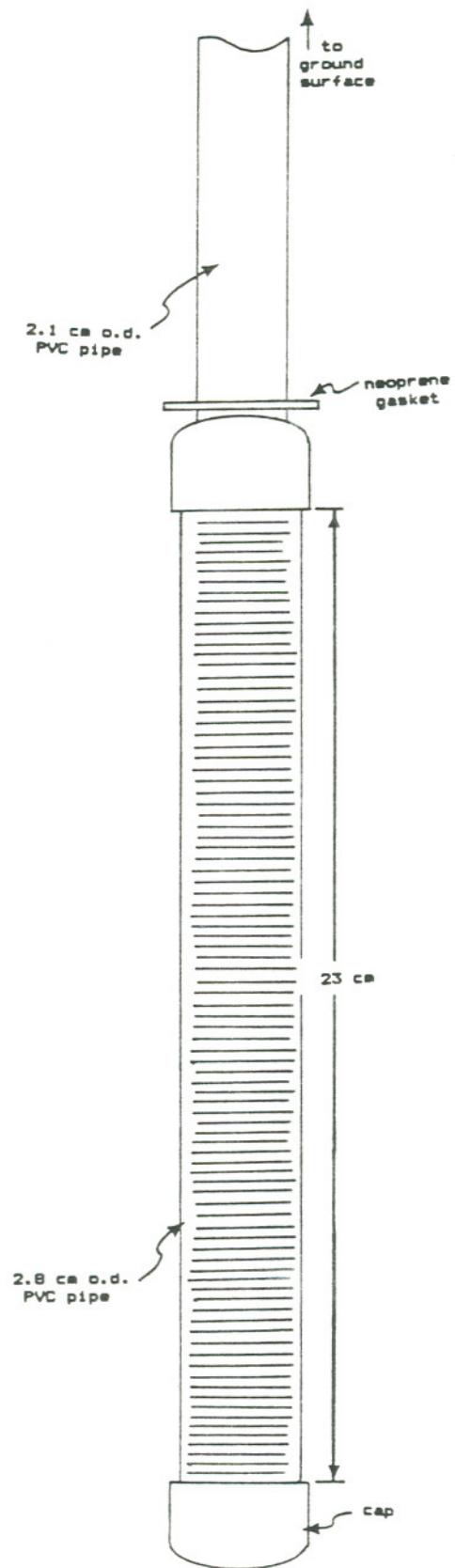


Figure II.B.4 Schematic drawing of single-discrete-level sampler.

tests (Section IV.C).

All of the methods used to install sampling devices at the CDS disturbed the soil structure and groundwater flow immediately surrounding the samplers. To minimize this, all of the samplers were "developed" prior to use. This was typically accomplished by addition and removal of water to the device by gasoline- or hand-powered pumps. In addition, prior to each sampling, several well volumes of water were removed to ensure that the sample, when collected, was from a portion of the aquifer unaffected by sampler installation.

II.C GROUNDWATER CHARACTERIZATION

II.C.1 WATER TABLE MEASUREMENTS

All of the previously described samplers, with the exception of the small stainless steel probes, were surveyed to allow the preparation of water table maps. Water table measurements have been made at the "ODEQ-type" wells since the burial of the materials at the site (ODEQ, 1977-1984). Figure II.C.1 gives water levels for Wells 2 and 8 (at the east and west ends of the site) during that period. (The water table was referenced to the top of the casing of Well 2, which has been

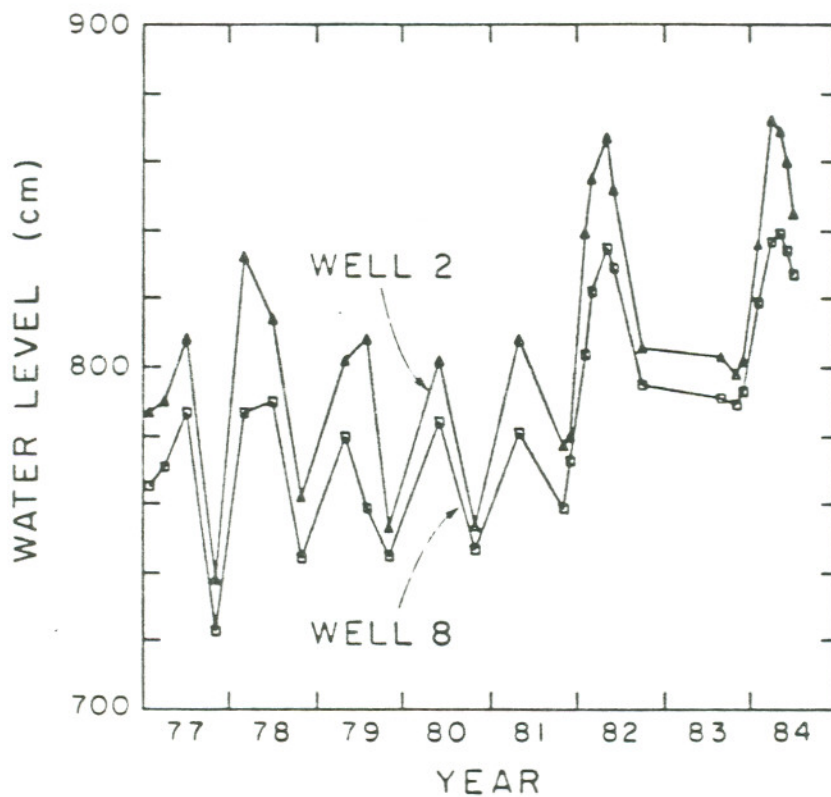


Figure II.C.1 Water table at "ODEQ" Wells 2 and 8 as a function of time over the period 1977-1984. The data are relative to the datum: top of Well 2 casing = 1000 cm.

arbitrarily set at 1000 cm.) In the site area, the hydraulic gradient remains towards the west throughout the year. Figure II.C.2 shows values of the gradient as estimated between Wells 2 and 8 for the period 1977-84. The data of Figures II.C.1-2 have been replotted as a function of month of the year in Figures II.C.3-4. Both water table and hydraulic gradient were highest in the late winter and early spring, with the gradient typically decreasing in the late summer and fall to less than half of the maximum value.

Water table contour maps for four times of the year are plotted in Figure II.C.5. It can again be seen that the gradient near the site is highest in the early months of the year, and lowest in the fall. In April 1984, a detailed mapping of the water table was made using the 0.9 cm I.D. tubes (S-series, Figure II.B.1). Figure II.C.6 presents contours generated from this data.

II.C.1.a CONDUCTANCE-WATER TABLE MEASUREMENT PROBES

Water table measurements for the April 1984 sampling were made using specially designed conductance probes (Figure II.C.7). These were designed to fit inside the 1.4 cm O.D. PVC tubes used in several of the sampler designs. They consisted of 0.64 cm O.D. 0.46 cm I.D. SS tubing with a machined Delrin tip. 0.025 cm

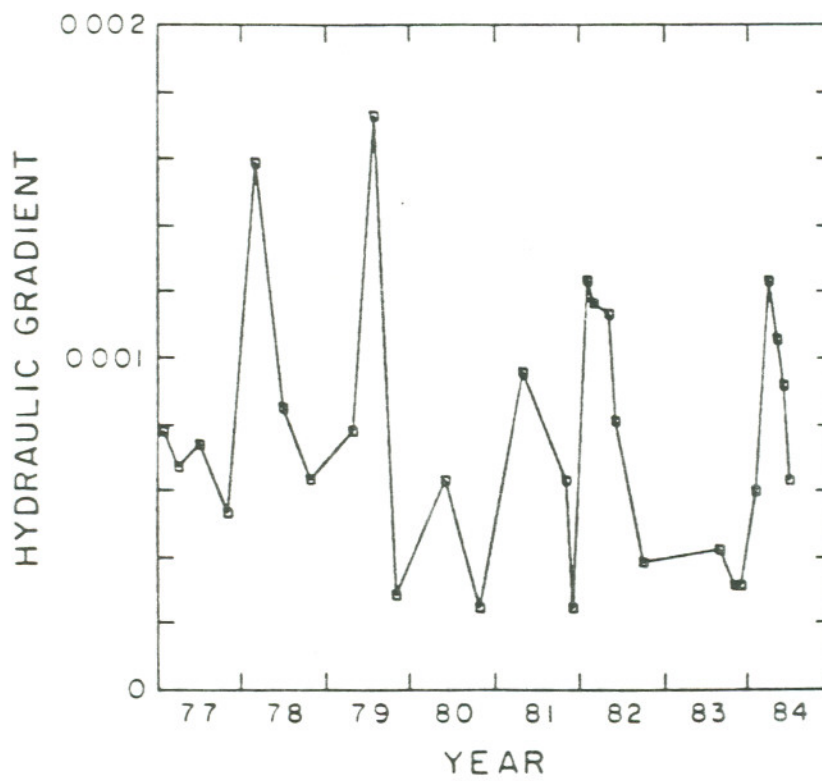


Figure II.C.2 Hydraulic gradient between "ODEQ" Wells 2 and 8 as a function of time over the period 1977-1984.

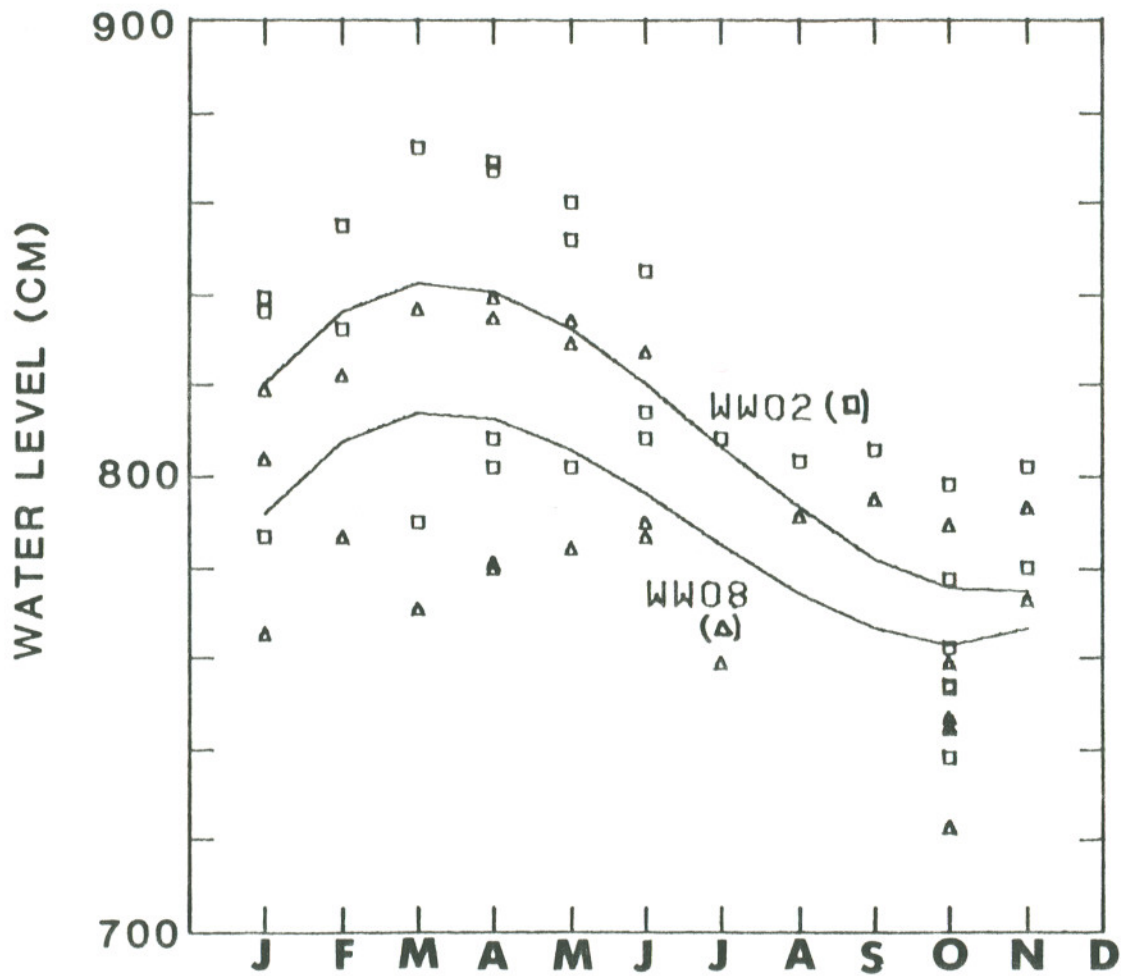


Figure II.C.3 Water table as a function of month of the year over the period 1977-1984. The data are relative to the datum: top of Well 2 casing = 1000 cm.

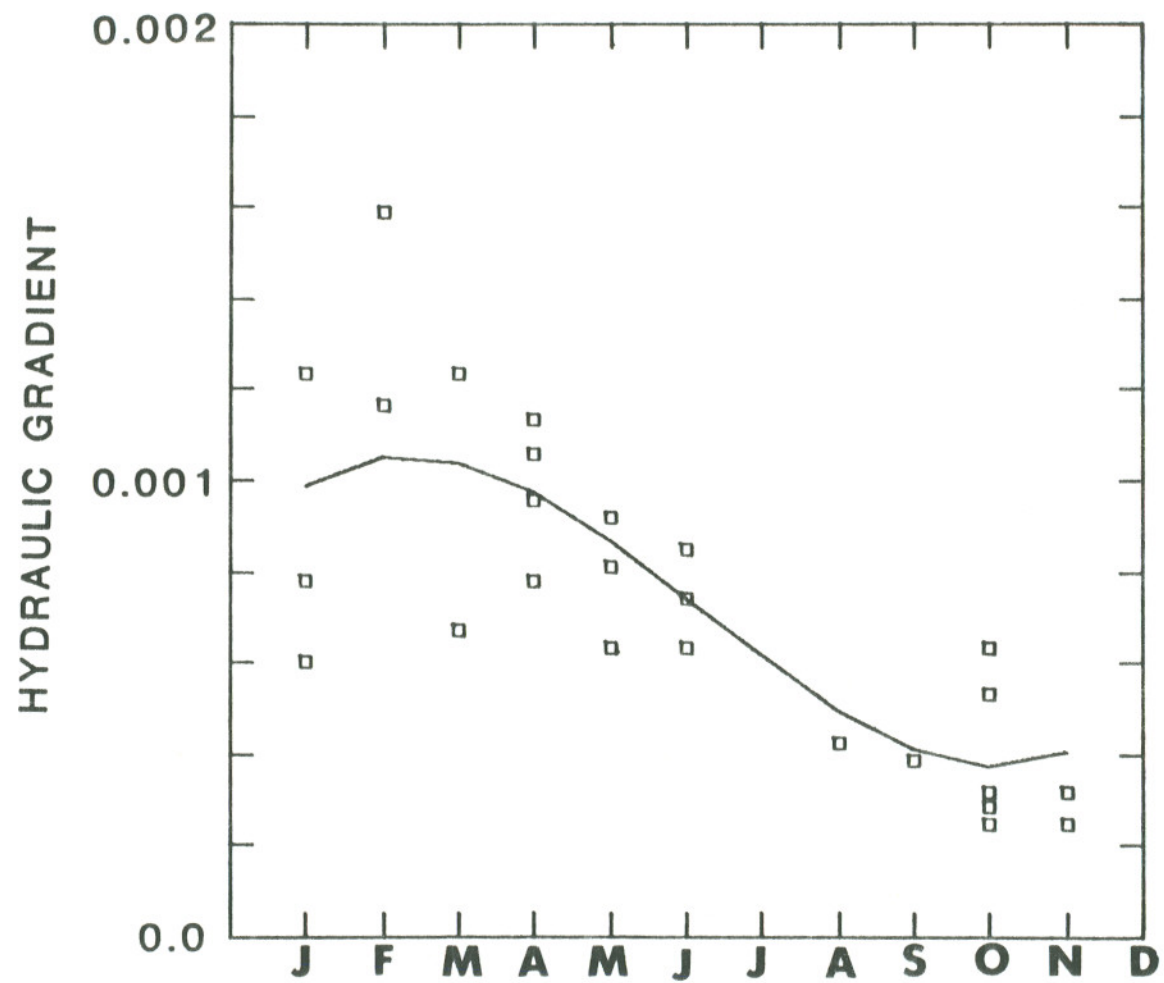
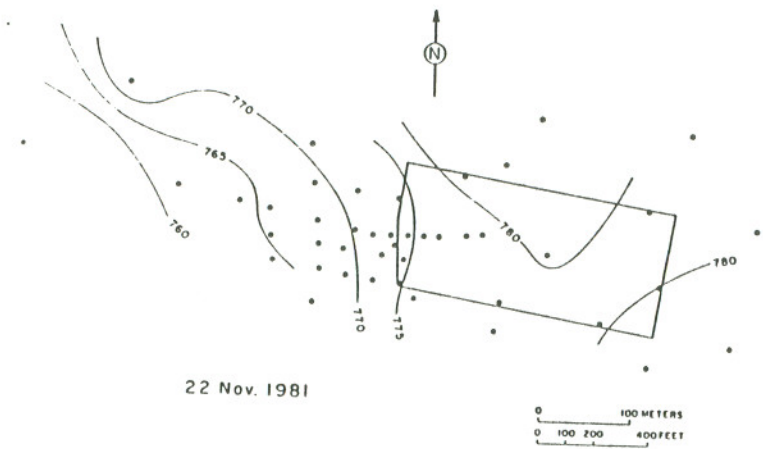
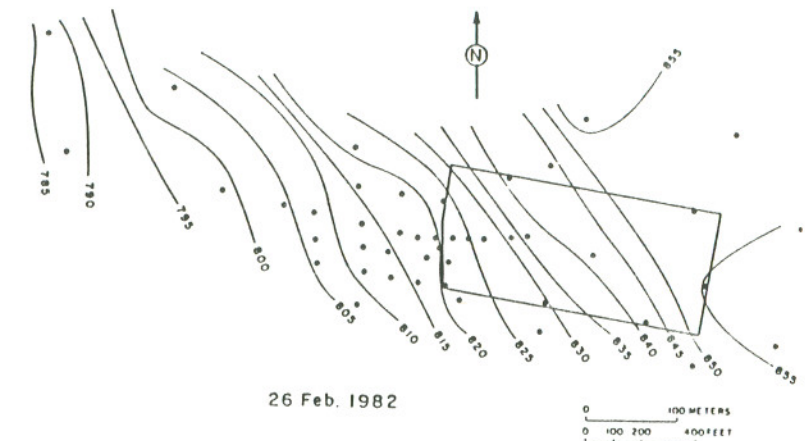


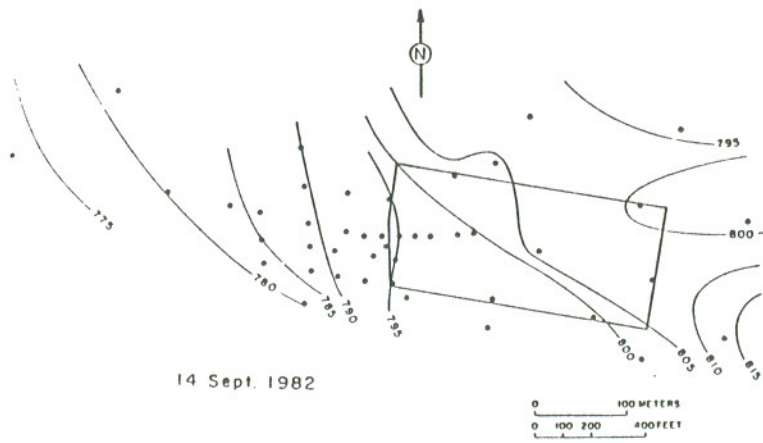
Figure II.C.4 Hydraulic gradient between "ODEQ" Wells 2 and 8 as a function of month of the year.



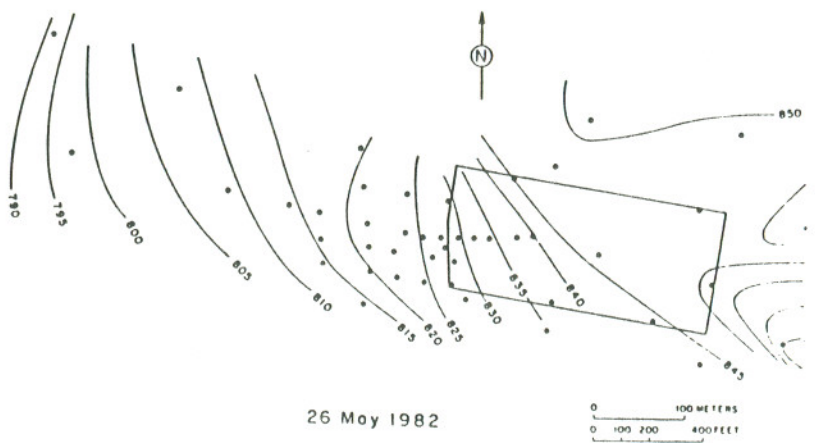
22 Nov. 1981



26 Feb. 1982



14 Sept. 1982



26 May 1982

Figure II.C.5 Water table maps in centimeters obtained during November 1981, and February, May and September 1982. The data are relative to the datum: top of Well 2 casing = 1000 cm.

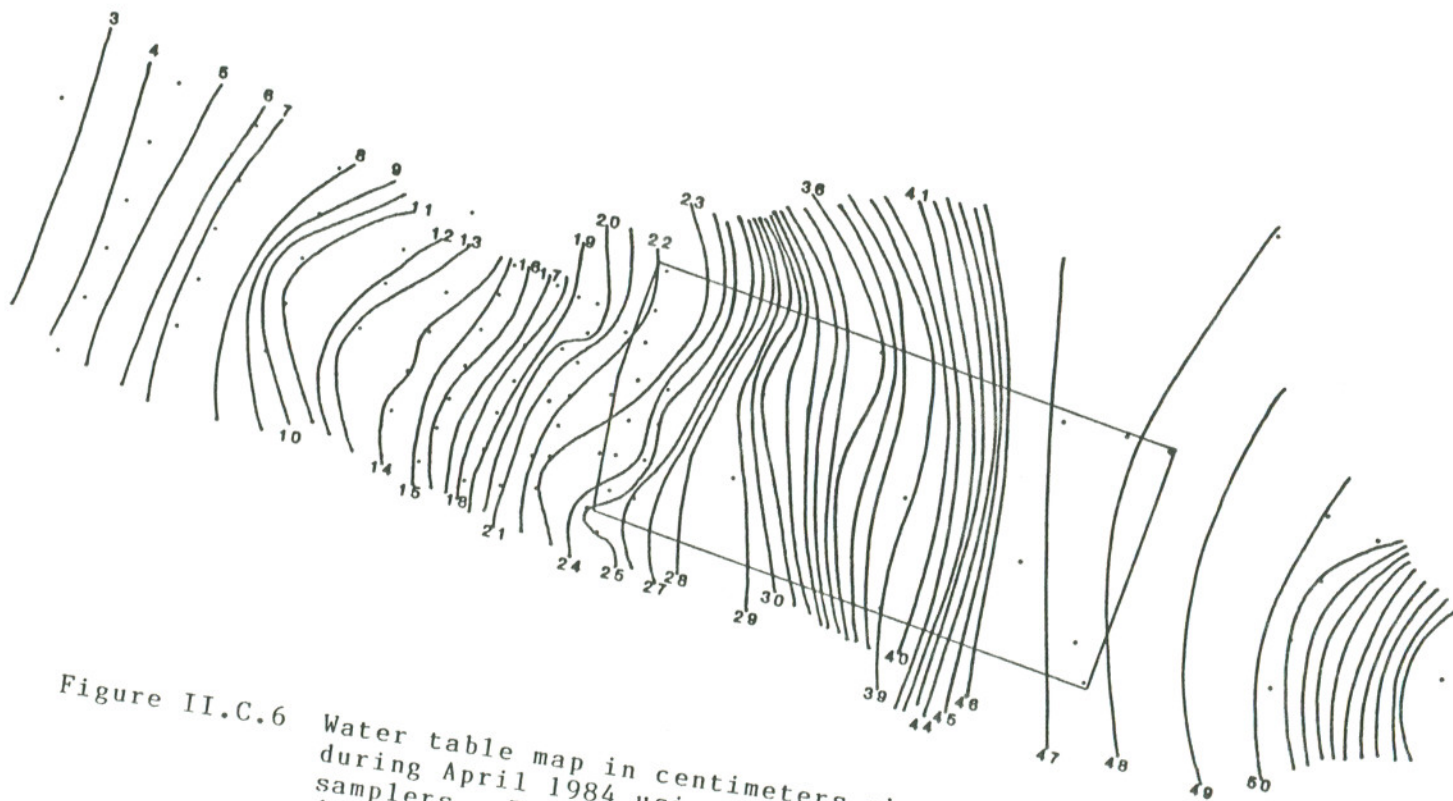


Figure II.C.6 Water table map in centimeters obtained during April 1984 using the S-series samplers. The data are relative to the datum: top of Well 2 casing = 200 cm.

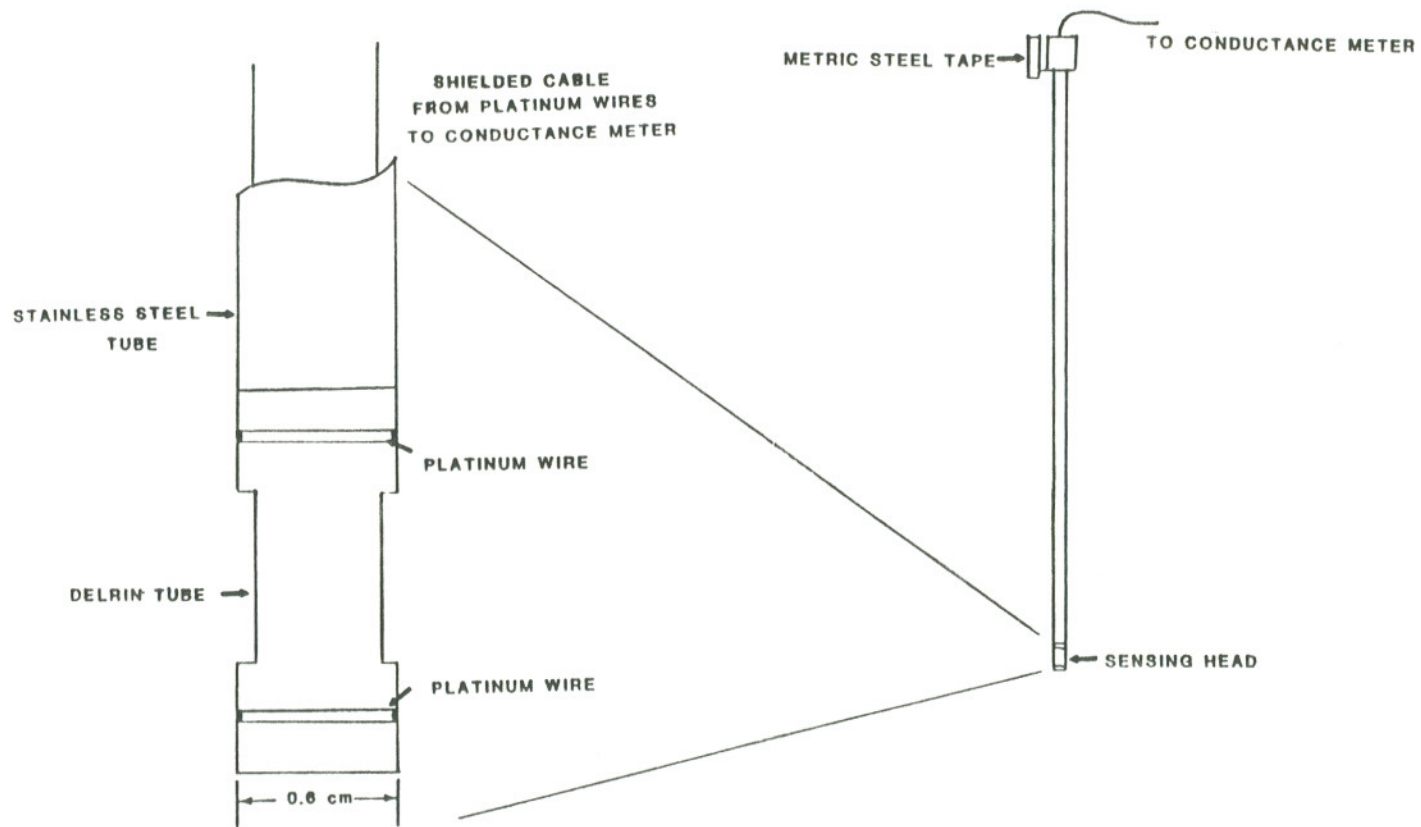


Figure II.C.7 0.64 cm O.D. probes used to monitor specific conductance of the groundwater and the water table.

diameter platinum wire was wrapped in grooves around the tip and connected to a shielded cable which was in turn connected to a specific conductance meter (Yellow Springs Instruments, Yellow Springs, OH). The probes could thus be used to monitor conductance as well as water level. The platinum wires were spaced 1.0 cm apart on the tip, which was not the same as for the YSI probe, thus the meter readings required correction. A calibration curve for the 0.64 cm O.D. probes is presented in Figure II.C.8. For the water table measurements, a metric steel tape was fixed to the top of the probe allowing direct measurement of the distance from the top of the casing to the water surface.

II.C.2 SPECIFIC CONDUCTANCE MEASUREMENT

Groundwater flowing from the springs east of the site is essentially fresh. As it moves west through the site, the concentrations of dissolved salts increase, as does the pH. Water quality measurements typical of the spring water and of the site are presented in Table II.C.1. It has been possible to map the direction of flow of the groundwater at the site by plotting specific conductance isopleths moving west from the springs, through the site towards West Alkali Lake. A detailed survey of specific conductance was made in April 1983 using samples collected from the small stainless-steel probes previously

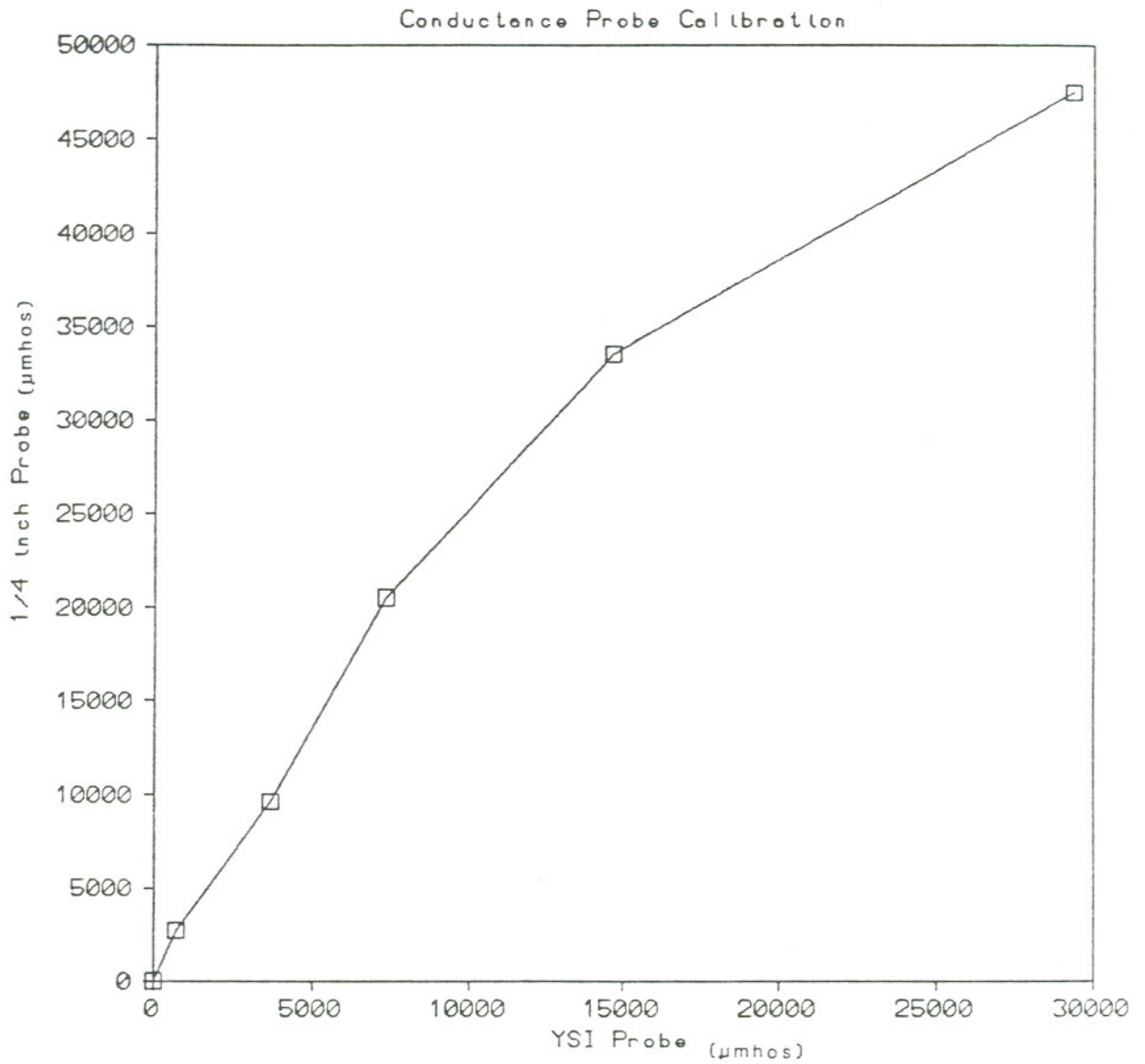


Figure II.C.8 Calibration curve for the 0.64 cm O.D. conductance probes versus the YSI probe.

TABLE II.C.1. GROUNDWATER QUALITY DATA

ARTESIAN SPRING WATER

TOTAL DISSOLVED = 200-500 mg/L
SOLIDS

CONDUCTANCE = 100-200 umhos/cm

pH = 7.5-8.5

GROUNDWATER BENEATH THE CDS

TOTAL DISSOLVED = 10,000-15,000 mg/L
SOLIDS

CONDUCTANCE = 10,000-20,000 umhos/cm

pH = 10.0

described. Specific conductance isopleths are plotted in Figure II.C.9 (Pankow et al., 1984). The contours suggest that the primary path of groundwater flow may be along the southern edge of the site. The flow path may also narrow as it moves out of the site to the west, and may broaden at 200-300 m downgradient from the site. This behavior is generally consistent with the observed water table data.

II.D. SOIL CHARACTERIZATION

II.D.1 MINERALOGICAL ANALYSES

Samples for mineralogical examination and grain size analyses were taken in the area of Well 34 (Figure I.A.4) at depths of 1.2 and 2.4 m. After collection each sample was extracted with 4:1 methanol:water to remove contaminants. Mineral and grain size characterizations were performed by Schlicker and Associates, Portland, OR. Mineral content was determined by X-ray analysis and by examination with a petrographic microscope. Grain size analyses were carried out by sieving with a series of standard U.S. screens (Nos. 40, 50, 100 and 200). The portions of each sample passing through the number 200 screen were further size segregated by hydrometer analyses. The two soil samples showed similar grain size distributions

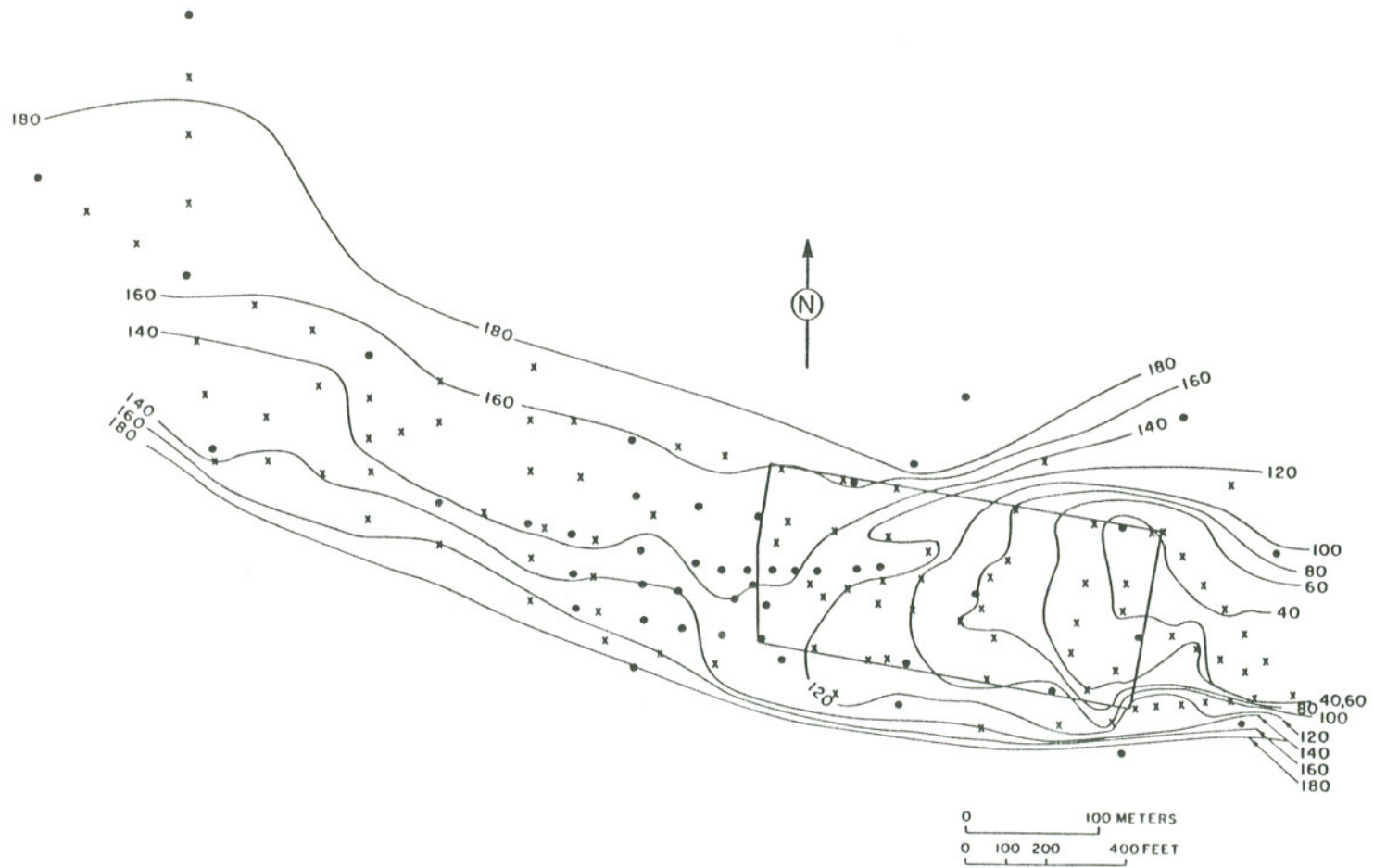


Figure II.C.9 Specific conductance isopleths (April 1983),
micromhos/cm $\times 10^{-2}$.

(Figure II.D.1). In both cases, 90% of the material was greater than 0.006 mm, very little being found in the operationally defined "clay" size range. Almost no clay minerals were found by X-ray analysis. This is consistent with the size distribution data, however field observation of all of the cores obtained by hand augering showed a highly plastic soil suggestive of clay.

II.D.2 POROSITY AND BULK DENSITY DETERMINATIONS

The porosity and bulk density values of the aquifer material were determined. Core samples of soil materials were taken below the water table downgradient (west) of the site in the zone of contamination. The samples contained intact angular blocks which appeared relatively undisturbed by sampling. The blocks were weighed and their volume determined by immersion in water. They were re-weighed after immersion to verify that no water had been absorbed, then dried at 50°C to a constant weight. The porosity was calculated as the weight loss to volume ratio. Porosity values found for a number of samples obtained near Well 25 (Figure I.A.4) ranged between 0.60 and 0.70. The bulk density of the soil was estimated to be in the range 0.8 to 1.0 g dry soil/cm³.

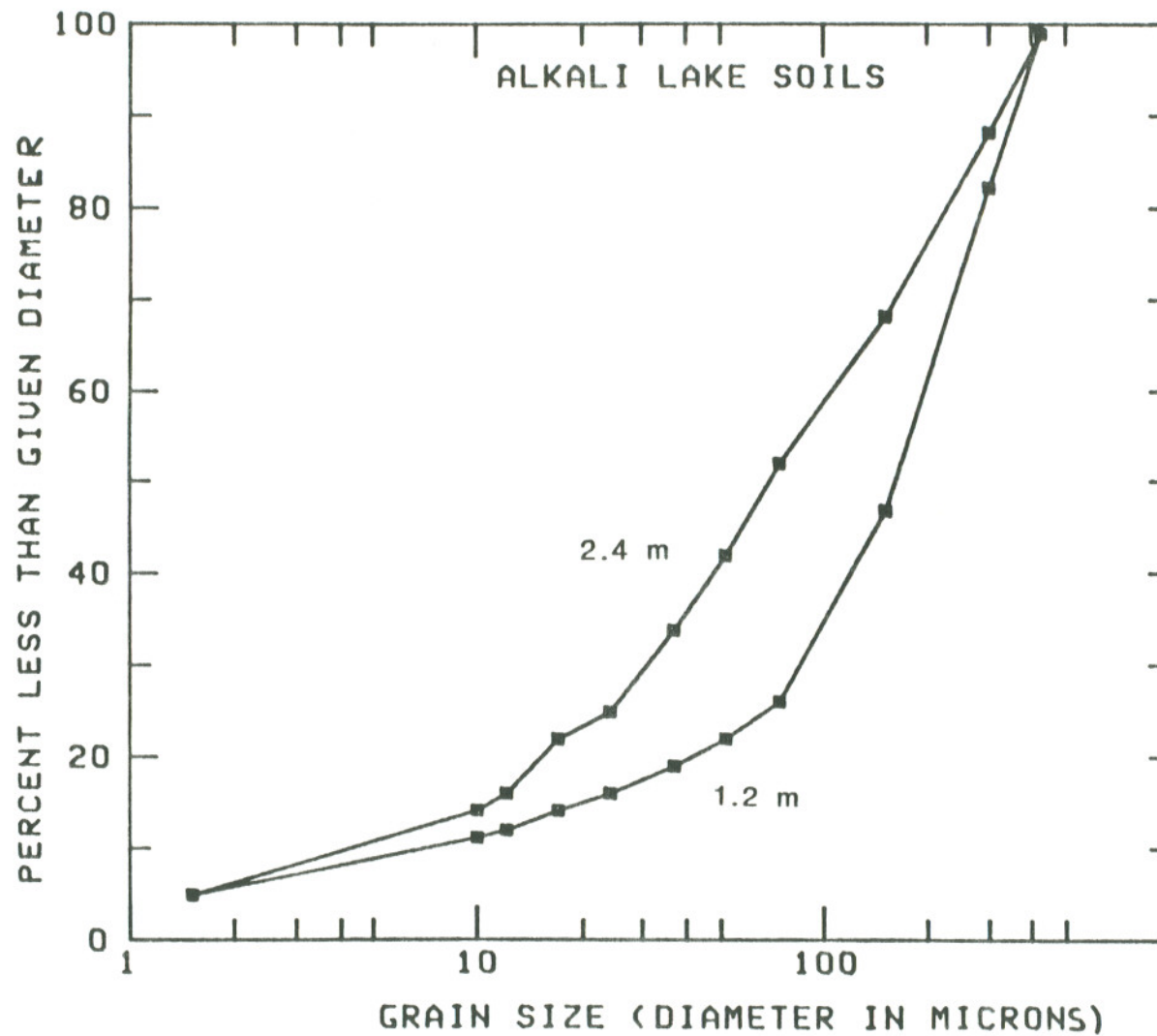


Figure II.D.1 Percent of soil material below a given grain size versus grain size for two samples taken near Well 34 at 1.2 and 2.4 m below groundlevel.

II.D.3 SOIL ORGANIC CARBON DETERMINATIONS

Soil organic carbon (SOC) determinations were made using an apparatus developed by Johnson (1981). Samples of soil (0.1 g) were: 1) placed in 0.6 cm diameter copper combustion boats; 2) treated with 200 uL of a 5% stannous chloride, 3 N HCl solution; 3) heated for 4 hours at 50°C to drive off inorganic carbon (carbonate and bicarbonate) as CO₂; and 4) combusted at 700°C in a 10% O₂-90% He gas mixture. The CO₂ formed by combustion was catalytically converted to methane and measured in a flame ionization detector (FID). Calibration of the FID with CO₂ injections and combustion of known amounts of organic compounds allowed the computation of the amount of organic carbon in the samples. The stannous chloride was used in the carbonate degradation step to prevent premature oxidation of the SOC (Allison and Moodie, 1965). The SOC content was determined on a soil sample obtained and composited from the depth range 1-3 m from a location 10 m east of Well 2 (Figure I.D.4). The measured SOC values for the soil on a dry weight basis gave a mean and standard deviation 2.4+/-0.3% for 12 replicates. These determinations were difficult because of the high level of carbonate present in the samples. That presence caused the possibility of artificially high SOC values.

II.E SOIL HYDRAULIC CONDUCTIVITY (K_H) USING "SLUG TESTS"

II.E.1 EXPERIMENTAL

Slug tests to determine K_H were carried out on a number of the single and multi-level (J- and L-series) wells described in Section II.B. The data were analyzed using the method of Hvorslev (1951). Because the values of K_H were quite large, the procedure for conducting and interpreting the tests had to be modified somewhat from that described by Hvorslev. In order to make the "basic time lag" sufficiently long to allow its measurement, it was necessary to quickly add a large volume of water to the well. The reservoir used to accomplish this is presented schematically in Figure II.E.1. To carry out the test on the multi-level devices, a tube similar to Figure II.B.2.(b) was inserted in the well to the desired level. The reservoir was then fitted to the top of the tube and filled with water. When the ball valve at the bottom of the reservoir was opened, there was an initial drop of approximately 3 cm due to compression and loss of air in the tube above the water table. Water then started to flow into the well. The water level in the reservoir was monitored with a translucent nylon tube mounted on the exterior of the reservoir. The time required for the water

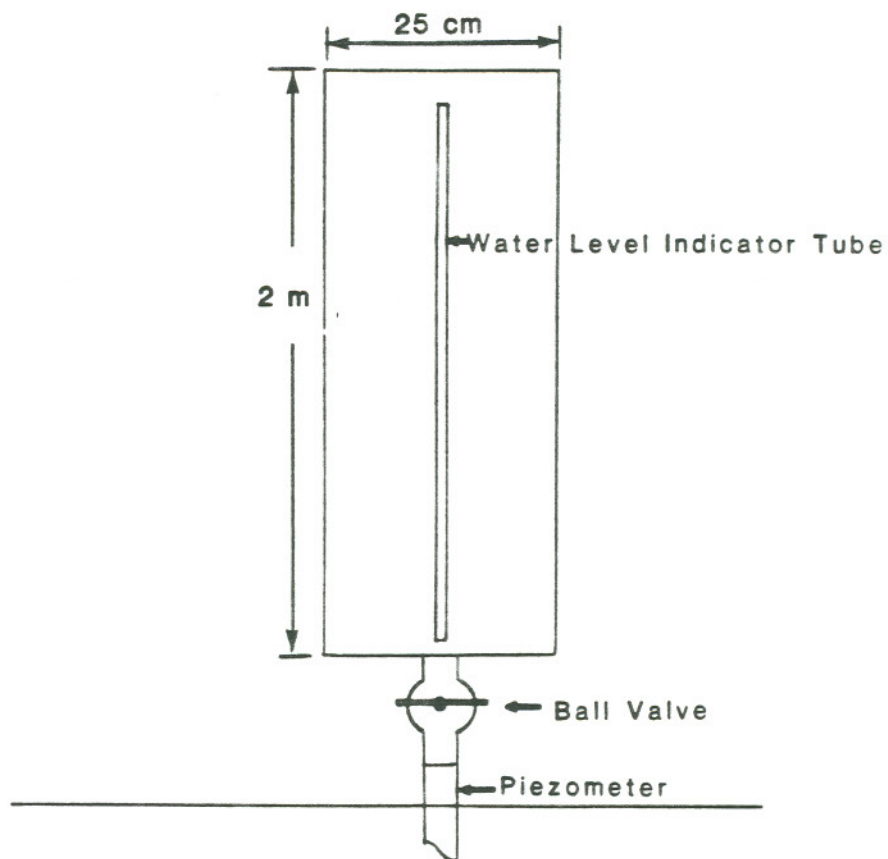


Figure II.E.1 Water reservoir used for the "slug tests".

level to reach several pre-set values was recorded.

II.E.2 RESULTS

Data were plotted as time vs. "water level at time(i)/water level at time(0)" to determine the basic time lag (T_0). (The datum was the water level before testing had begun = 0.) Test results are found in Appendix C. For an isotropic medium the equation to estimate K_H is:

$$K_H = r^2 \ln(L/R) / 2LT_0 \quad \text{for } L/R > 8 \quad (\text{II.1})$$

where L=length of the screened interval

R=radius of the screened interval

r=radius of the standpipe.

Values of K_H at various locations and depths are presented in Table II.E.1. The locations of the testing points are given in Figure II.E.2. The test results indicate the aquifer is not isotropic, and that K_H decreases with depth.

The preceding analysis is for porous media flow. In reality, the groundwater flow in the vicinity of the CDS is believed to be controlled by a highly permeable network of fractures. Barker and Black (1983) investigated the application

TABLE II.E.1 HYDRAULIC CONDUCTIVITY (K_H) DATA

SLUG TEST LOCATION	K_H ($\times 10^4$ m/s)
J1-3	4.2
J1-4	4.1
J1-5	2.5
J2-3	8.1
J2-4	7.0
J2-5	5.6
J2-6	2.7
J3-3	5.8
J3-4	5.5
J3-5	4.4
J4-3	5.5
J4-4	4.7
J4-5	4.6
J4-6	3.5
J5-3	9.3
J5-4	6.7
J5-5	6.7
J5-6	3.9
L4-3	3.5
L4-4	4.1
L4-5	2.0
L4-6	1.4
L10-4	3.3
L10-5	2.1
L10-6	0.8
PPA	1.2
PPB	2.9
PPC	3.5
PPD	2.1
PPG	2.9
PPH	2.4

J1

B C D
A J2 E
F

H
J3
G

L4 L10
J4 J5

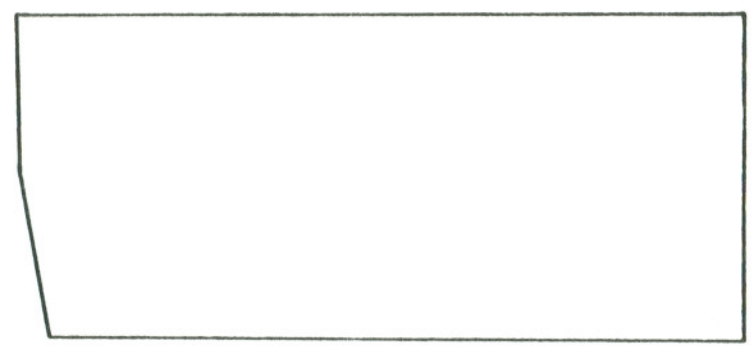


Figure II.E.2 Map showing locations of the "slug tests" used to determine K_H values.

of slug tests to fissured aquifers and found that such tests probably give K_H values to within a factor of three of the "correct" value. Comparisons of the Alkali Lake slug test-derived K_H values with other hydrological data (pumping tests, tracer tests, etc.) suggest that the slug test data are probably within a factor of three of the "correct" K_H values.

II.F PUMPING-DRAWDOWN TESTS

Pumping-drawdown tests were conducted primarily to investigate the vertical anisotropy of the aquifer. It was hoped that this information could then be used to interpret the pumping tracer tests to be discussed in Section IV. The thoroughness with which these tests were carried out was, however, significantly limited by three problems: 1) the installation of piezometers of greater than approximately 4 m below the water table would have caused the vertical spreading of the contaminants down into previously uncontaminated portions of the aquifer; 2) the process of pumping brought large quantities of contaminated water to the surface; and 3) the process of pumping accelerated the transport of contaminants out of the site and onto private land. For all of the above reasons, the number, duration, and pumping rate of the tests were all minimized.

The basic layout of one test is shown in Figure II.F.1. Discrete piezometers were installed at two depths, 1.8 and 3.5 m below the water table. Water levels in the piezometers were determined using the 0.64 cm O.D. conductance probes described in Section II.C. Water was pumped from the pumping well at a rate of approximately 1 L/s by a gas-powered pump. Data from the pumping test are presented graphically in Figures II.F.2-7.

No interpretation of this data will be presented here. The data are included here primarily as background information for the pumping tracer tests discussed in Section IV.

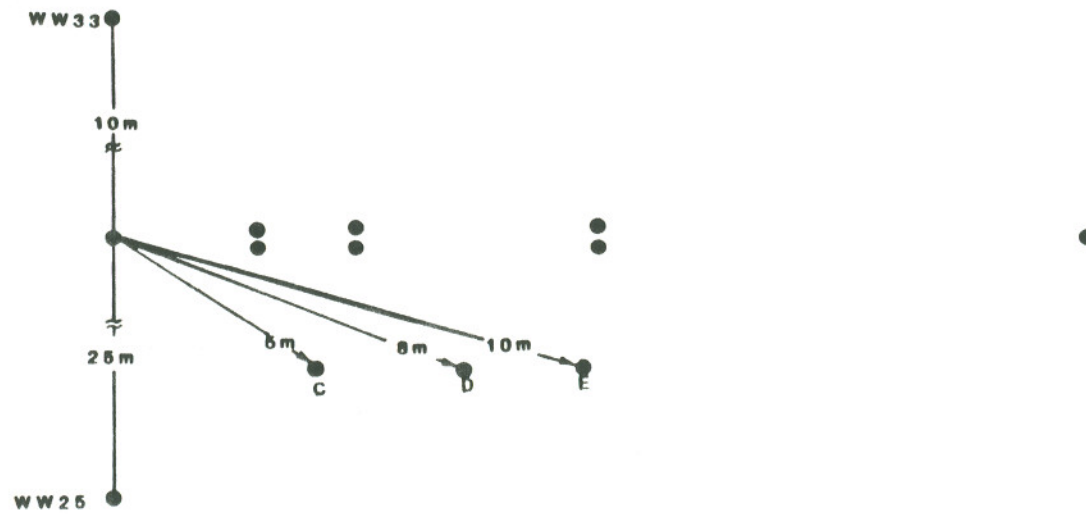
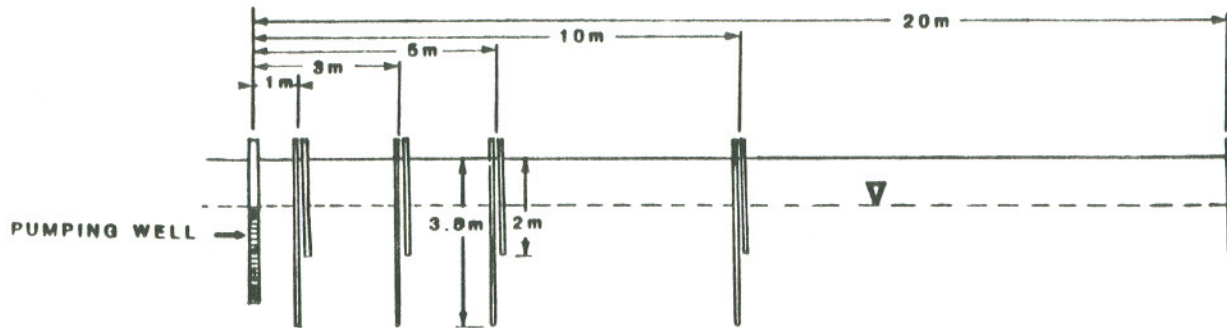


Figure II.F.1 Piezometer layout for pumping drawdown test T7P. (Located near wells 33 and 25, Figure I.D.4.)

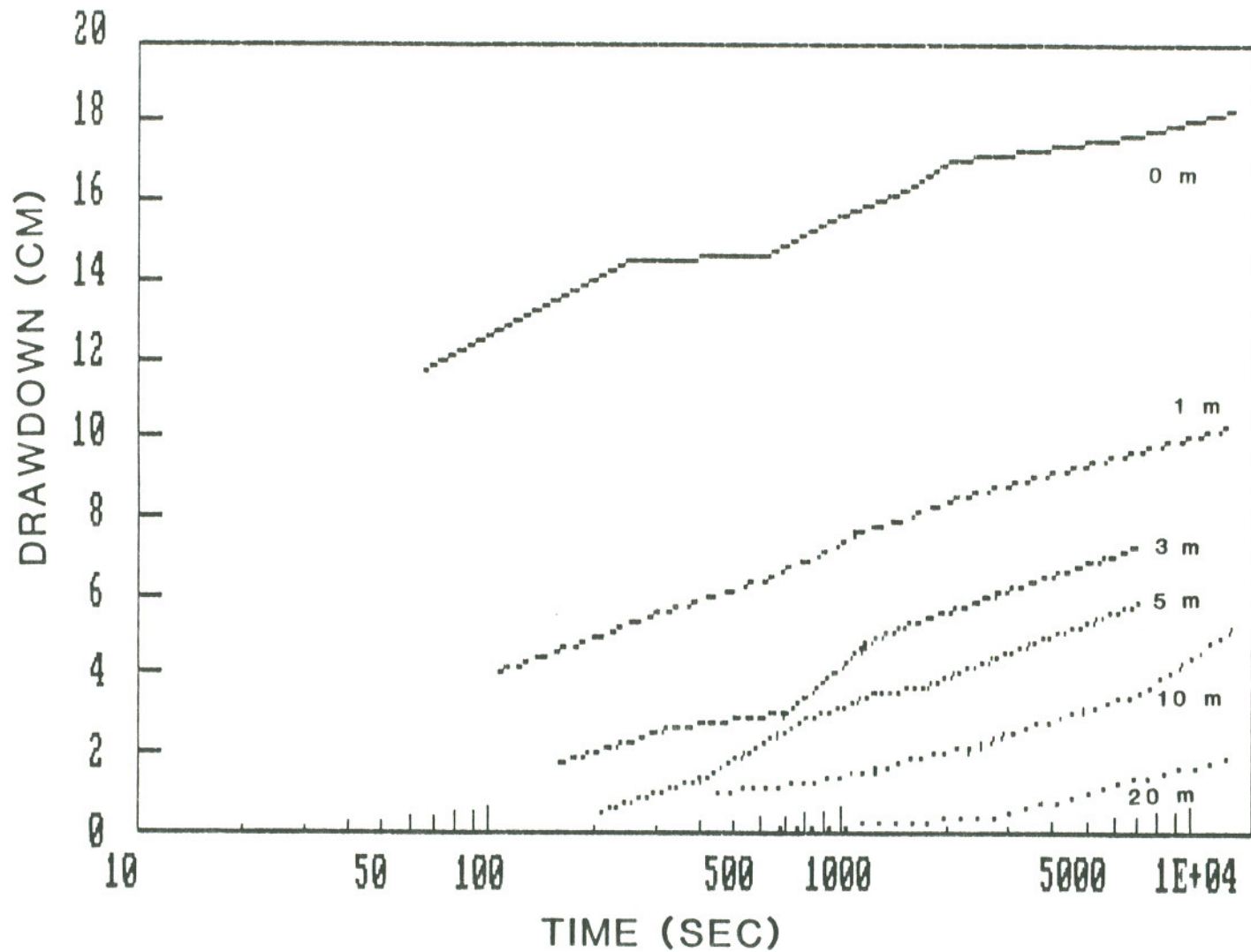


Figure II.F.2 Drawdown (cm) versus time for pumping test T7P (Located near wells 33 and 25, Figure I.D.4.) for piezometers open at approximately 1 m below the water table at 0,1,3,5,10 and 20 m from the pumping well.

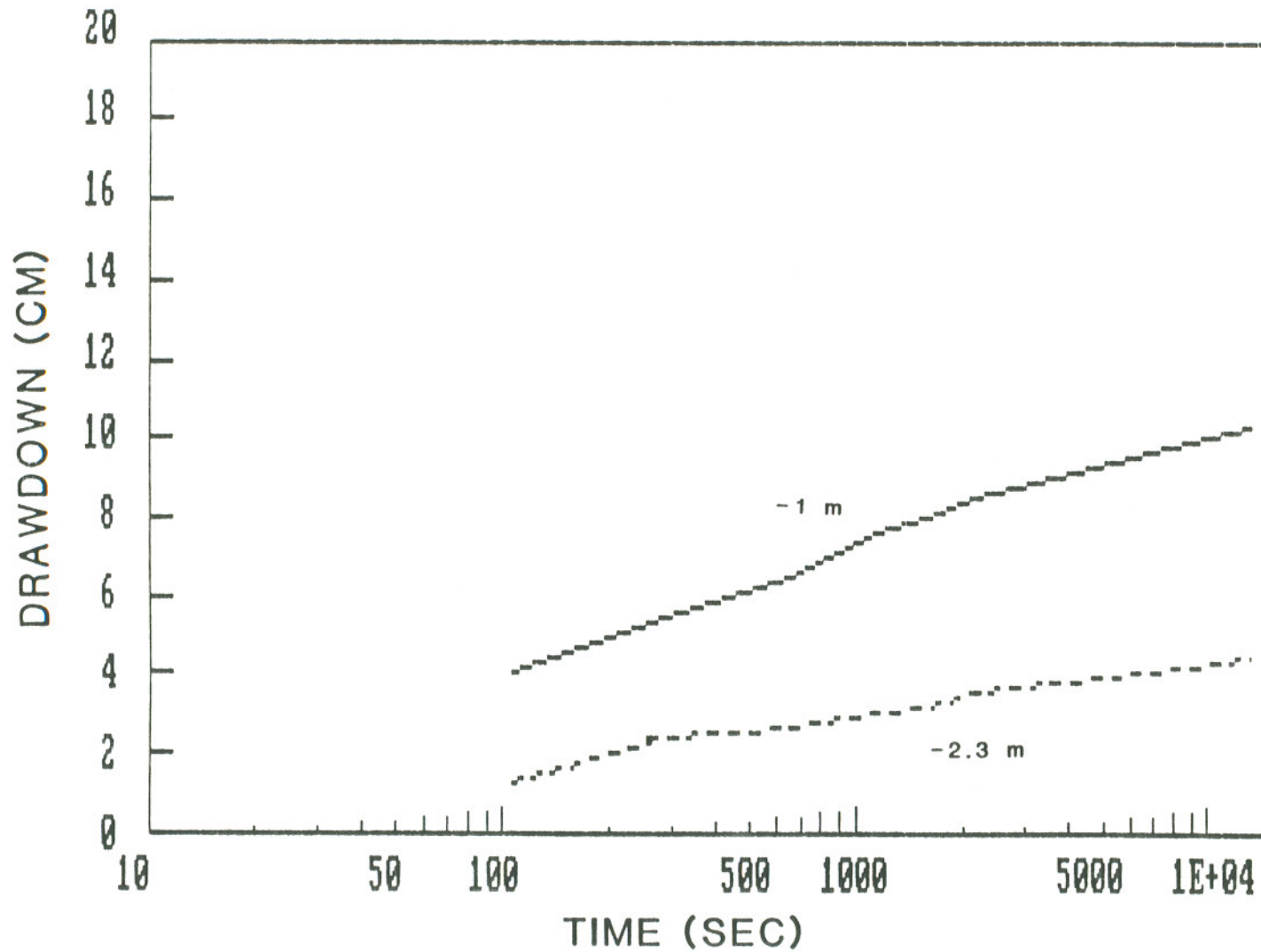


Figure II.F.3 Drawdown (cm) versus time for pumping test T7P (Located near wells 33 and 25, Figure I.D.4.) for piezometers open at approximately 1 and 2.3 m below the water table at 1 m from the pumping well.

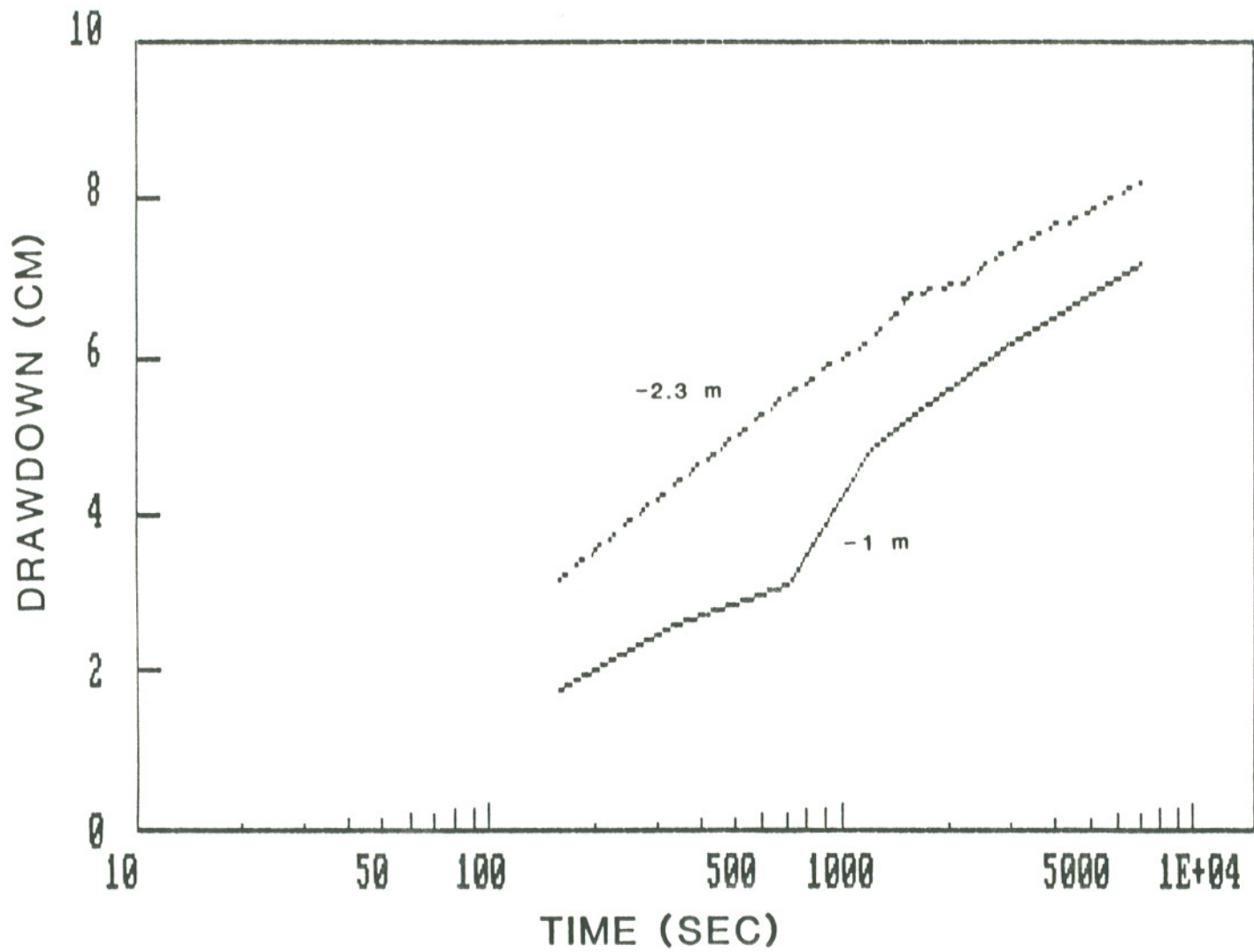


Figure II.F.4 Drawdown (cm) versus time for pumping test T7P (Located near wells 33 and 25, Figure I.D.4.) for piezometers open at approximately 1 and 2.3 m below the water table at 3 m from the pumping well.

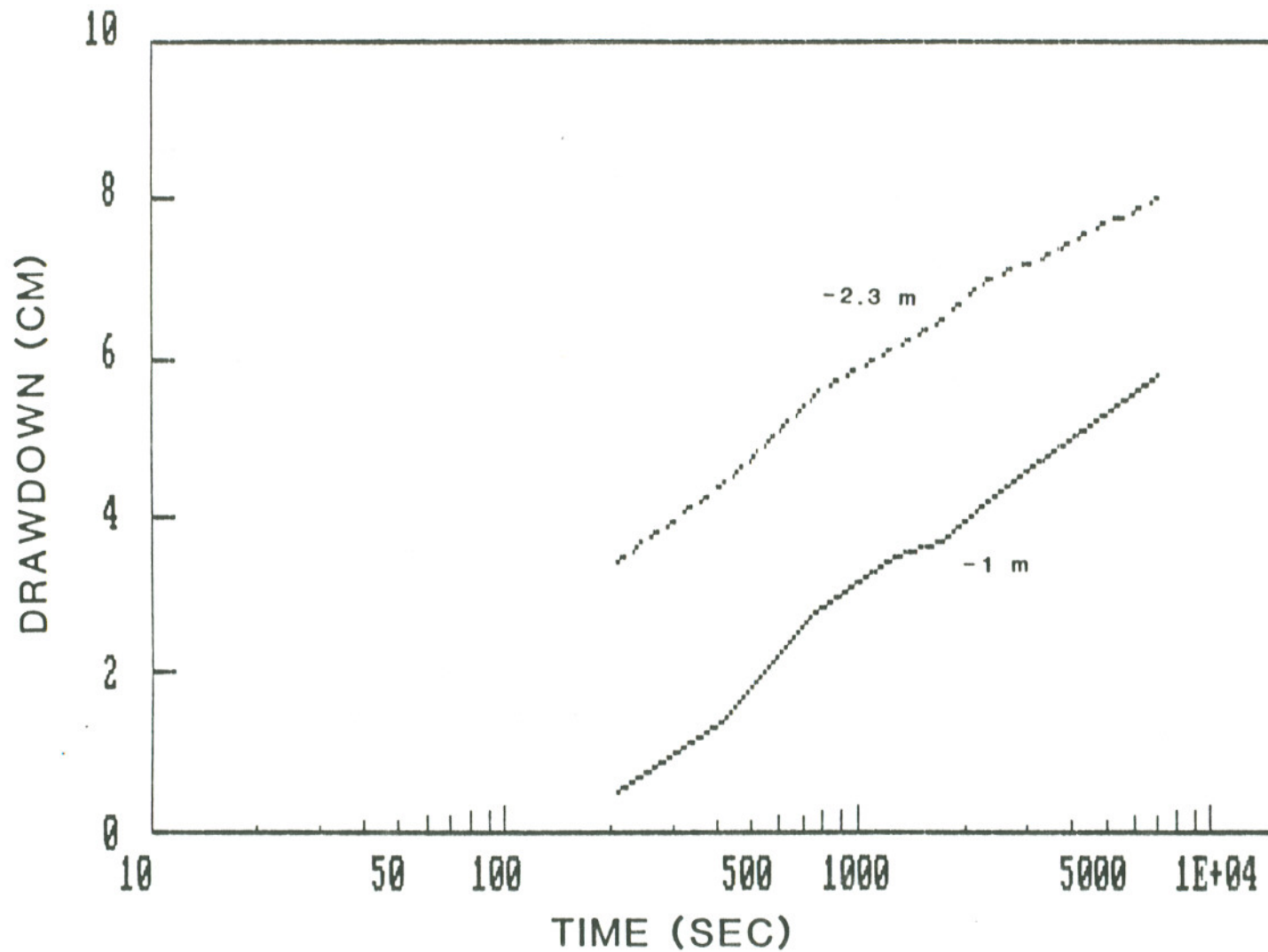


Figure II.F.5 Drawdown (cm) versus time for pumping test T7P (Located near wells 33 and 25, Figure I.D.4.) for piezometers open at approximately 1 and 2.3 m below the water table at 5 m from the pumping well.

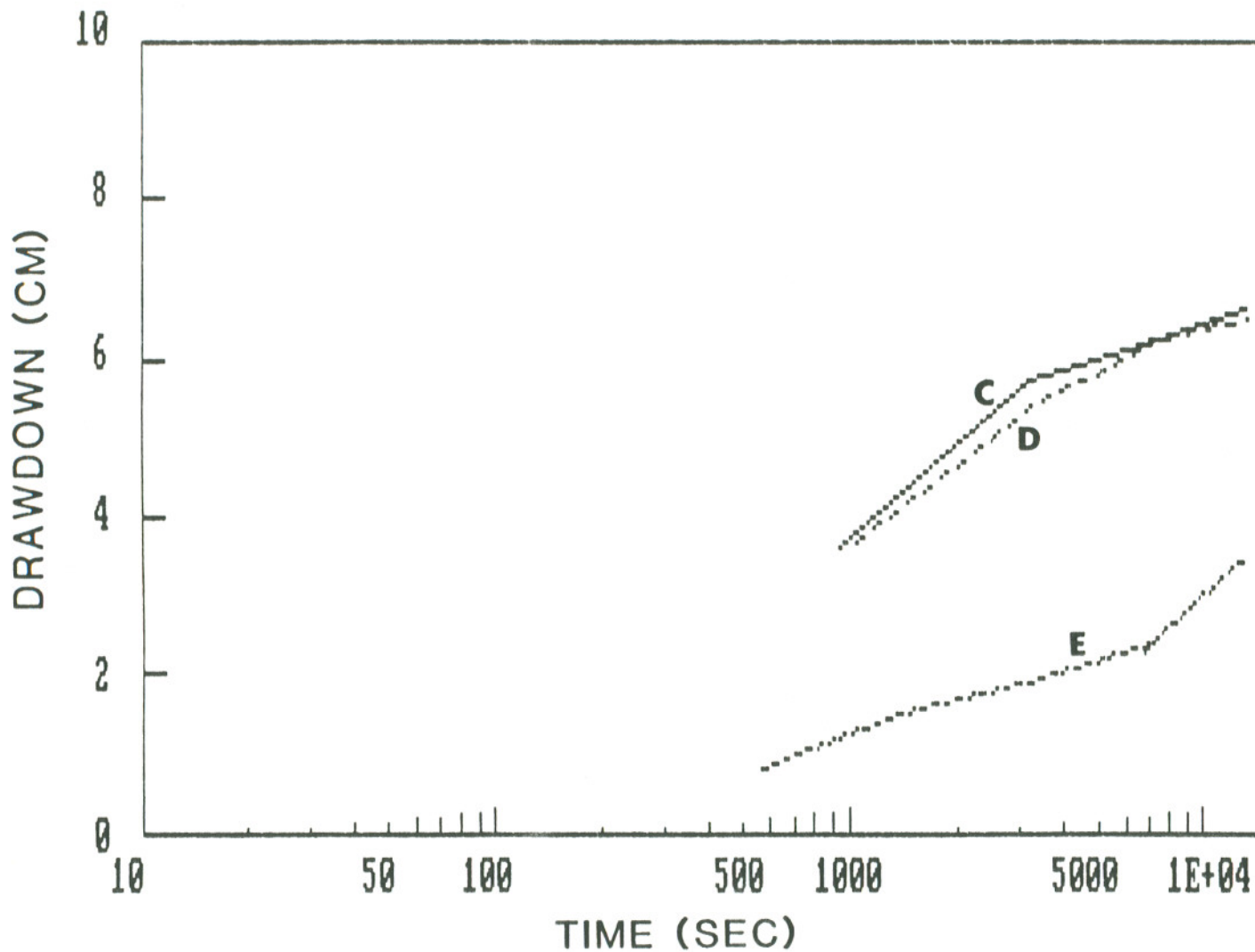


Figure II.F.6 Drawdown (cm) versus time for pumping test T7P (Located near wells 33 and 25, Figure I.D.4.) for piezometers open at approximately 1 m below the water table at 5, 8 and 10 m from the pumping well (piezometers C, D and E, respectively, Figure II.F.1).

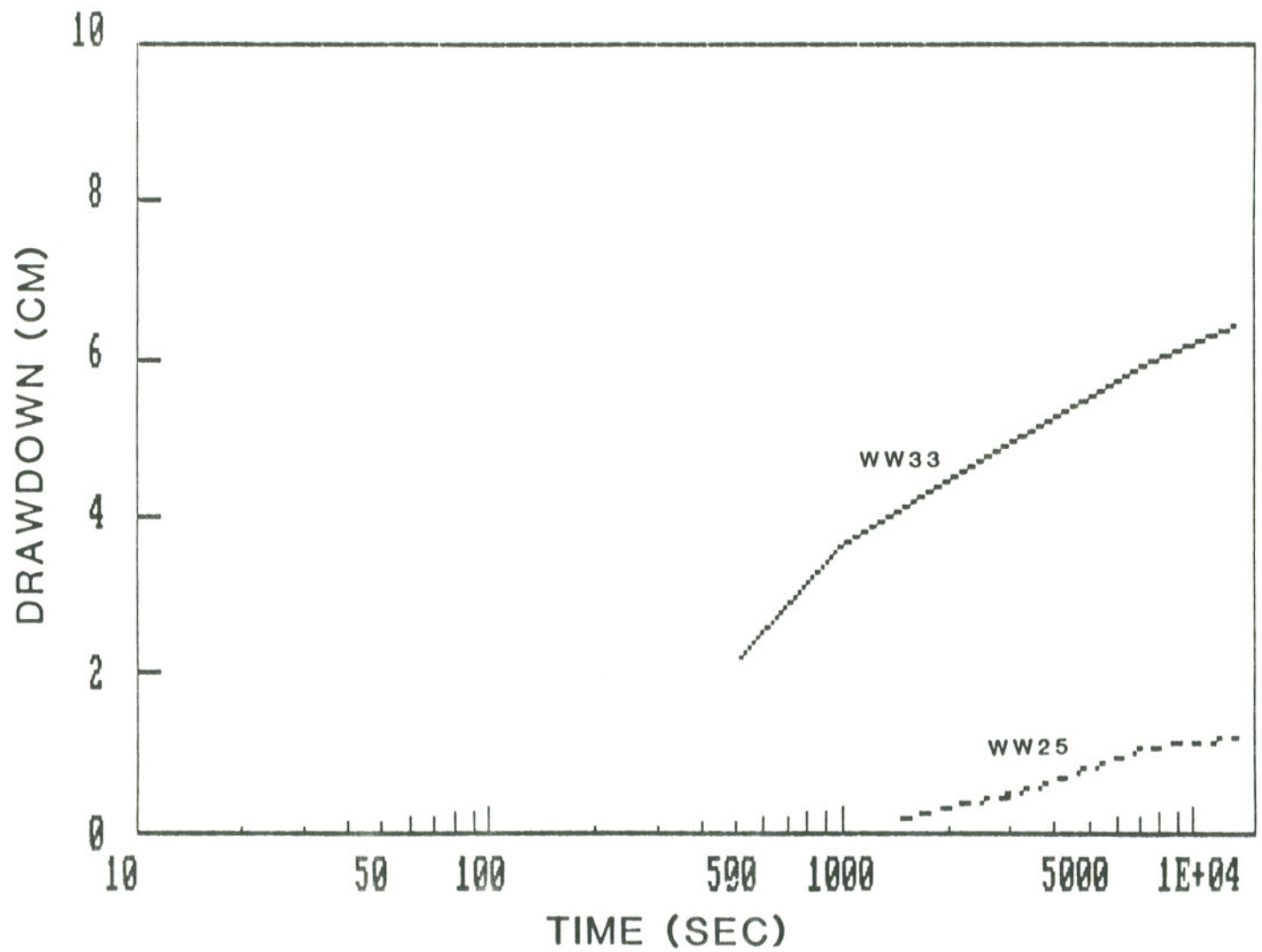


Figure II.F.7 Drawdown (cm) versus time for pumping test T7P for piezometers open from approximately 1 to 3 m below the water table at 10 and 25 m from the pumping well (Wells 33 and 25, respectively, Figure I.D.4).

III. CONTAMINANT DISTRIBUTIONS AT THE ALKALI LAKE CDS

III.A. INTRODUCTION

This section will deal specifically with the quantitative measurement of 2,3,4,6-tetrachlorophenol (TeCP), pentachlorophenol (PCP), and the chlorophenoxyphenols (CPP) in the area immediately downgradient of the Alkali Lake CDS. The emphasis is on this area primarily because the flow of contaminants there is less complex. Within the boundary of the site the physical process of crushing and burying the drums perturbed the aquifer to an unknown extent. In contrast, the area downgradient of the site was undisturbed and was probably free of contaminants at the time of burial. In the following sub-sections: 1) the nature of the waste materials will be discussed; 2) the methods of quantitative analysis will be covered; and 3) the results of mapping of the contaminant plume will be presented.

III.B. THE WASTE MATERIALS

During the period 1960-1970, large quantities of the

herbicide 2,4-D (2,4-dichlorophenoxyacetic acid) were manufactured for use as a defoliant in Vietnam (Young et al., 1978). The 2,4-D was produced by the etherification of 2,4-dichlorophenol (2,4-DCP) and chloroacetic acid. The 2,4-DCP used in this process was manufactured by the direct Cl_2 chlorination of phenol (Figure III.B.1). During the chlorination step, a large number of competing side reactions occurred leading to a variety of unwanted by-products. These included 2,6-dichlorophenol, 2,4,6-trichlorophenol, TeCP, PCP (Figure III.B.2) and the CPP polymerization products. The CPP dimers are also known by the class name "hydroxydiphenyl ethers". The 2,4-DCP was separated from the chlorination process mixture by fractional distillation, leaving behind a concentrated residue of the by-products. These residues, in addition to wastes from the etherification step make up the bulk of the materials disposed of at the Alkali Lake CDS.

An example of the polymerization of chlorophenols to form a CPP dimer is presented in Figure III.B.3. In this example, two 2,4-DCP molecules combine to form a trichlorophenoxyphenol. Because there are a number of different chlorophenols present, and because they can combine in a number of ways, a large number of other CPP dimer isomers are also possible. The polymerization process can continue to form trimers, tetramers, etc. (Figure III.B.3). Pankow et al. (1981) have reported CPP containing up

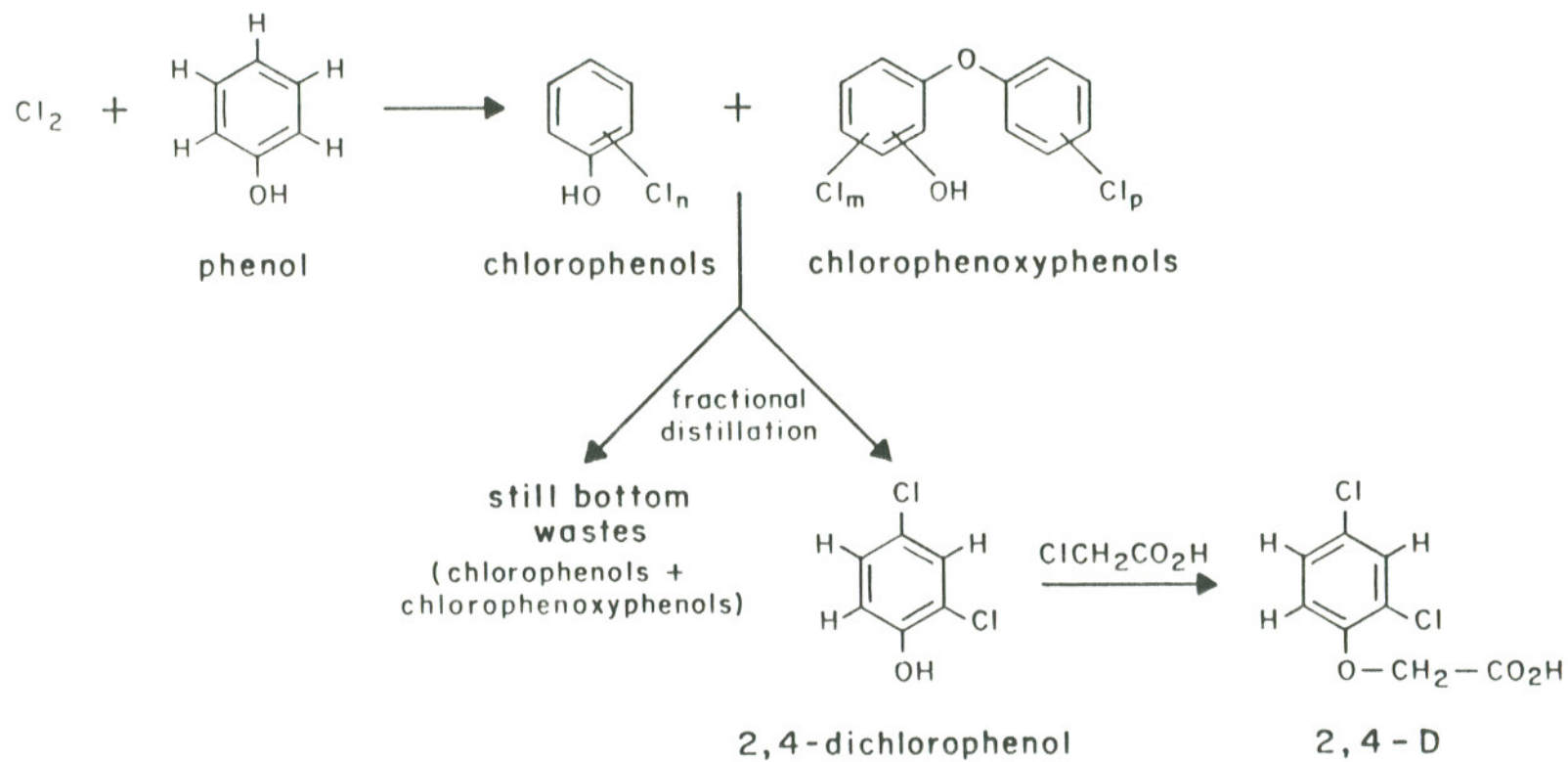
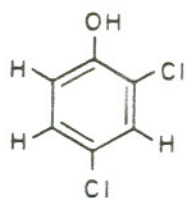
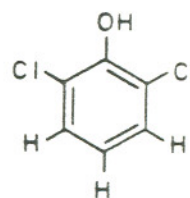


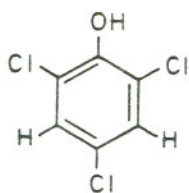
Figure III.B.1 Reaction scheme for the production of 2,4-D from phenol showing the major waste products which result from side reactions.



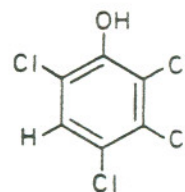
2,4 - DCP
(2,4-dichlorophenol)



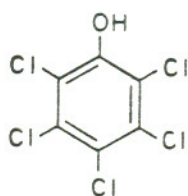
2,6 - DCP
(2,6-dichlorophenol)



2,4,6 - TCP
(2,4,6-trichlorophenol)



TeCP
(2,3,4,6-tetrachlorophenol)



PCP
(pentachlorophenol)

Figure III.B.2 Structures of the chlorophenols found in the materials disposed of at Alkali Lake.

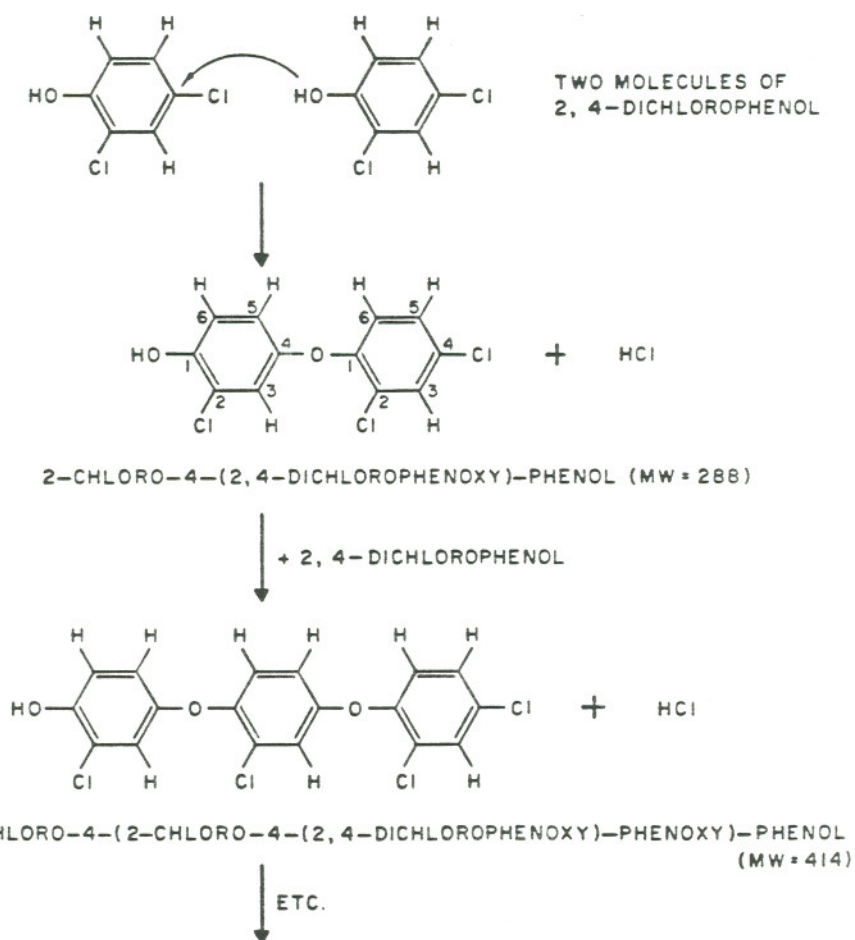


Figure III.B.3 Polymerization of 2,4-DCP molecules to form CPP.

to 5 aromatic rings and with 2 to 7 chlorine atoms in the materials disposed of at Alkali Lake.

III.C. CHEMICAL ANALYSIS

Quantitative determinations of TeCP, PCP and the CPP in samples of Alkali Lake groundwater were at once straightforward and difficult. They were straightforward in that contaminant concentration levels were high enough so that very little sample concentration was necessary to allow detection by capillary column gas chromatography/mass spectrometry (GC/MS). They were difficult for three main reasons: 1) the compounds were found in the presence of very large concentrations of chlorophenols and phenoxy acids; 2) the large number of CPP isomers made separation of many of the individual compounds difficult, even on a capillary column; and 3) there were few standards available for the CPP compounds. The first point led to: a) overloading of the sample concentration cartridge used in sample preparation; and b) serious degradation of the analytical GC column in the course of one day of analyses. Points two and three meant that both exact compound identification and absolute mass determinations of the CPP were not possible. It was, however, possible to select for study a number of the CPP compounds in the mixture which occurred as single component peaks

in the chromatogram. Mass calibration for these compounds was estimated by analysis using capillary gas chromatography with a flame-ionization detector (GC/FID).

The areal distributions of three CPP are reported here. The CPP have been designated as CL2D2, CL3D3 and CL4D2. They are all dimers (hence the "D"), and contain 2,3 and 4 chlorines, respectively. Mass spectra for TeCP, PCP, and the CPP and a sample chromatogram may be found in Appendix D.

III.C.1 SAMPLE COLLECTION

A number of sampling well types were used during the course of this work. Most of the data reported here were for samples collected using the 0.9 cm I.D. (1.4 cm O.D.) samplers (S-series). The probes provided samples whose concentrations represented averages over a ~ 2 m slotted interval. The concentration distribution data presented in Section III.D came from this type of sampler. Samples were withdrawn by vacuum suction. Compound loss due to volatilization during collection was not a problem for TeCP, PCP and the CPP because their vapor pressures are very low at the pH of the groundwater (pH = 10). Samples were collected into amber bottles (40, 125 or 500 mL), stored in the dark, and kept in a cold room upon return to the lab until they were extracted for analysis. Stability studies

have shown that there were no changes in the chlorophenol concentrations during sample storage periods of up to six weeks (Brillante, 1985). All samples were processed in less than that period of time.

III.C.2. SAMPLE PREPARATION AND ANALYSIS

Sample workup was carried out using a special apparatus (Figure III.C.1.) by means of the following steps: 1) 10 mL of sample placed in the apparatus; 2) stirrer activated, pH electrode inserted, and sample acidified to pH 2-3 with 6 N HCl to protonate all organic acid analytes; 3) electrode rinsed with 1-2 mL of organic-free water, then removed; 4) apparatus capped; 5) Sep-Pak C-18 cartridge (Waters Assoc., Milford, MA) placed on the apparatus, and apparatus pressurized to 10 psi with nitrogen gas to obtain a 5 mL/min flow rate; 6) Sep-Pak removed from the apparatus and aspirated for 30 s to remove residual water; 7) organics eluted with 2 mL of methylene chloride, the first drop (residual water) having been discarded; 8) volume reduced to 1.0 mL using a micro Kuderna-Danish/Snyder column in a hot (95°C) water bath); 9) 10 uL of external standard added (1 ng/uL each of chrysene and fluoranthene); 10) concentrate transferred to a pre-cleaned 3.5 mL amber glass vial (Pierce Chemical Co., Rockford, IL); 11) sample stored at 0°C; and 12) GC/MS analysis. For quality assurance (QA), every tenth

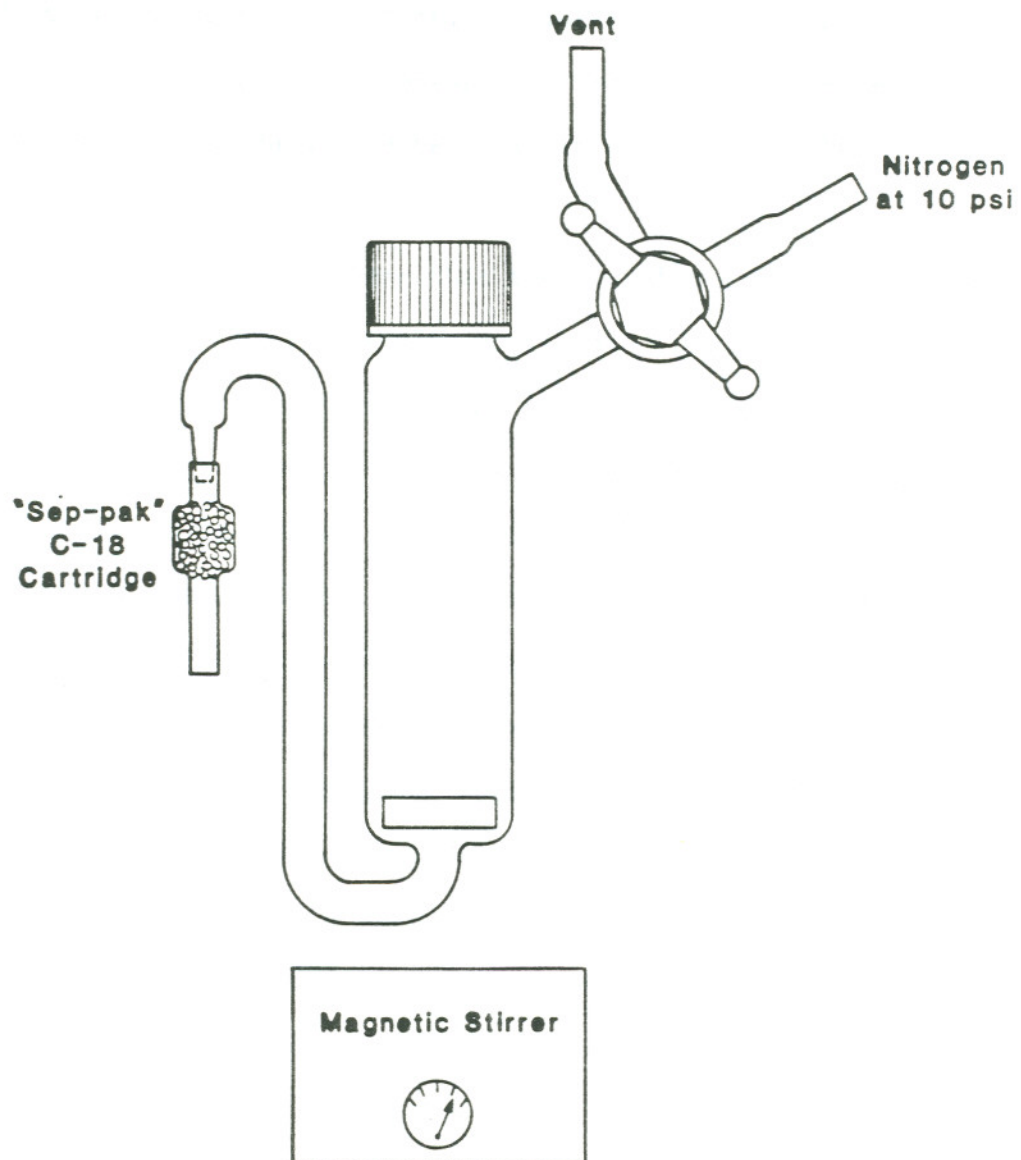


Figure III.C.1 Apparatus used for the separation and concentration of the chlorophenolics in the groundwater from Alkali Lake.

sample was analyzed both in duplicate and spiked with the recovery standards TeCP and 5-chloro-2-(2,4-dichlorophenoxy)-phenol. The chlorophenoxyphenol was obtained as Irgasan DP300 (Ciba-Geigy, Basil, Switzerland). The recovery standards were added to the samples prior to extraction. (Since both compounds may have been present in the samples, they were called recovery standards, rather than internal standards.

It should be noted here that the use of the term "external standard" (ES) in this section is consistent with the definition used in the Master Analytical Scheme (Research Triangle Institute, 1983). That is, an ES is a standard compound which is added to the sample extract just prior to the analytical determination step. (It is "external" to the work-up.) The purpose of the ES is to allow compensations to be made for: 1) changes in instrument response between calibrations; and 2) variation in volume of sample injected into the analytical instrument. An "internal standard" (IS) on the other hand would be a compound added to the sample prior to extraction and used to evaluate the recovery efficiency of the extraction process. (It is "internal" to the work-up.)

Analyses were carried out by injection of 1.0 uL of the extract using an on-column injector mounted in an HP 5790 GC interfaced to a Finnigan GC/MS/DS (Pankow and Isabelle, 1984).

The column used was a 30 m, 0.25 mm I.D., 0.25 μ m film thickness DB-5 (SE-54) fused silica capillary column (J&W Scientific, Rancho Cordova, CA.). The transfer line, source and MS manifold temperatures were maintained at 225, 225, and 100 $^{\circ}$ C, respectively. The carrier gas linear velocity used was 30 cm/s (at ambient temperature). The on-column injections were carried out with the oven at 80 $^{\circ}$ C. After injection the GC was immediately temperature programmed at 10 $^{\circ}$ C/min to 300 $^{\circ}$ C. The analytes were detected using multiple ion detection (MID or "selected ion monitoring"). The ions monitored for each of the compounds were: TeCP (131,232,234); PCP (266,268); CL2D2 (184,252,254); chrysene (202,101); CL3D3 (225,254,288,290); CL4D2 (146,322,324); and fluoranthene (228,114).

The presence of PCP and TeCP in the samples was confirmed by comparison of the GC retention times and the mass spectra with those of reference compounds. (The latter were obtained from Chem Services, Inc., West Chester, PA and Ultra Scientific, Inc., Hope, RI, respectively.) Specific structures for the chlorophenoxyphenols found at the site were not determined because adequate reference compounds were not available.

TeCP and PCP concentrations in the sample extracts were determined by comparison of peak areas to those obtained with standards of known TeCP and PCP concentrations. Standard

solutions were prepared in a series of concentrations which bracketed the range of sample concentrations. These standards also contained the external standard compounds, and allowed a determination of the absolute amounts of TeCP and PCP in each sample extract. This procedure could not be used for the CPP because, as noted above, adequate CPP reference compounds do not exist. It was possible, however, to determine the concentrations of the CPP in the extracts relative to a "standard sample". The standard sample selected was collected from Well 8 (Figure I.A.4) on 14 September 1982. 200 mL of this sample was extracted shortly after collection and the extract stored at 0°C to protect against degradation. Several vials of the extract were prepared. 10- and 100-fold dilutions of the standard sample extract were also prepared and stored at 0°C. This range of extract concentrations bracketed the downgradient sample extract concentrations. The standard sample extracts all contained the ES compounds, and were used in quantitation in the same manner as the TeCP and PCP standard solutions.

The measurement of transport distances of the chlorophenolics (Section III.D) was made using relative concentrations of the ambient samples, rather than absolute concentrations, and thus absolute mass calibration was not necessary. Nevertheless, in order to better estimate the impact of the CDS, the absolute concentrations of the CPP were estimated

in the standard sample, and thereby in all samples. To accomplish this, the standard sample was analyzed several times using GC/FID. An HP 5700 GC with an on-column injector and the same column used in the GC/MS/DS analyses was used. The assumption was made that all of the compounds gave the same response per carbon atom in the FID. The mass of carbon associated with each compound was then divided by the weight percent carbon of each compound to give the estimated mass of each compound per unit volume of the standard. The response factors used in mass estimations were derived from the GC/FID analysis of a standard solution of the CPP compound Irgasan DP300.

A formal error propagation analysis has not been carried out for the analytical quantitation work reported here because it is believed that the dominant source of uncertainty is sample collection error, which has not been determined. The quantitative analysis procedure outlined in Section III.C.2 ensured that uncertainties in the analytical procedure were less than +/- 20%. Spatial variability, particularly as a function of depth for the CPP could probably have resulted in an error several times that large, and make the analytical uncertainties small by comparison. Fortunately, as seen in the next section, the concentrations of the contaminants decrease by a factor of 100 or more as one moves away from the CDS, and so even the

uncertainty introduced by sampling variability does not seriously interfere with the characterization of the contaminant distributions at the site.

III.D CONTAMINANT DISTRIBUTIONS

The purpose of this section is to describe the current distributions of the chlorophenolics within and downgradient of the Alkali Lake CDS. This data will be used in subsequent sections to estimate the input parameters to be used in modeling the site. Primary effort has been given to characterizing the areal distributions of the contaminants at the site, rather than the vertical. This was because there appeared to be very little vertical movement (advection or dispersion) compared to the scale of longitudinal transport. This was probably due to both: a) the horizontal nature of the fractures; and b) the decrease in the hydraulic conductivity with depth. Transverse dispersion appears to be limited by the local geography and geology.

The areal distributions of eight chlorophenolic compounds are reported here (Figures III.D.1-8). These distributions delineate the extent of the contamination as of April 1984. The distributions of 2,4-dichlorophenol (2,4-DCP), 2,6-dichlorophenol (2,6-DCP), and 2,4,6-trichlorophenol (2,4,6-TCP) were determined

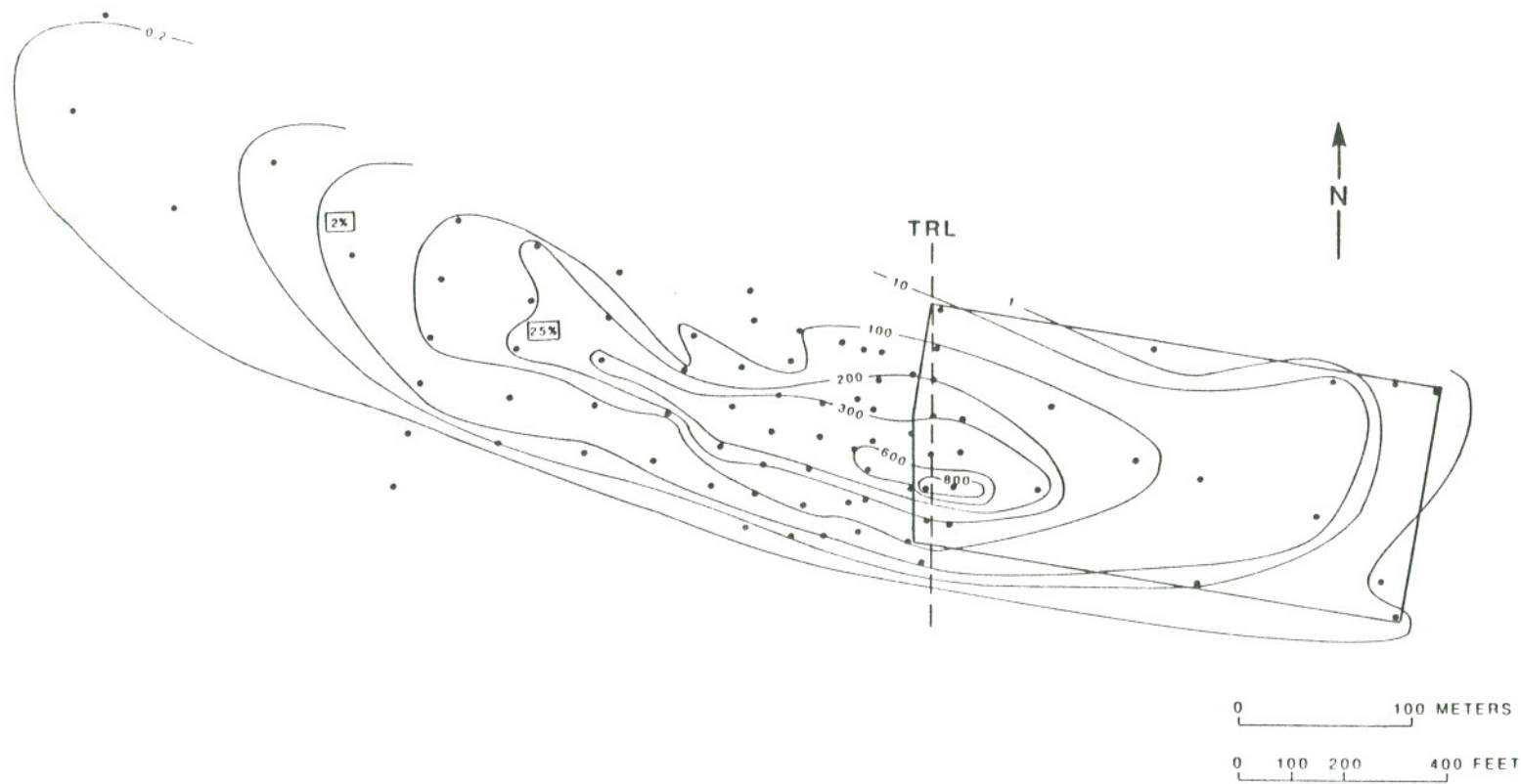


Figure III.D.1 Concentration contours for 2,4-DCP (in ppm) in the vicinity of the Alkali Lake CDS as of April 1984. (from Johnson et al., 1985)

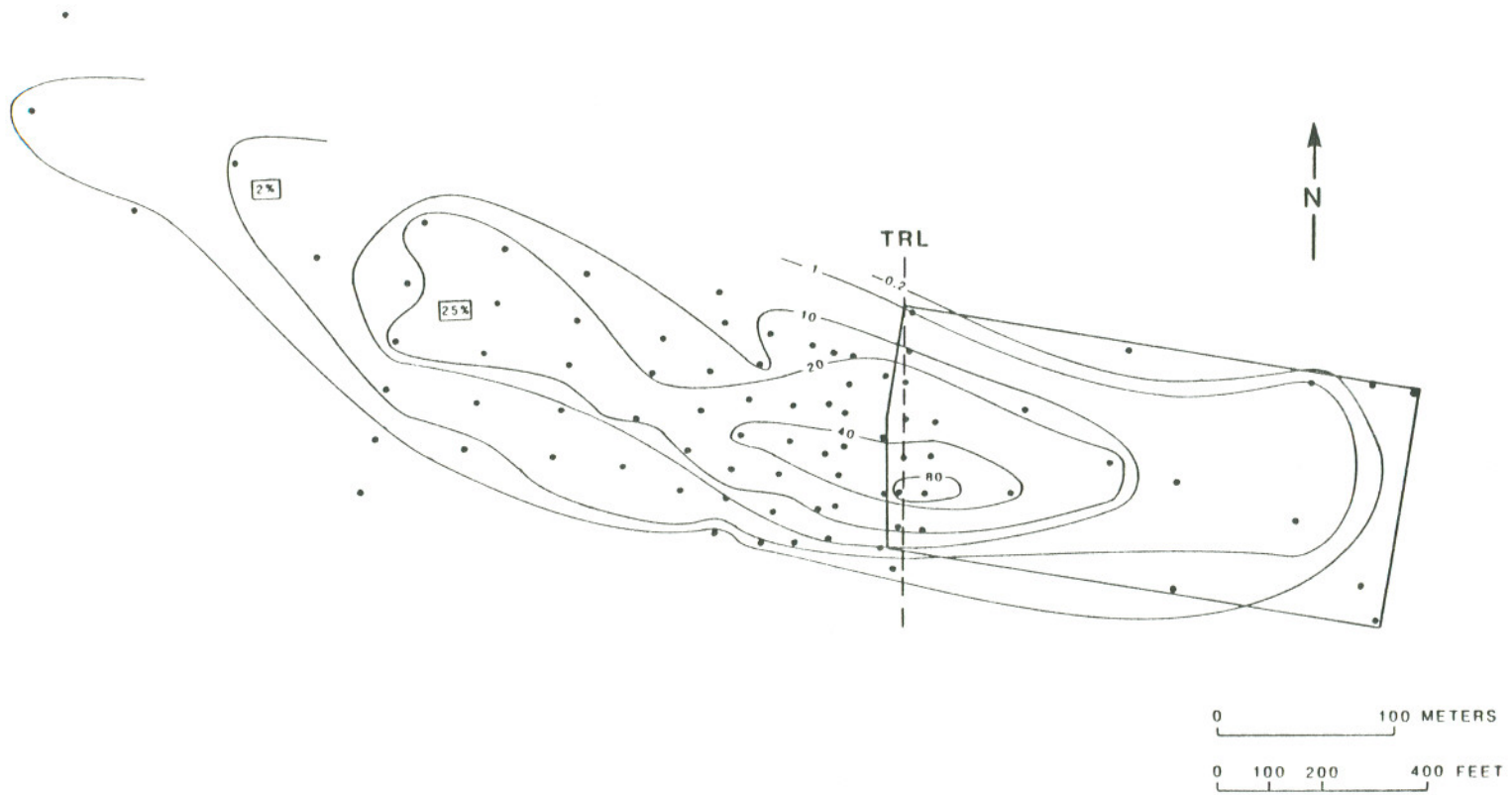


Figure III.D.2 Concentration contours for 2,6-DCP (in ppm) in the vicinity of the Alkali Lake CDS as of April 1984. (from Johnson et al., 1985).

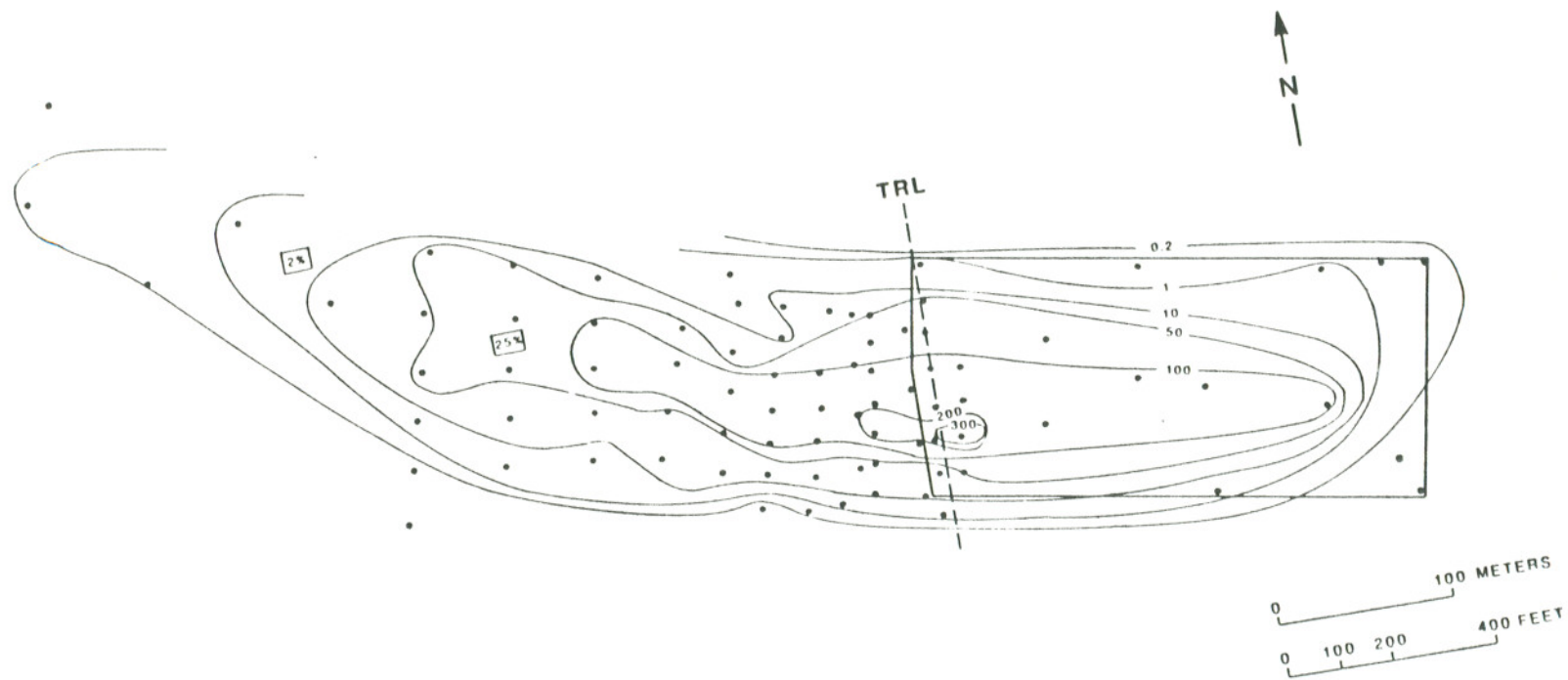


Figure III.D.3 Concentration contours for 2,4,6-TCP (in ppm) in the vicinity of the Alkali Lake CDS as of April 1984. (from Johnson et al., 1985)

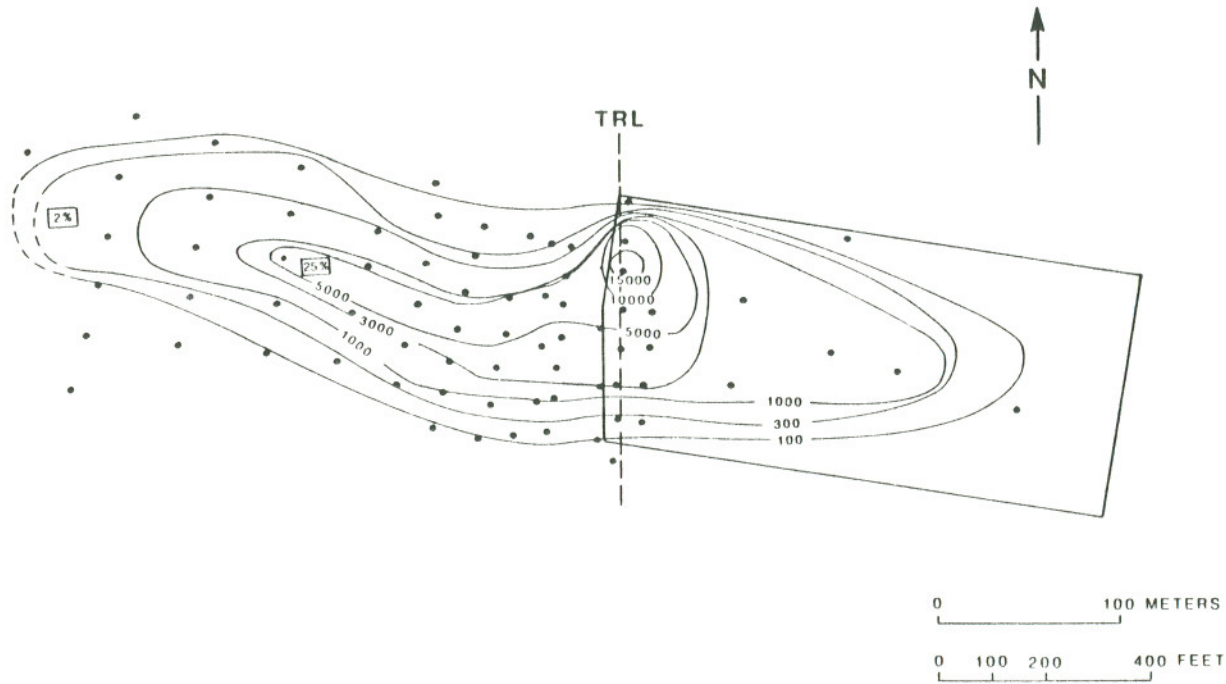


Figure III.D.4 Concentration contours for TeCP (in ppb) in the vicinity of the Alkali Lake CDS as of April 1984.

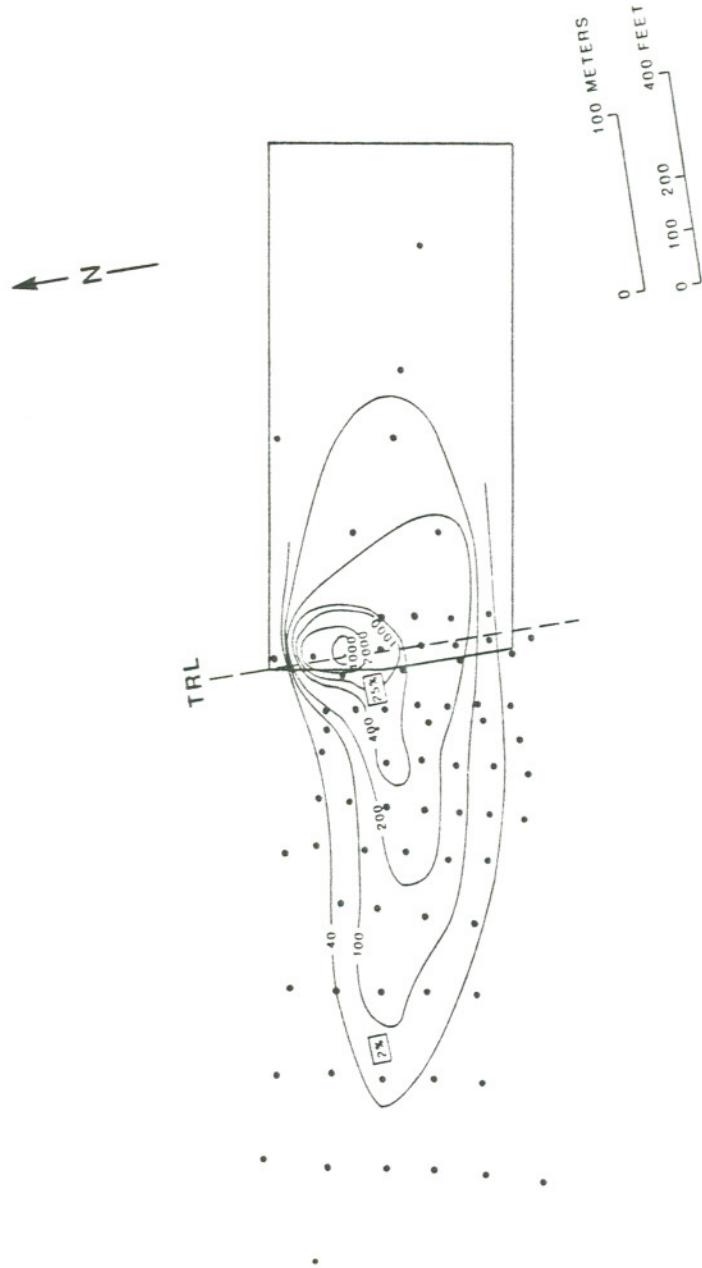


Figure III.D.5 Concentration contours for PCP (in ppb) in the vicinity of the Alkali Lake CDS as of April 1984.

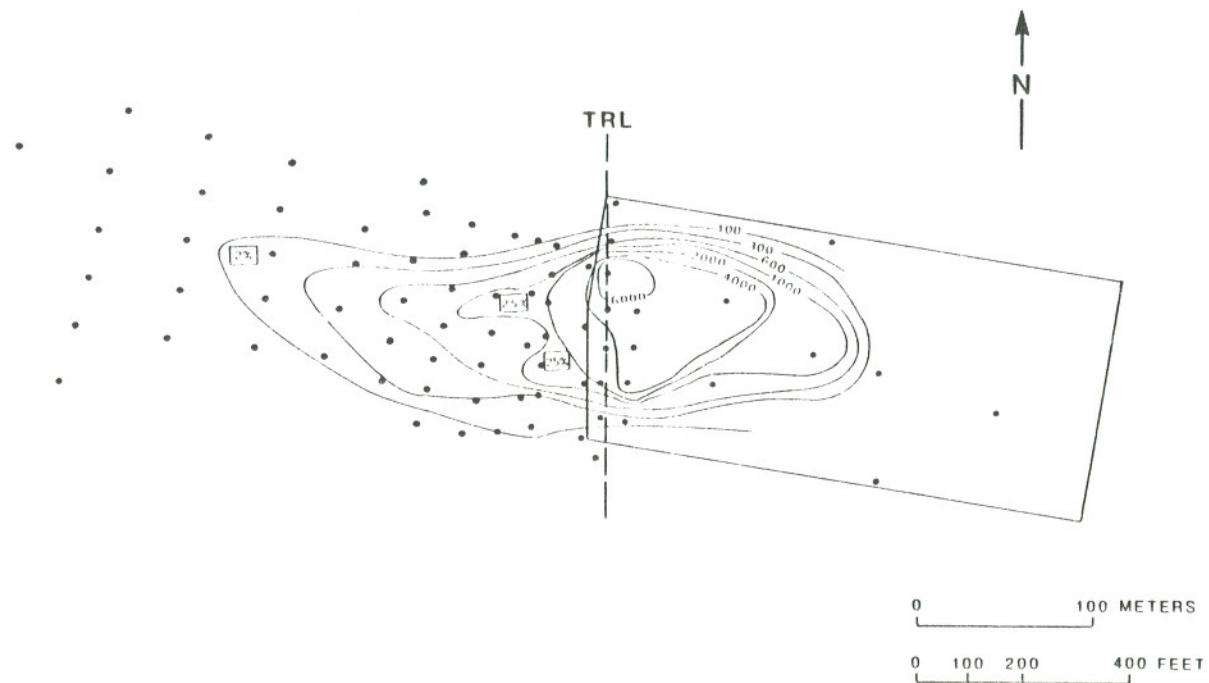


Figure III.D.6 Concentration contours for CL2D2 (in ppb) in the vicinity of the Alkali Lake CDS as of April 1984.

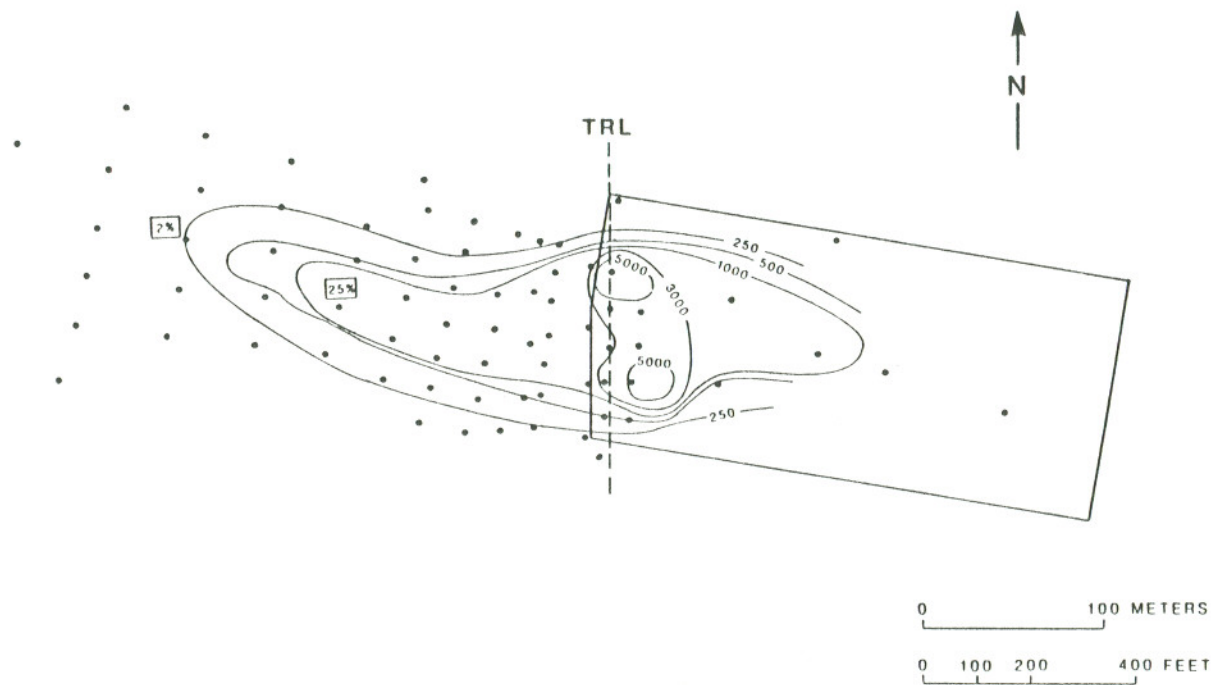


Figure III.D.7 Concentration contours for CL3D3 (in ppb) in the vicinity of the Alkali Lake CDS as of April 1984.

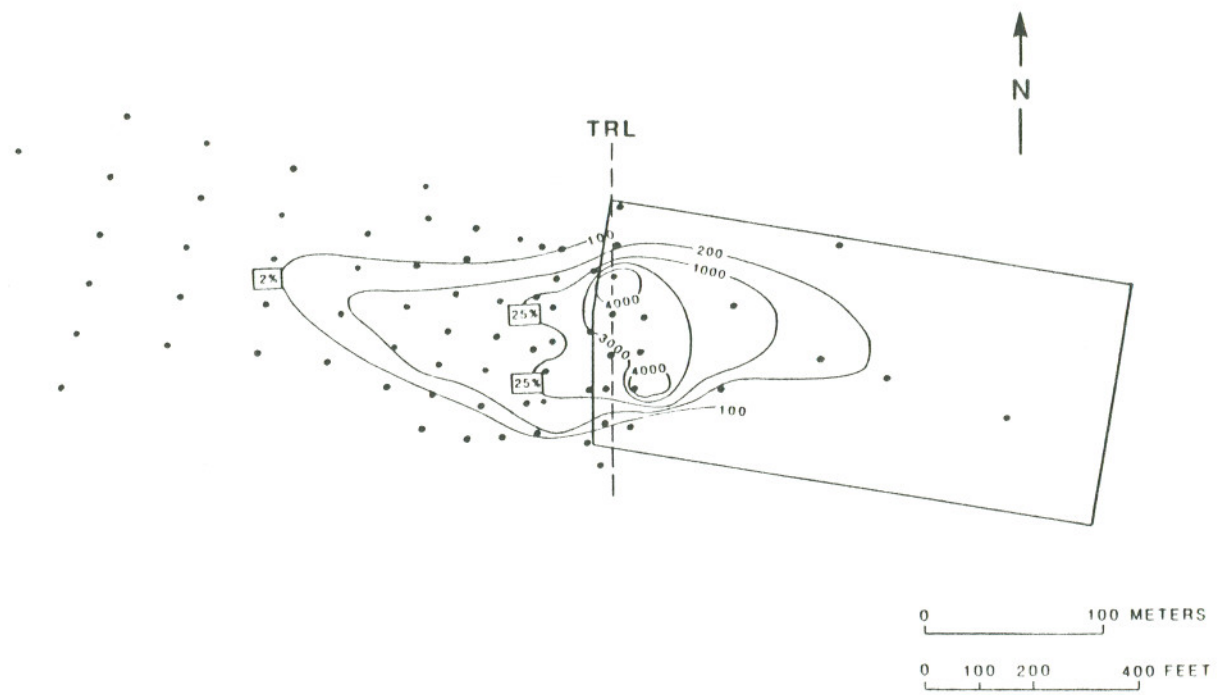


Figure III.D.8 Concentration contours for CL4D2 (in ppb) in the vicinity of the Alkali Lake CDS as of April 1984.

by Brillante (1985), and have appeared elsewhere (Johnson et al., 1985, see Appendix B.). They have been included in this work for comparison with the distributions of the higher molecular weight compounds obtained for this thesis. The latter compounds include 2,3,4,6-TeCP, PCP, and the CPP compounds designated CL2D2, CL3D3, and CL4D2.

The distributions of 2,4-DCP, 2,6-DCP and 2,4,6-TCP display almost identical patterns. This implies that these chlorophenols: 1) have similar source functions; 2) have been subject to the same hydrology; and 3) have experienced similar degrees of sorption or lack thereof. Based on the pH of the groundwater (approximately 10), the acidity of these compounds, and their low molecular weights, one could predict that sorption would be similarly unimportant for all three. Because the sampling network used was fairly extensive and the analytical precision for these compounds was quite good (relative standard deviation 5%), it is possible to infer areas of decreased hydraulic conductivity to the north and south of the plume which control the shape of the contaminant plume (Johnson et al., 1985).

Due to the larger relative standard deviations for the low ($\mu\text{g}/\text{l}$) level determinations of TeCP, PCP and the CPP (14-20%) it was not possible to draw the concentration contours of these

compounds (Figures III.D.4-8) with the same degree of detail present in the 2,4-DCP, 2,6-DCP and 2,4,6-TCP contours. Nevertheless, the general patterns of contamination for the TeCP, PCP and the CPPs were similar to those of the di- and trichlorophenols, though the concentrations were approximately 100 times lower. Minimum detectable concentrations were an order of magnitude below the lowest values reported.

The true north-south line which passes through the northwest corner of the site was selected as the uniform transport reference line (TRL) from which to measure transport distances. This line, marked on the figures, was selected because it: 1) corresponds roughly to the best line drawn through the points of maximum concentration for the eight compounds studied; and 2) represents a line nearly orthogonal to the direction of groundwater flow at that point.

For each compound, the point selected as the reference point for the measurement of transport distances is the point at which the concentration of the compound is at a maximum on the TRL. In Figures III.D.1-8, boxes are used to mark the points (as positioned on the line of shallowest rate of descent, i.e., approximate plume centerline for each compound) at which the concentration drops to 2% and 25% of the reference point value. It would be physically more meaningful to use the point at which

the concentration is 50% of the reference value, as this point is more directly related to the average velocity of the contaminant. (Dispersion causes the leading edge of the contaminant front to travel faster than the average velocity). Because of the discrete nature of the sampling network and the uncertainty in assigning the position of the transport reference line, this would have introduced excessive errors in estimating transport distances. (As will be discussed in Section V.E., the apparent retardation of the sorbed compounds is artificially reduced by from 9 to 45% by using the 2% and 25% concentration front distances instead of the 50% distance.)

The 2% and 25% transport distances in April 1984 are listed in Table III.D.1. The transport distances for TeCP, PCP and the CPP are shorter than those for the di- and trichlorophenols. This is primarily the result of sorption of the TeCP, PCP and the CPP compounds.

It has not been possible to observe changes in the distributions of the contaminants with time over the years 1981-1984. The contaminant concentrations observed at the "ODEQ-type" wells during this period do not demonstrate any trends with time (Brillante, 1985). It is hoped that the S-series sampling network installed at the end of this period, and the data reported here will provide the basis for observing

TABLE III.D.1. TRANSPORT DISTANCES OF THE CHLOROPHENOLICS

COMPOUND	X(2%) (in m)	X(25%) (in m)
2,4-DCP	400.	250.
2,6-DCP	420.	270.
2,4,6-TCP	400.	270.
TeCP	330.	210.
PCP	260.	40.
CL2D2	230.	70.
CL3D3	280.	150.
CL4D2	210.	40.

changes in the contaminant distributions in the future.

III.E PARTITION COEFFICIENT (K_p) DETERMINATIONS

III.E.1 EXPERIMENTAL

Batch equilibrium experiments to determine K_p for the chlorophenolics were carried out using samples of contaminated water and uncontaminated soil taken from the site. The water was collected at Well 38 (Figure I.D.4), and spiked with naphthalene (12 mg/L) as a control compound. The soil was from the same composite examined in the SOC analyses. Dry soil (2 g) was mixed in a 35 mL glass vial with 20 mL of contaminated water. The samples were rotated end-over-end at $20 \pm 3^\circ\text{C}$ for 24 hours (30 inversions/min). After equilibration, each sample was centrifuged at 1200 rpm for 10 min. 12-15 mL of the supernatant were decanted into a 20 mL syringe, forced through a glass fiber prefilter followed by a silver membrane filter (Selas Corp., Huntingdon Valley, PA). 10 mL of filtrate were then processed as described in Section III.C.2.

Determinations were made at two different contaminant levels: 1) the concentrations represented by Well 38 water; and 2) Well 38 water concentrations divided by 10 (a 9:1 mixture of

Well 2 water: Well 38 water). Each of the experiments was run in triplicate. In addition, a set of three samples at the lower concentration were equilibrated with an additional 500 ppm 2,4-dichlorophenol. This was done because the di- and trichlorophenols were found at the site at approximately that level, and it was felt that at these concentrations they might affect the sorption of the other chlorophenolic materials.

III.E.2 RESULTS

The presence of the additional dichlorophenol was found to not effect sorption. The results from all of the batch experiments were therefore averaged. K_p values for the chlorophenolics ranged from 0 to 28 (Table III.E.1). The inclusion of the control compound naphthalene in the experiments permitted an independent measure of the SOC content of the soil. Based on the literature value of organic carbon partition coefficient (K_{oc}) for naphthalene of 870 (Karickhoff, 1981), and on the partition coefficient of $16. \pm 2$. measured by batch experiments in this work, an SOC content of $1.8 \pm 0.5\%$ may be calculated for 9 replicates.

TABLE III.E.1 PARTITION COEFFICIENT (K_p)^a DATA
FOR THE CHLOROPHENOLICS

2,4-DCP	0.0+/-0.5
2,6-DCP	0.0+/-0.5
2,4,6-TCP	0.0+/-0.5
TeCP	1.8+/-1.0
PCP	9.0+/-1.8
CL2D2	24.+/-5.
CL3D3	14.+/-3.
CL4D2	28.+/-5.

^a Determined at pH = 10, temperature = 20+/-3°C.

IV. TRACER TESTS

This section describes the field tracer experiments carried out at Alkali Lake to characterize the important physical parameters (advective velocity, diffusion, dispersion, etc.) which control contaminant transport at the site. Three types of tracer tests will be discussed. The first, a natural gradient tracer test, gave an estimate of average velocity and overall dispersion (dispersion plus matrix diffusion) for the aquifer. Two other types of pumping tracer tests were designed to investigate the properties of the fracture system, specifically the average fracture aperture and the matrix diffusion coefficient.

Unlike flow through porous media, the velocity of non-sorbing contaminants in fractured porous systems often cannot be estimated directly via Darcy's Law. Diffusion of the contaminants from the fractures into the surrounding matrix retards solute transport relative to the water velocity in the fractures. To understand contaminant transport in such systems it is necessary to have some estimate of the: 1) size distribution of the fracture apertures; 2) distances between the

fractures; 3) water velocities in the fractures; and 4) diffusion coefficients for the contaminants in the matrix.

The distances between fractures can often be observed from cores of the aquifer material. Fracture apertures, however, often cannot be measured directly and must be estimated by some indirect means. The two types of pumping tracer tests employed were chosen to provide such estimates. These tests were also used to estimate the mean matrix diffusion coefficient. In addition, as will be seen in Section V., the fracture water velocity can be estimated from the solution of the Navier-Stokes equation if fracture aperture and hydraulic head values are known. Thus, the pumping tracer tests can be used to estimate three important parameters for describing contaminant transport in fractures: fracture aperture, matrix diffusion coefficient and fracture water velocity.

IV.A THE NATURAL GRADIENT TRACER TEST

IV.A.1 EXPERIMENTAL

In March 1983 approximately 5 grams of fluorescein dye in 20 L of water were injected into the ground approximately 300 m west of the Alkali Lake CDS. The purpose of this experiment was

fractures; 3) water velocities in the fractures; and 4) diffusion coefficients for the contaminants in the matrix.

The distances between fractures can often be observed from cores of the aquifer material. Fracture apertures, however, often cannot be measured directly and must be estimated by some indirect means. The two types of pumping tracer tests employed were chosen to provide such estimates. These tests were also used to estimate the mean matrix diffusion coefficient. In addition, as will be seen in Section V., the fracture water velocity can be estimated from the solution of the Navier-Stokes equation if fracture aperture and hydraulic head values are known. Thus, the pumping tracer tests can be used to estimate three important parameters for describing contaminant transport in fractures: fracture aperture, matrix diffusion coefficient and fracture water velocity.

IV.A THE NATURAL GRADIENT TRACER TEST

IV.A.1 EXPERIMENTAL

In March 1983 approximately 5 grams of fluorescein dye in 20 L of water were injected into the ground approximately 300 m west of the Alkali Lake CDS. The purpose of this experiment was

to estimate the average groundwater velocity and dispersion of the tracer by observing its movement in the groundwater under the effect of the natural hydraulic gradient. A network of 0.64 cm O.D. stainless steel sampling probes was inserted into the ground in a roughly radial pattern at increasing distances of 1-3 m over approximately 75 degrees of arc (Figure IV.A.1). The position of the injection well in relation to the CDS is identified as SW1 on Figure II.B.2. The injection was made into the top three meters of the water table, and samples were collected at depths between 1 and 2 m below the water table.

Fluorescein Tracer Analysis Procedure

Fluorescein analysis was by laser induced fluorescence (LIF). A block diagram of the analysis apparatus is presented in Figure IV.A.2. The analysis procedure was : 1) sample diluted by 1:10 or 1:100 with a 25 mM Na_2HPO_4 solution buffered to pH=7 and placed in a 40 mL vial; 2) vial placed in the sample holder; and 3) fluorescence signal recorded. The purpose of dilution was two-fold. First, it ensured that the signal was in the linear portion of the calibration curve, and second it minimized the effect of absorption of fluoresced light by phenolic contaminants in the sample.

Calibration of the LIF system was accomplished with a

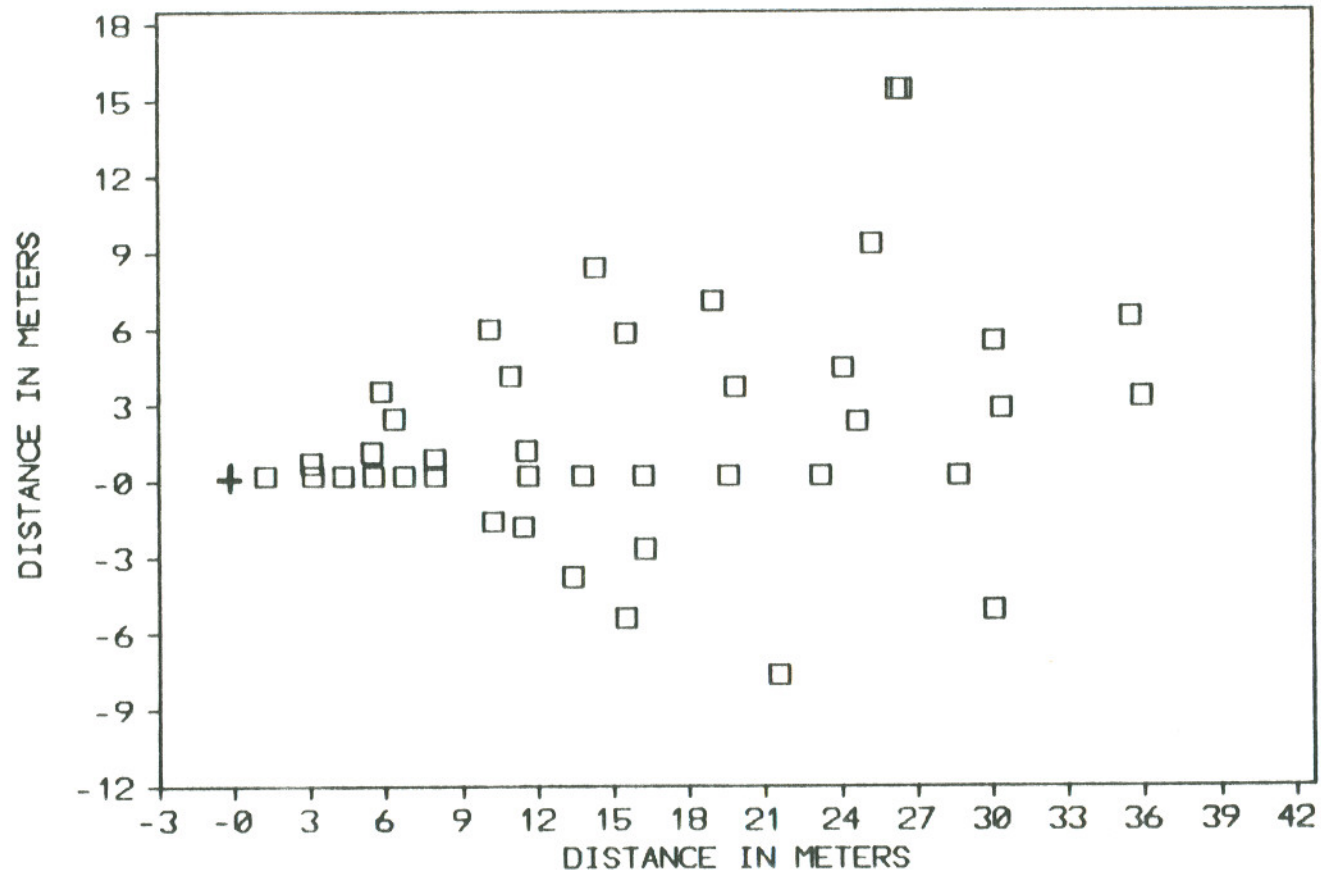


Figure IV.A.1 Map showing the locations of the source well and sampling points for the natural gradient tracer test.

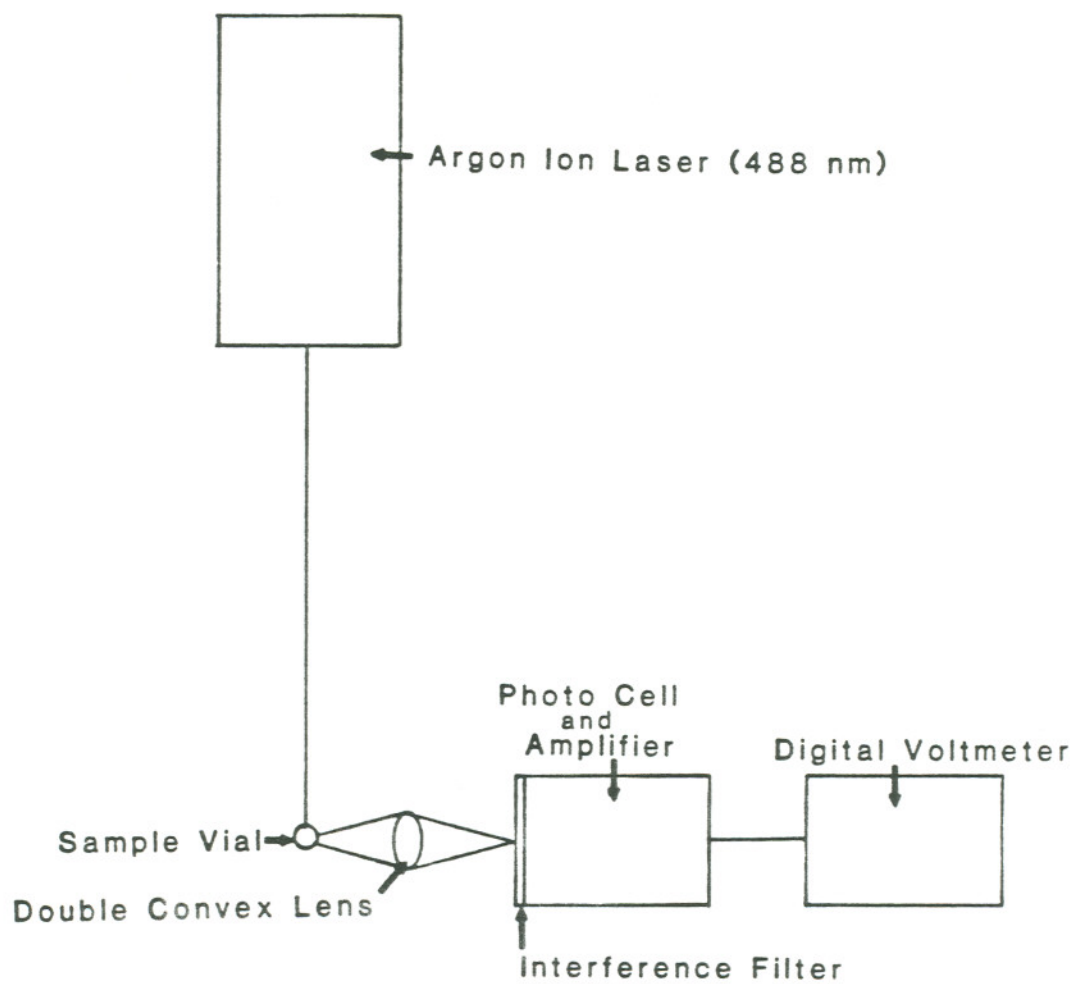


Figure IV.A.2 Block diagram of the laser induced fluorescence system used for fluorescein detection.

series of buffered fluorescein standards spanning the concentration range 10^{-9} - 10^{-5} M. Figure IV.A.3 contains a typical calibration curve. Above a concentration of 10^{-6} M self-absorption by the fluorescein became important, and the calibration curve was non-linear. The effects of the chlorophenolic compounds on fluorescence can also be seen in Figure IV.A.3. A series of standards was prepared using undiluted groundwater from Well 9. The reduced signal from these standards was the result of absorption of the fluorescence of the fluorescein by the contaminants in the groundwater.

Sodium iodide was also injected at the same time as the fluorescein. All of the iodide appears to have been oxidized to iodine and lost from the system. No iodide could be detected after one year.

IV.A.2 RESULTS

Samples were collected from the probes three times in the first two months. Results from these samplings suggested that the physical act of sampling might have influenced the spread of the tracer. At that point, sampling was therefore discontinued until November 1983. The probes located in the center of the plume were then re-sampled, and additional probes were installed at greater distances from the injection point in an attempt to keep

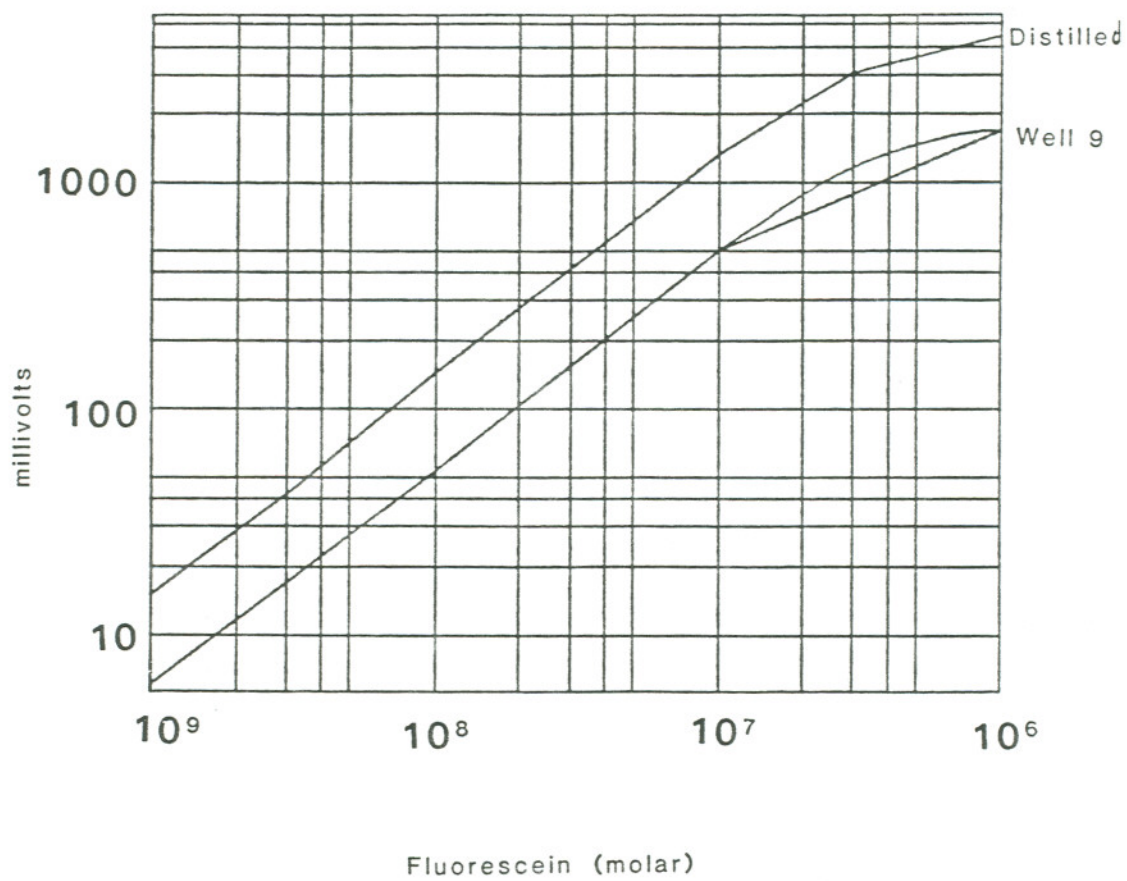


Figure IV.A.3 Typical calibration curve for the LIF procedure used for the fluorescein analyses.

pace with the leading edge of the tracer plume. All of the probes were sampled again in April 1984. The distribution of tracer from the source is presented in Figure IV.A.4. For the April 1984 samples a very rough mass balance was attempted on the fluorescein. A total of approximately 1.6 grams was accounted for within the area defined by the contours. This corresponded to 24% of the injected mass. This analysis assumed a bulk soil porosity of 0.65. The procedure used was to integrate the area contained within each of the contours and assume the plume was a constant 3 m thick (i.e. no vertical dispersion). By making these assumptions some of the mass of the dye was missed, either because of vertical dispersion or because it occurred outside of the $2 \times 10^{-9} \text{M}$ concentration contour. There may also have been losses due to degradation. The uncertainty in the mass balance procedure was probably +100%/-50%. In spite of this, it was possible to characterize the processes of advection and longitudinal dispersion from the test.

The average velocity of the fluorescein was estimated from the location of the center of mass of the tracer plume relative to the source well approximately one year after injection. The plume was fairly symmetrical, with the point of maximum concentration nearly on the same line as the apparent principle direction of transport. The center of mass has been estimated graphically from Figure IV.A.5. In this figure integrated

NATURAL GRADIENT TEST AT ONE YEAR

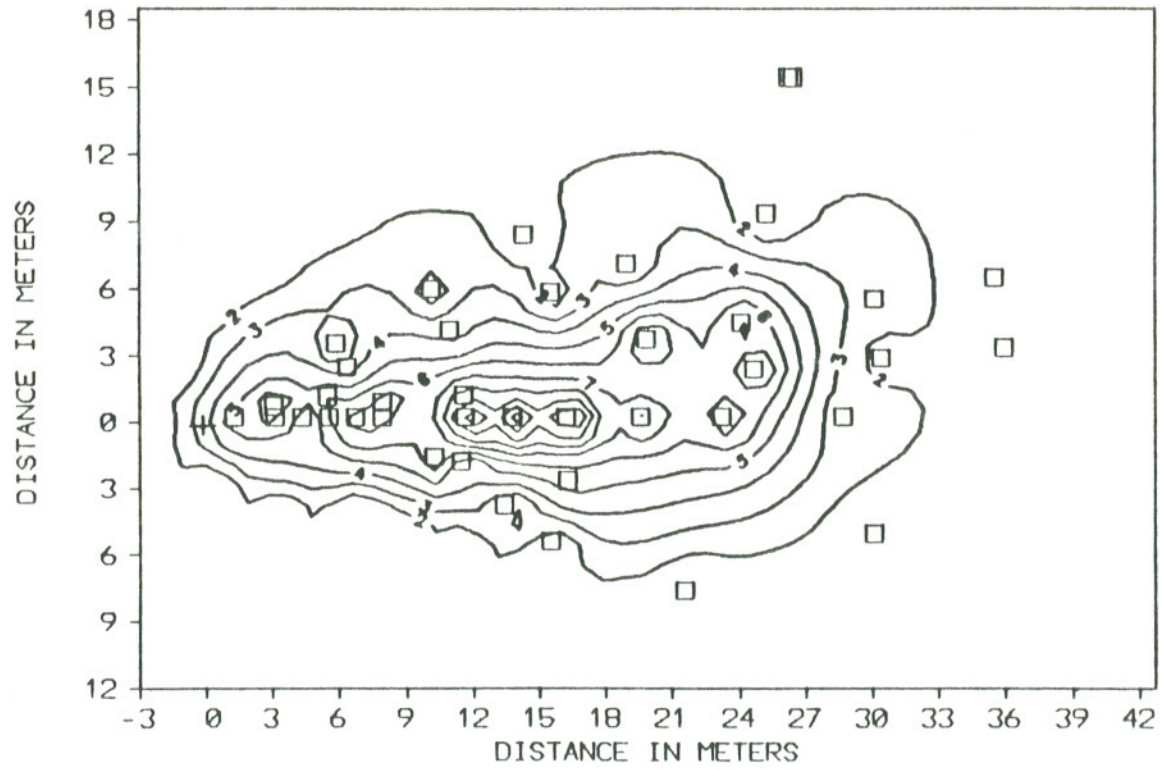


Figure IV.A.4 Tracer distribution for the natural gradient tracer test during April 1984 (at approximately 1 year). Concentration units are nM.

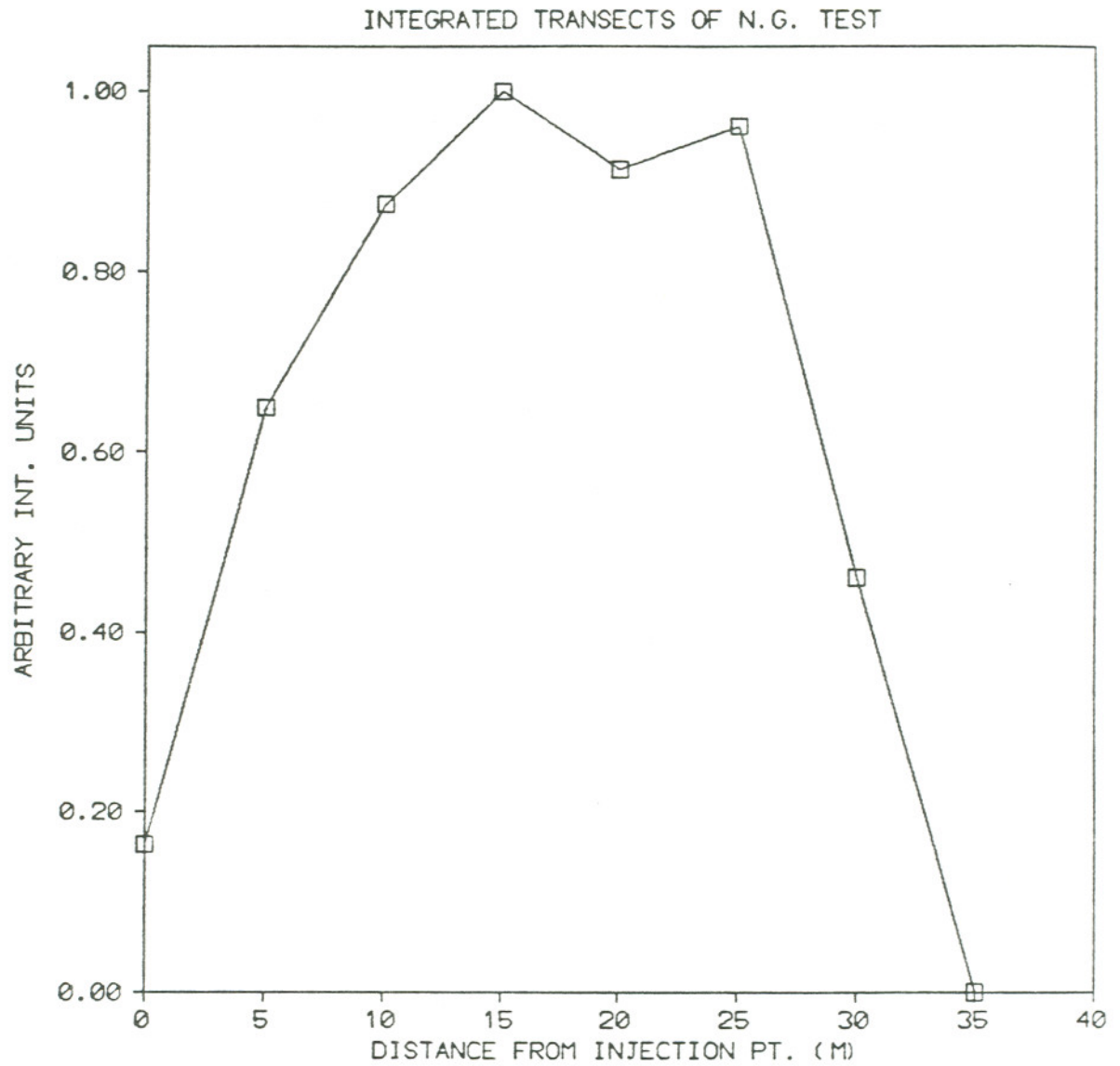


Figure IV.A.5 Integrated transects of fluorescein concentration constructed from Figure IV.A.2 plotted versus distance from the source well.

transect concentrations from Figure IV.A.4 are plotted at eight distances from the injection point. The points generated for Figure IV.A.5 were integrated to determine the center of mass. The center of mass was estimated at 18 m from the injection point at approximately 370 days. This corresponds to an average velocity of just under 5 cm/day. The direction of transport was northwest ($310^{\circ} \pm 15^{\circ}$), consistent with the direction of groundwater transport of the contaminants from the CDS.

IV.A.3 SIMULATION OF THE NATURAL GRADIENT TRACER TEST

A one-dimensional equivalent porous medium (EPM) model was used to simulate results of the natural gradient tracer test. A one-dimensional model was selected to be consistent with the modeling of the contaminant plume from the CDS. Injection of the tracer in the natural gradient test was made at a point source. Thus, unlike the contaminant plume, transverse dispersion was important in the tracer test. In order to make the one-dimensional solution applicable, the tracer concentrations were integrated across the plume at several distances downgradient from the injection point. (The same process which was used to determine the center of mass.) Justification for using the EPM approach at Alkali Lake will be presented in Section V.

Observed and calculated distributions for the natural gradient test are seen in Figure IV.A.6. The values of the input parameters for the model are a velocity of 0.049 m/day and a dispersion coefficient of $0.15 \text{ m}^2/\text{day}$. A sensitivity analysis has been carried out to estimate the uncertainties in the assigned parameter values. For the EPM model, velocity and dispersion coefficient have been varied by +100% and -50% (Figures IV.A.7 and IV.A.8). This analysis suggests that the model does provide estimates of aquifer parameters to within a factor of two. This is the same magnitude of uncertainty as observed in the other aquifer testing procedures (e.g. slug tests, pumping tests, etc.).

IV.B TWO-WELL PUMPING TRACER TESTS

IV.B.1 EXPERIMENTAL

As a result of the sampling induced difficulties in the early stages of the natural gradient tracer test, the decision was made to conduct some small scale pumping tracer tests. The primary goals of the tests were to: 1) estimate the effective porosity (total fracture volume) of the soil; and 2) observe the role of matrix diffusion in transport. There were two important

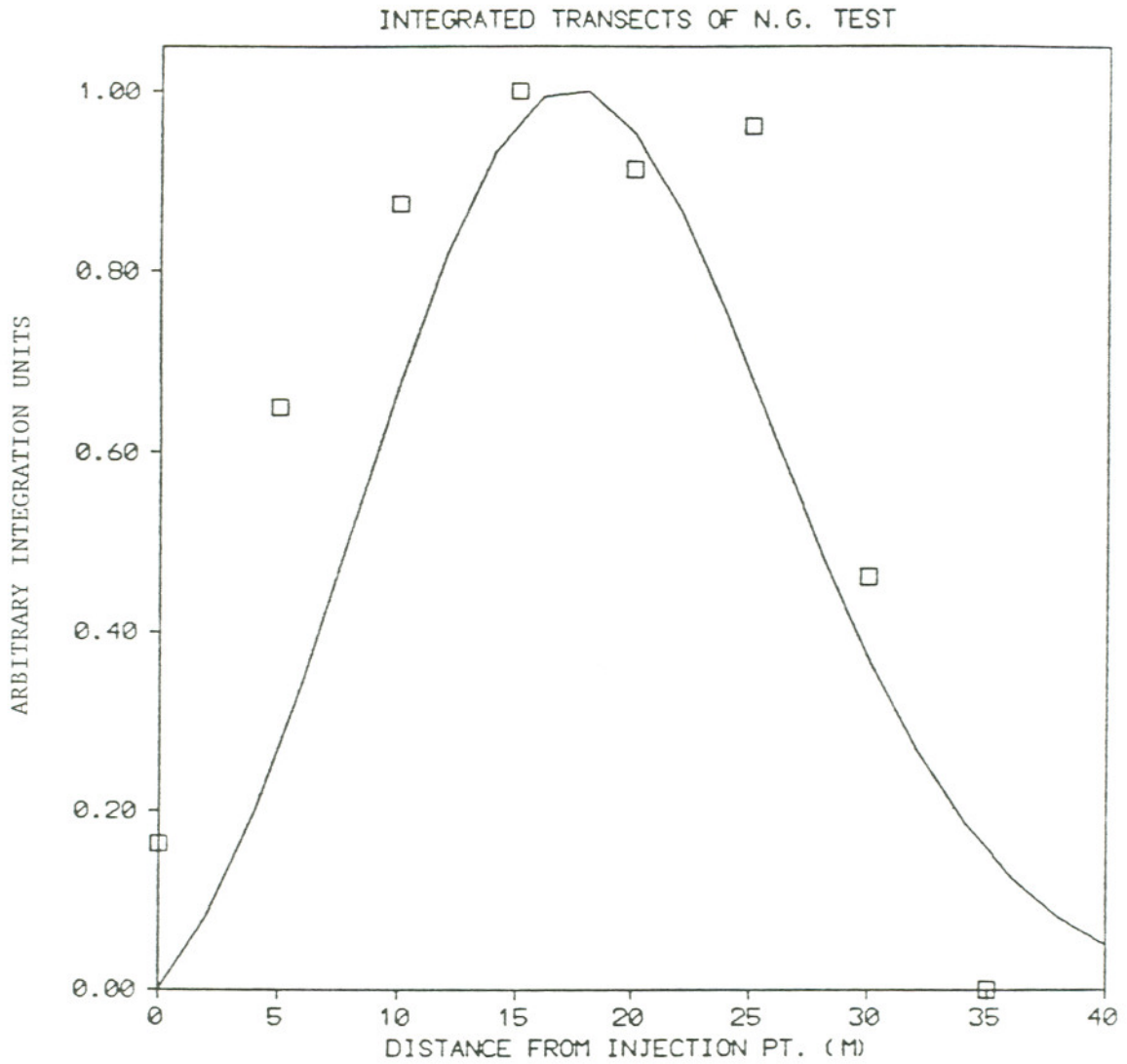


Figure IV.A.6 "Best fit" one-dimensional EPM simulation of the natural gradient test data (Figure IV.A.5) plotted with the observed integrated transects versus distance from the source well.

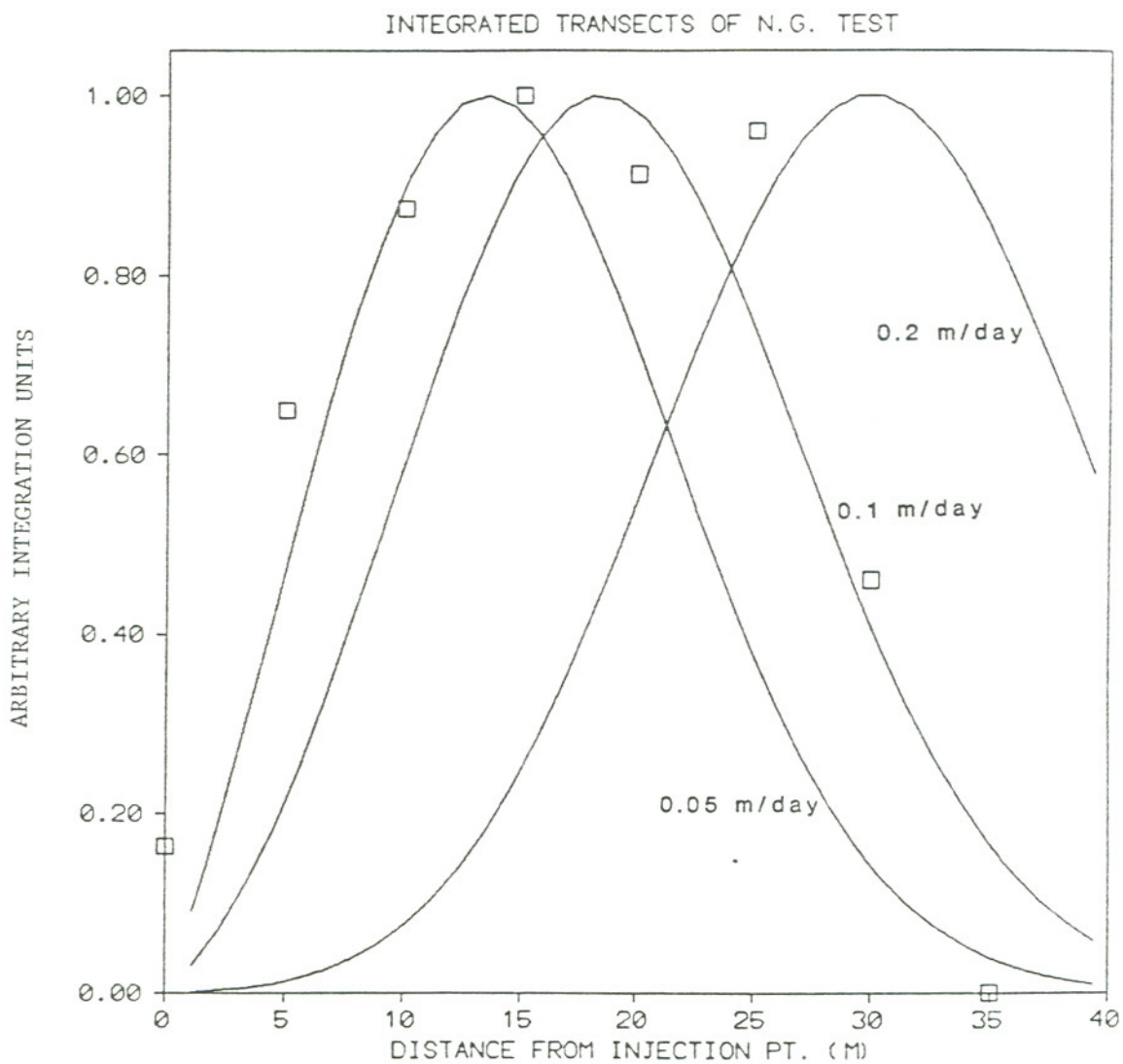


Figure IV.A.7 Sensitivity of EPM simulation of the natural gradient tracer test to velocity. Simulations have been plotted along with observed integrated transects versus distance from the source well. (1 year after injection, April 1984.)

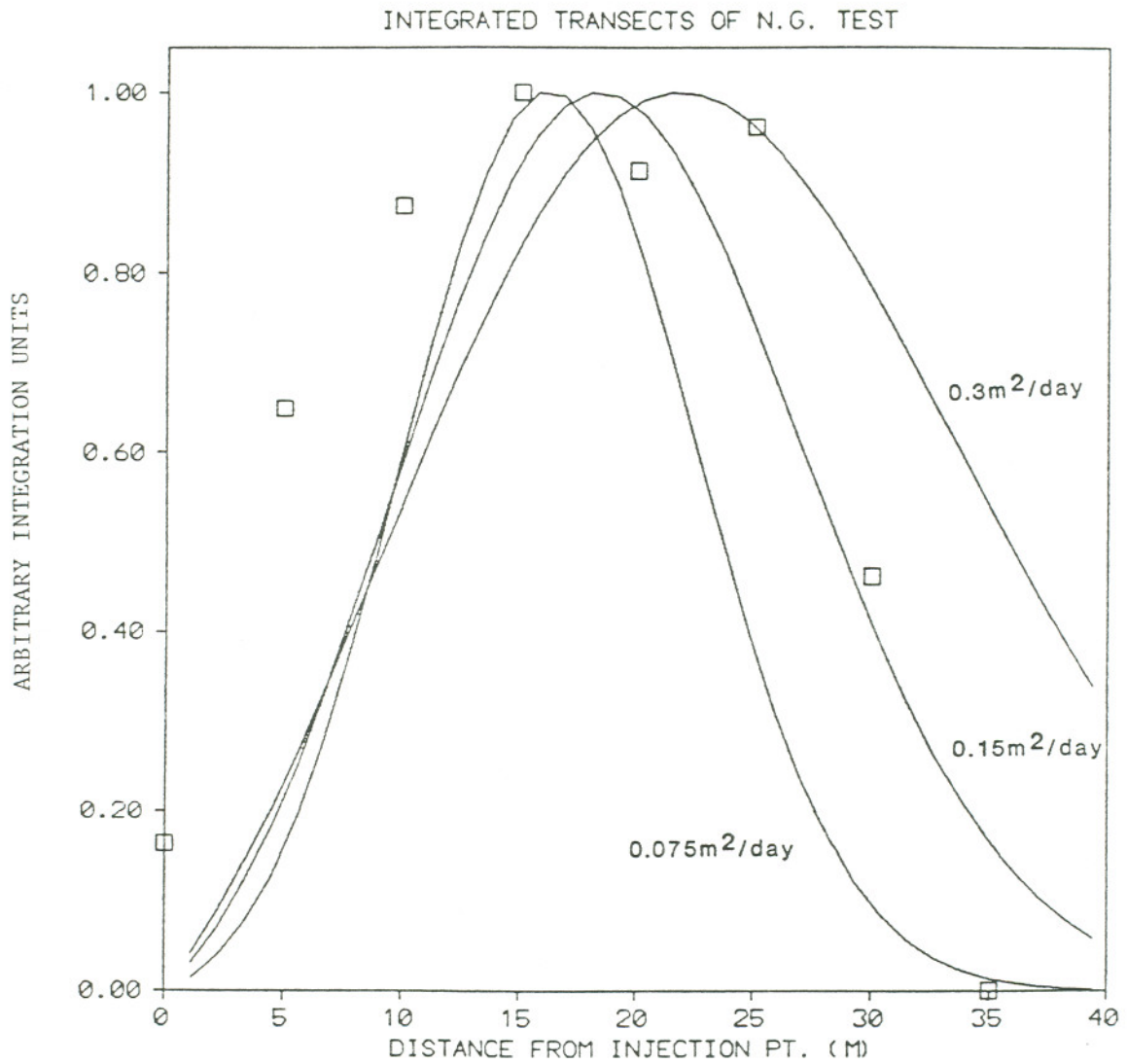


Figure IV.A.8 Sensitivity of EPM simulation of the natural gradient tracer test to longitudinal dispersion. Simulations have been plotted along with observed integrated transects versus distance from the source well. (1 year after injection, April 1984.)

advantages of the pumping tests over the natural gradient test. The first was that the flow field could be perturbed in a more or less known manner via the pumping rate. Second, a pumping tracer test required much less time to conduct than a natural gradient test. As previously mentioned, the primary difficulties with such a test are that: 1) large volumes of contaminated water was brought to the ground surface; and 2) to accurately describe the flow system, values of the horizontal and vertical hydraulic conductivities, as well as the gradient, are needed as a function of depth. It was not possible to obtain this information in sufficient detail to model the flow system. As a result, two approximate models of flow were used to estimate the effective porosity.

The pumping tracer experiments were carried out at the same field site used for the draw-down test (Section II.F). Injection of the tracer was made after pumping for approximately 2 hours. At this point the drawdown was changing quite slowly. The points of injection were approximately 1 meter below the water table at distances of 3 and 6 meters from the pumping well. As with the drawdown test, the pumping rate was approximately 1 L/s. 1 L of a 1 mM fluorescein solution was injected in separate tests, at 3 and 6 meters. Samples were collected at 5 minute intervals using an ISCO Model 1392 (Instrument Specialties Co., Lincoln, Neb.) automatic sample

collector which took the sample directly from the discharge end of the pump. Samples were collected in 40 mL vials and stored in the dark until returned to the lab where they were stored at 4°C until analyzed. Analyses were conducted using the procedure described in Section IV.A.

IV.B.2 RESULTS

An injection well to pumping well distance of 3 meters was selected for this test to provide a residence time of the tracer in the ground which was sufficiently short to minimize the effects of matrix diffusion, while being long enough to provide a reasonable estimate of the effective porosity of the system. The overall shape of the breakthrough curve (Figure IV.B.1) suggests that the tracer was not subject to a great deal of matrix diffusion. The tailing of the curve was due in part to matrix diffusion, although a significant portion of the tailing was probably due to 1) the injection having some "non-point source" character; and 2) dispersion during flow through the fractures. (Dispersion was also evidenced in the "push-pull" tests discussed in the following section.) Because of the uncertainty in the flow regime, no attempt was made to mathematically model the tracer behavior. Instead, a relatively simple calculation was performed to estimate the upper limit of fracture porosity.

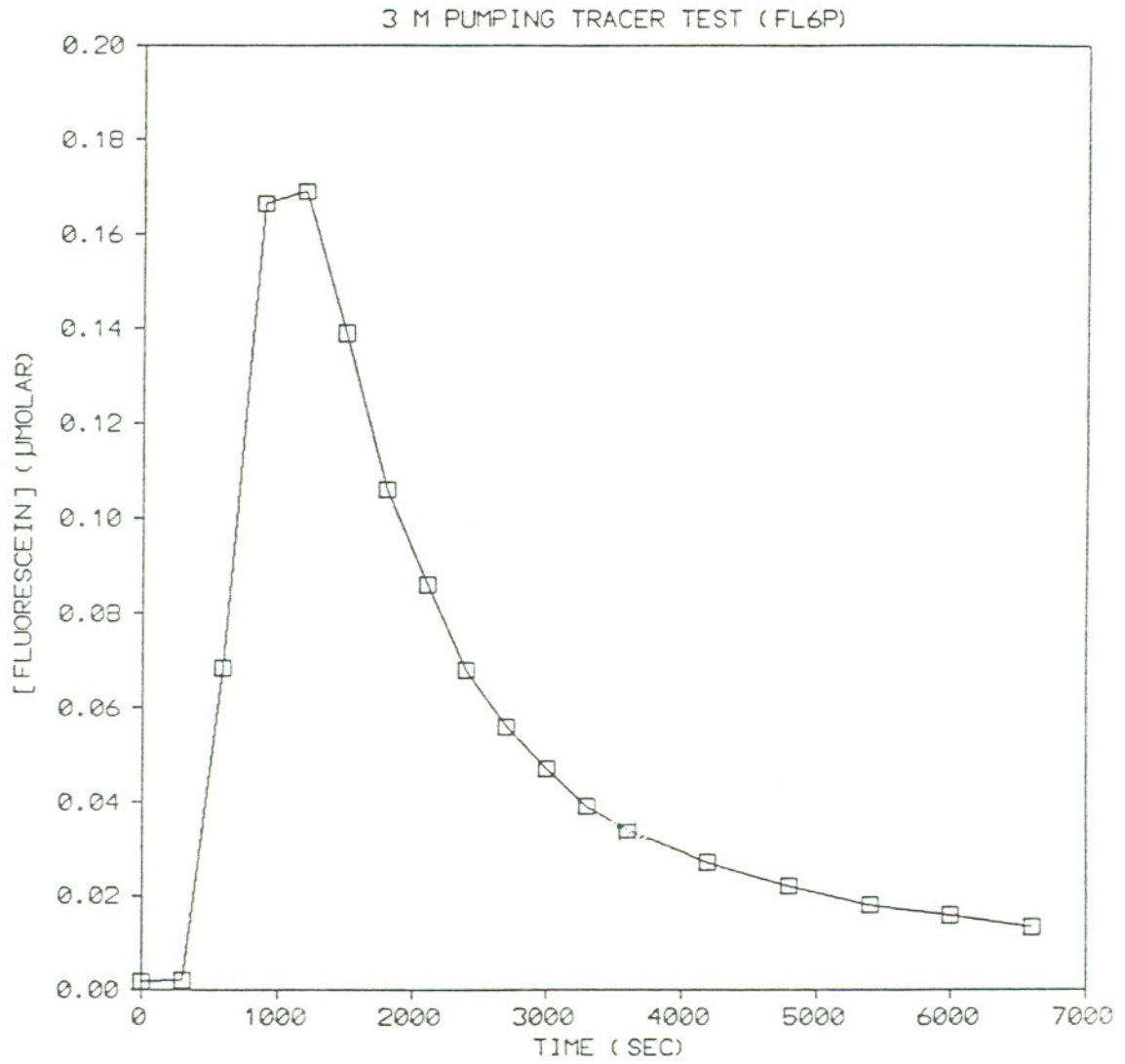


Figure IV.B.1 Breakthrough (recovery) curve for fluorescein in the 3-meter pumping tracer test. (Near Wells 33 and 25, Figure I.D.4.)

In this calculation, the pumping well was placed at the center of an imaginary volume element whose radius was the distance from the injection point to the pumping well. The effective porosity of the aquifer was estimated as the ratio of the volume of water which had to be pumped to recover the tracer to the volume of the element. In this analysis, the volume was taken as both a hemisphere and a cylinder (Figures IV.B.2 and IV.B.3, respectively). The volume of each element was calculated by the appropriate geometric formula. The volume of water needed to recover the tracer in the 3 meter test was approximately 1.5 m^3 . This corresponded to a point at approximately 1500 s (Figure IV.B.1) which was roughly the center of mass of the tracer recovered during the test. The total recovery of tracer for the pumping period was approximately 56%. The material not recovered was almost certainly lost temporarily to the matrix by diffusion (continued pumping would have eventually recovered all of the tracer). For the calculation of fracture porosity described above, it was important to know the breakthrough time for the center of mass of only that portion of the tracer which was not retarded by matrix diffusion. For the 3 meter test, this value probably occurred somewhat before 1500 s. Because an upper limit to the fracture porosity was being calculated, however, 1500 s was used. The volumes of the cylindrical and hemispherical elements were 56 and 113 m^3 , respectively. This led to upper limits of effective

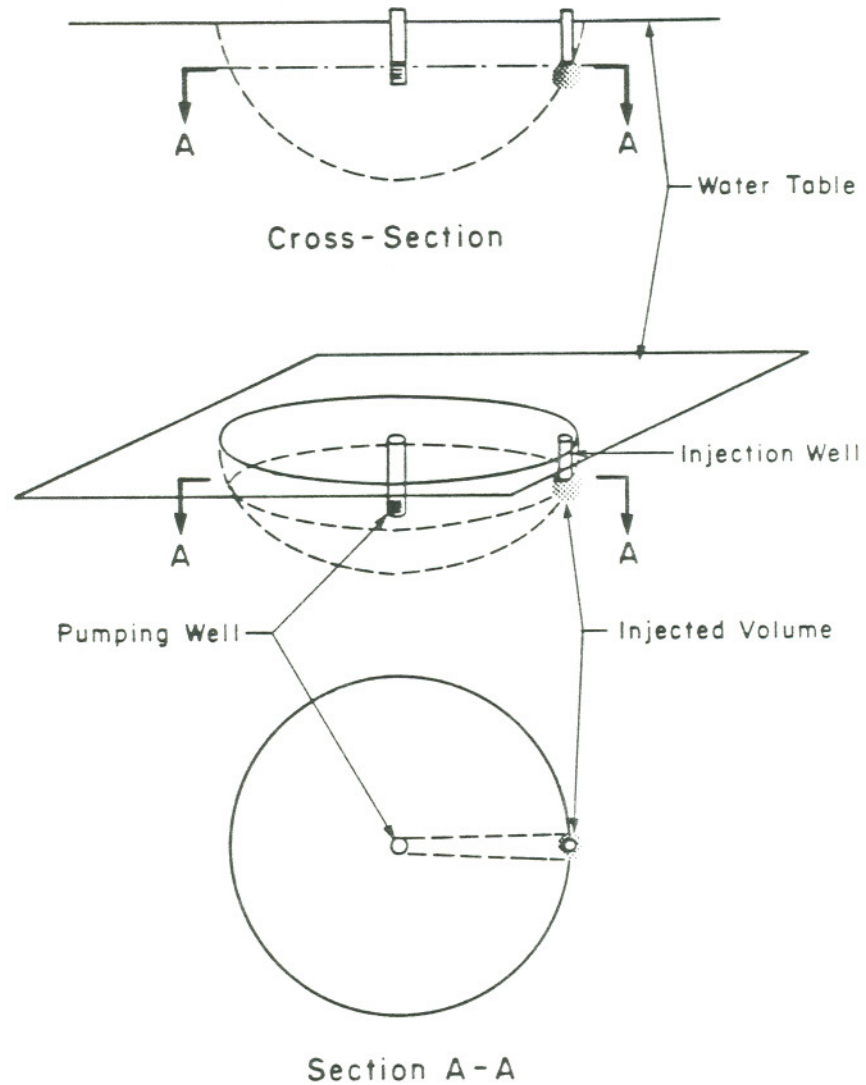
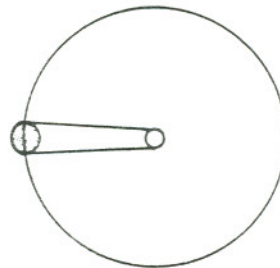
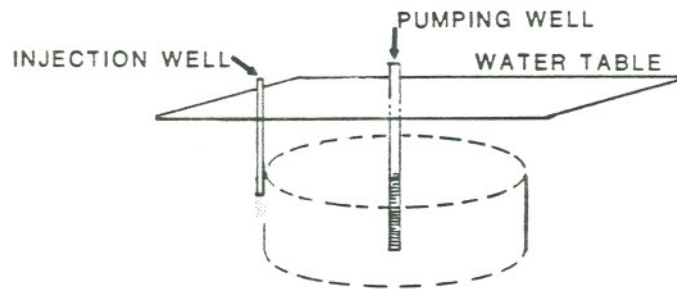
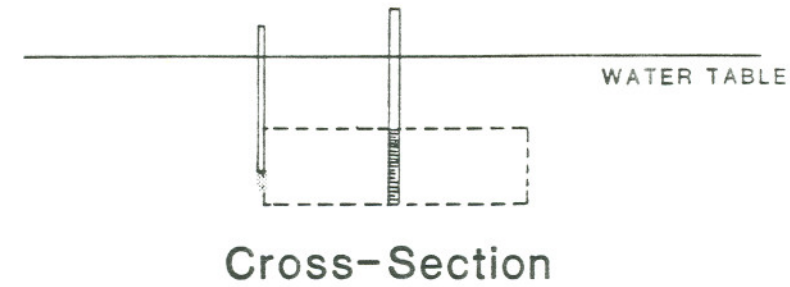


Figure IV.B.2 Conceptual drawing of the imaginary hemispherical volume element used in estimating total fracture porosity for the pumping tracer tests.



Plan View

Figure IV.B.3 Conceptual drawing of the imaginary cylindrical volume element used in estimating total fracture porosity for the pumping tracer tests.

(fracture) porosity of 2.7% and 1.3%, respectively. Because of the horizontal nature of the bedding plane fractures, and the decrease in hydraulic conductivity with depth, the cylindrical element was probably more representative of the actual flow system. The upper limit of effective porosity calculated by the above procedure is far less than the bulk porosity of the aquifer material (65%), and provided direct evidence of a dual porosity (i.e. fractured) system.

The 6 meter test was performed at the same flow rate as the 3 meter test to ensure the same flow regime. The shape of the breakthrough curve (Figure IV.B.4) for this test showed the effect of matrix diffusion. In the absence of matrix diffusion, a maximum in the breakthrough curve would have been expected at a time approximately four times as long as for the 3 meter test, with a peak concentration one fourth that of the 3 meter test (for the "cylindrical" flow regime). Instead, no maximum in concentration was observed over the pumping interval, although there was some suggestion of an inflection point at approximately the correct time (4000 s). The concentration of the pumped water at that point was more than a factor of 20 lower than the maximum for the 3 meter test. The total fluorescein recovery for the interval pumped for the 6 meter test was 5.4%. Both the shape of the curve and the low recovery for the 6 meter test were the result of loss of tracer from the fractures to the matrix by

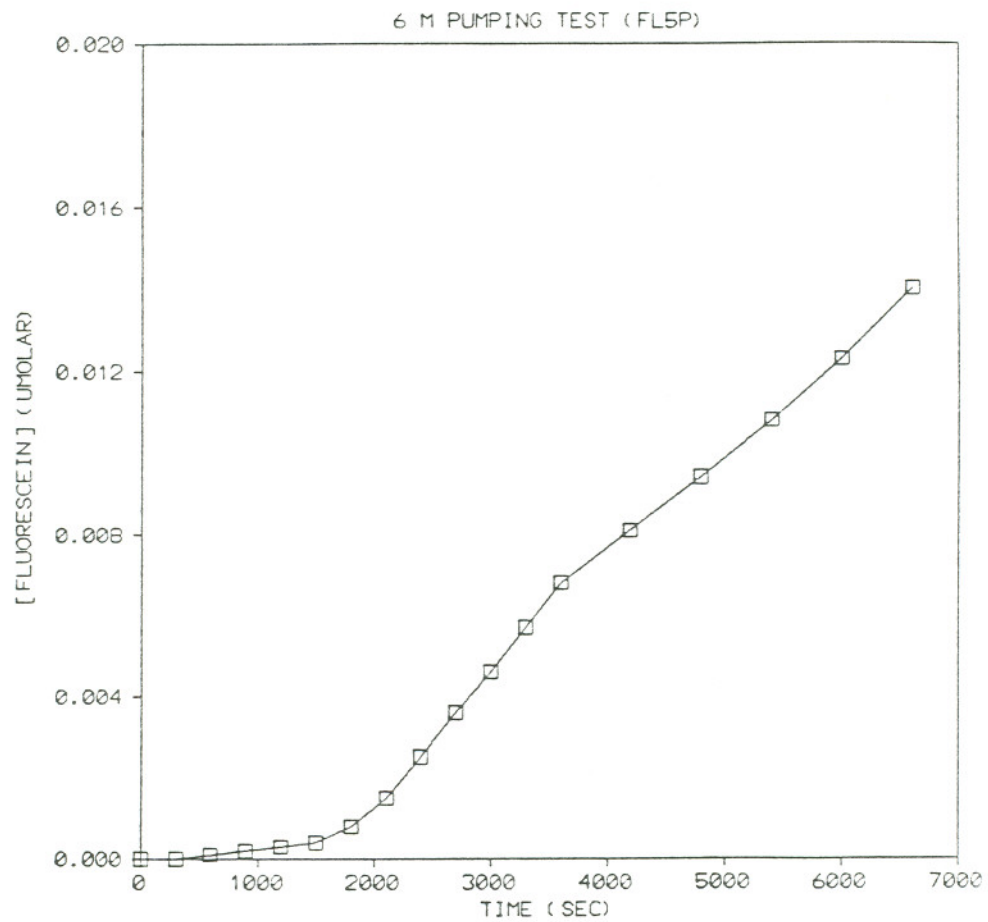


Figure IV.B.4 Breakthrough (recovery) curve for fluorescein in the 6-meter pumping tracer test. (Near Wells 33 and 25, Figure I.D.4.)

diffusion.

Given a more detailed understanding of the groundwater flow path (either by more detailed pumping drawdown tests, or by conducting two-hole recirculation tests), it should be possible to mathematically model pumping tracer tests at Alkali Lake. Short of that, the tests conducted here do demonstrate that: 1) groundwater flow occurs in only a small fraction of the total soil volume; 2) an upper limit to the effective porosity is probably less than 3%; and 3) diffusion from the mobile water (in the fractures) into immobile water in the matrix can significantly reduce the velocity of the tracer center of mass compared to the velocity of the mobile water.

IV.C ONE-HOLE "PUSH-PULL" TRACER TESTS

The push-pull tests represented an attempt to evaluate fracture aperture and spacing and matrix diffusion in situ in the absence of advection. These parameters are critical to an understanding of the extent to which matrix diffusion will retard the movement of solute relative to the groundwater velocity in the fractures.

IV.C.1 EXPERIMENTAL

A push-pull tracer test involved the injection of a non-sorbing tracer into the aquifer. The tracer was allowed to remain in the fractures for a pre-determined period of time during which the tracer could diffuse out of the fractures into the matrix. Pumping was then begun at the injection well. At that point, the tracer which remained in the fractures was quickly swept out and sampled. If pumping was continued, tracer in the matrix then began to diffuse back into the fractures and was swept out by the pumping. Recovery of the tracer in these tests showed both the initial recovery of the material which remained in the fractures and the diffusion back into the fractures from the matrix.

The apparatus used in these experiments is presented in Figure IV.C.1. The equipment was constructed of PVC. The two reservoirs were 2 m long pieces of 7.6 cm I.D. tube. These were connected with 2.1 cm O.D. tubing. The three ball valves had a minimum diameter of approximately 1.0 cm. The apparatus was designed to mount on 2.1 cm O.D. PVC wells. These were the same wells which were used in the slug tests described in Section II (Figure II.E.2, Wells A-H). The pump used was capable of pumping 1 L/s, but in these tests the flow rate was typically 0.4-0.6 L/s due to the relatively small screened interval.

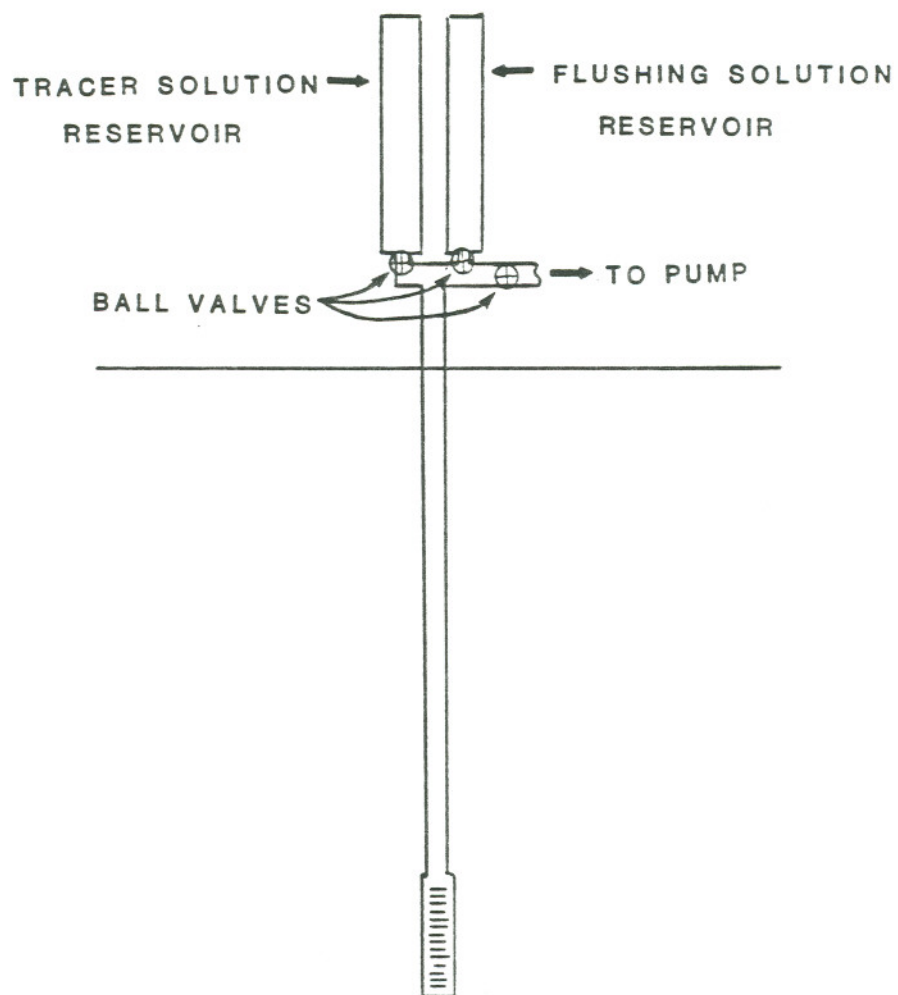


Figure IV.C.1 Schematic drawing of the apparatus used for the "push-pull" tracer tests.

The steps in the test were as follows: 1) the reservoirs were filled with tracer and flushing solutions (7 and 3 L, respectively); 2) the tracer ball valve was opened and the tracer solution flowed by gravity into the well; 3) the flushing solution valve was opened and the flushing solution flowed into the well; 4) the tracer was allowed to reside in the ground for some pre-determined period of time; and 5) the pumping line valve was opened, pumping was initiated and samples were collected. The purpose of the flushing solution was to ensure that all of the tracer was moved from the well into the matrix where diffusion could occur. Residence times ranged from 0 to 4 hours. (Preliminary tests indicated that equilibration was very nearly achieved in this period of time, yet the time was short enough to neglect advection.) When pumping was initiated, samples were collected from a well-mixed reservoir filled with the discharge of the pump. The volume of the reservoir was 10 L, i.e. equal to the sum of tracer and flushing solution volumes. Each time the reservoir was filled, a sample was collected and the reservoir was emptied. In this manner 16 or more aliquots were collected for each test. Samples were collected in 40 mL vials, which were stored in the dark while enroute to the lab, then stored at 4°C until analyzed.

Two tracers were used in these tests, fluorescein (1 mM) and iodide (1000 ppm). The tracers complemented each other well

in these tests in that they: 1) provided independent measures of recovery, one by fluorescence detection and the other by UV absorption; 2) fluorescein could be detected at very low concentrations; 3) both the free solution diffusion coefficient and the behavior of iodide in groundwater systems are well characterized; and 4) neither compound was present in the natural groundwater or the contaminants.

Fluorescein analyses were performed by LIF using the same procedure described for the natural gradient tracer test samples. Iodide analyses were by high performance liquid chromatography (HPLC) using UV absorption as the detection method. The basic HPLC operating conditions are listed in Table IV.C.1. In this procedure the samples were: 1) acidified to $\text{pH}=3.0\pm 0.5$; 2) injected (50-300 μL) onto a sample-loop concentrator (Brownlee Labs, Santa Clara, CA) which contained a 0.64 cm O.D. by 5 cm reverse phase (ODS) column; 3) eluted off of the concentrator by switching the concentrator on-line for 60 s to allow elution of the iodide off of the concentrator and onto the analytical column (while retaining the potentially interfering chlorophenolic compounds on the concentrator); and 4) chromatographed, detected and quantitated. Approximately every tenth run, chlorophenolic material began to bleed from the concentrator while it was on-line with the analytical column. To avoid this difficulty, the concentrator was cleaned approximately every fifth analysis

TABLE IV.C.1 HPLC CONDITIONS FOR IODIDE ANALYSES

Detector wavelength = 230 nm

Flow rate = 1.5 mL/min

Solvent = 10 mM PO_4 buffered
to pH=7 in 70:30 H_2O :Methanol

Column = Whatman Partasil SAX, 1/4" X 25 cm

by flushing with methanol and then with column eluent. Calibration was accomplished by a series of standards prepared using water collected in the vicinity of the "push-pull" tests.

IV.C.2 RESULTS

A total of 9 tests were carried out on 7 different sampling wells downgradient from the site. In the first two tests, the tracer and flushing solution were injected into the well and immediately (within 2 minutes) pumped out. The purpose of this was to evaluate recovery in the absence of diffusion. Just over 90% of the injected mass of the tracer was recovered in these tests, most of it within the first four aliquots. For the subsequent tests, the tracer was allowed to remain in the ground for a range of pre-determined times. The result was that as the residence time of the tests increased, there was a systematic decrease in the fraction of the input mass recovered during the pumping period (Figure IV.C.2). The fractions of the mass recovered for both fluorescein and iodide were very similar.

Data for all of the experiments are presented in Figures IV.C.3-9 for fluorescein and in Figures IV.C.10-17 for iodide. Several features of the figures should be noted: 1) the first aliquot was generally not the one of highest concentration; 2) there was some "tailing" in the recovery curve even for the

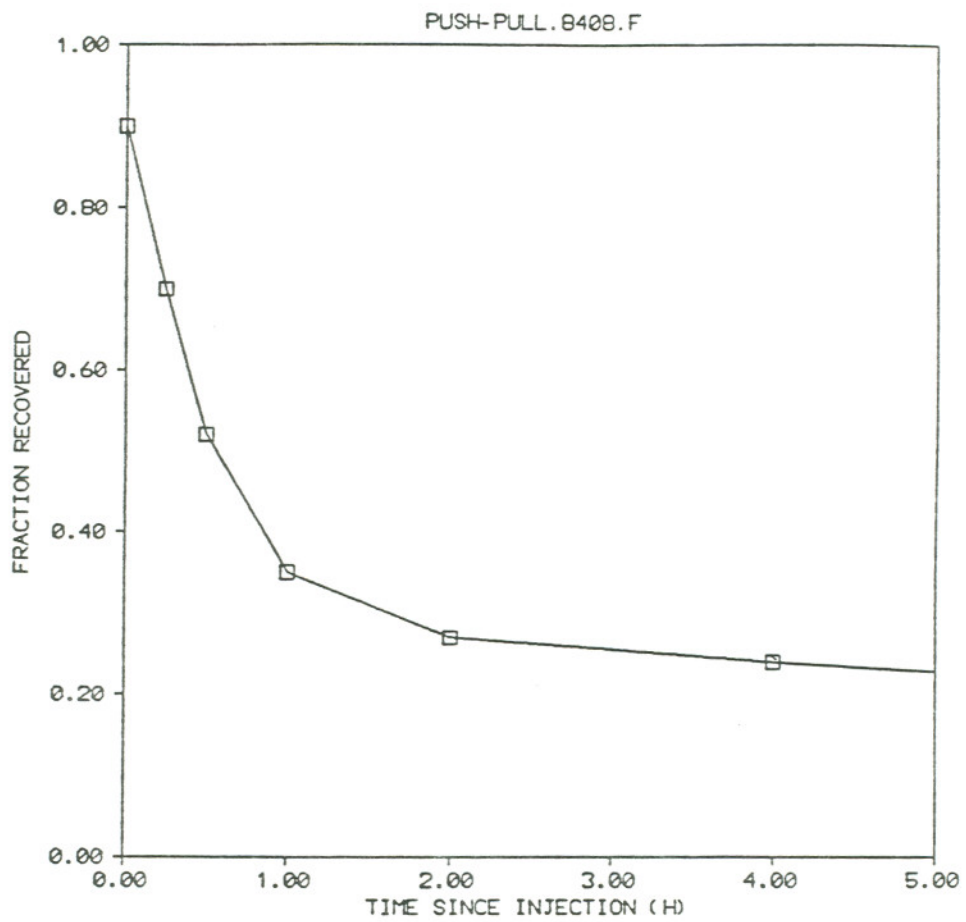


Figure IV.C.2 Fraction of mass recovered during pumping versus residence time of the tracer in the ground prior to beginning of pumping for the "push-pull" tests using fluorescein.

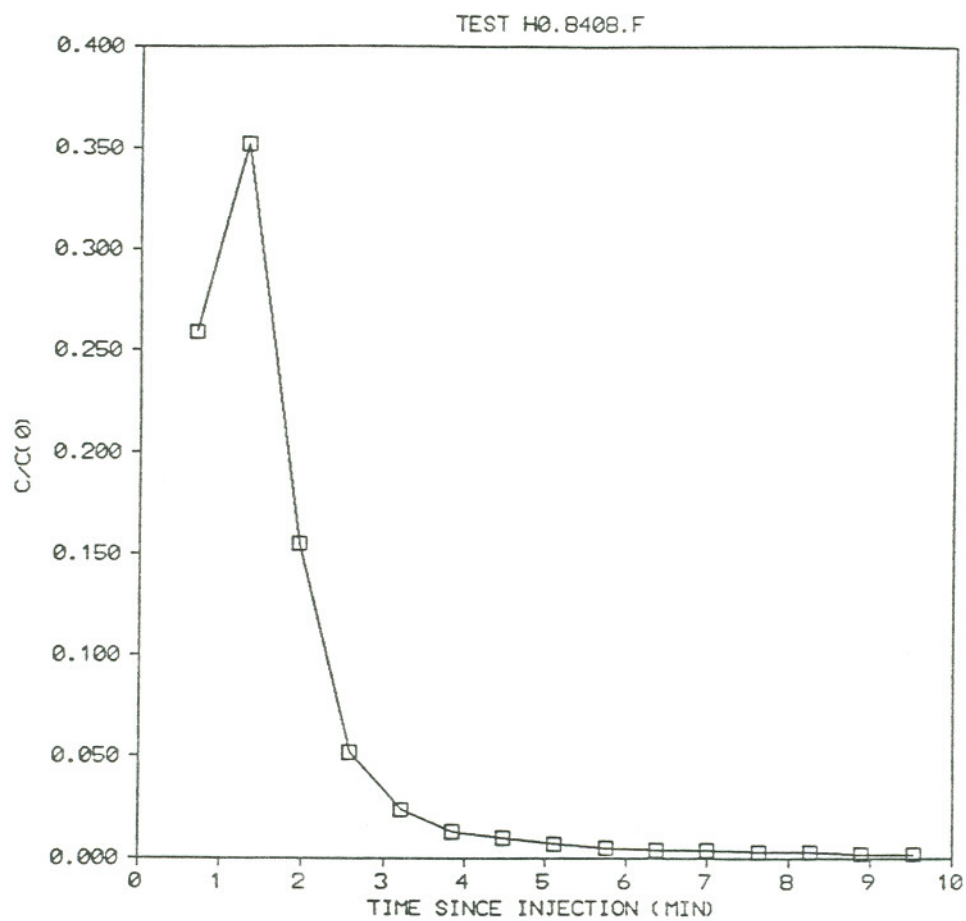


Figure IV.C.3 Fluorescein recovery curve for the "push-pull" test H0.8404.F with residence time = 0 hours. (Piezometer H, Figure II.E.2.)

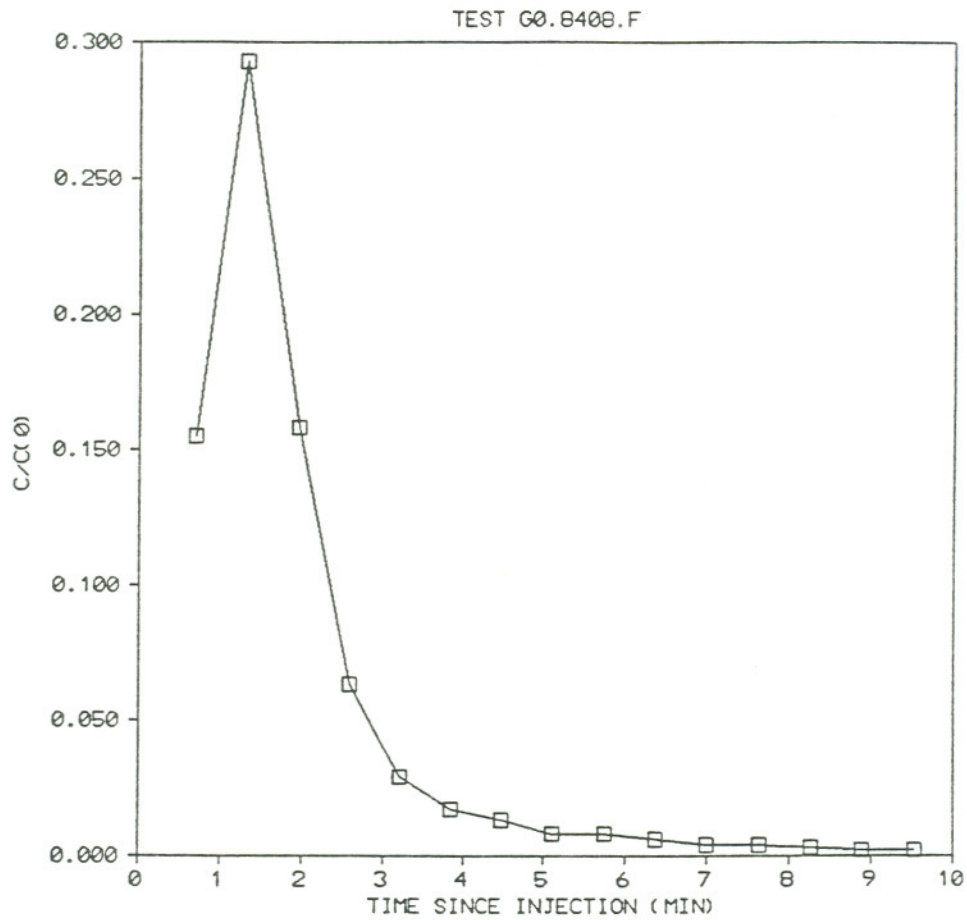


Figure IV.C.4 Fluorescein recovery curve for the "push-pull" test G0.8404.F with residence time = 0 hours. (Piezometer G, Figure II.E.2.)

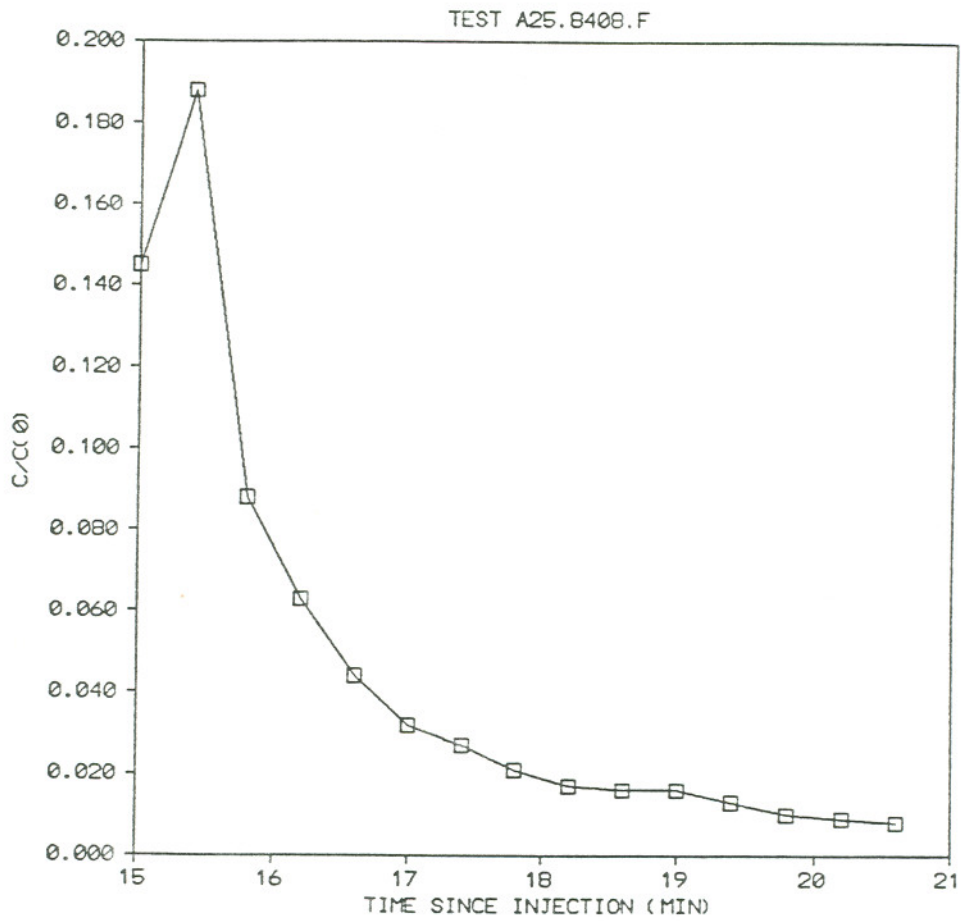


Figure IV.C.5 Fluorescein recovery curve for the "push-pull" test A25.8404.F with residence time = 0.25 hours. (Piezometer A, Figure II.E.2.)

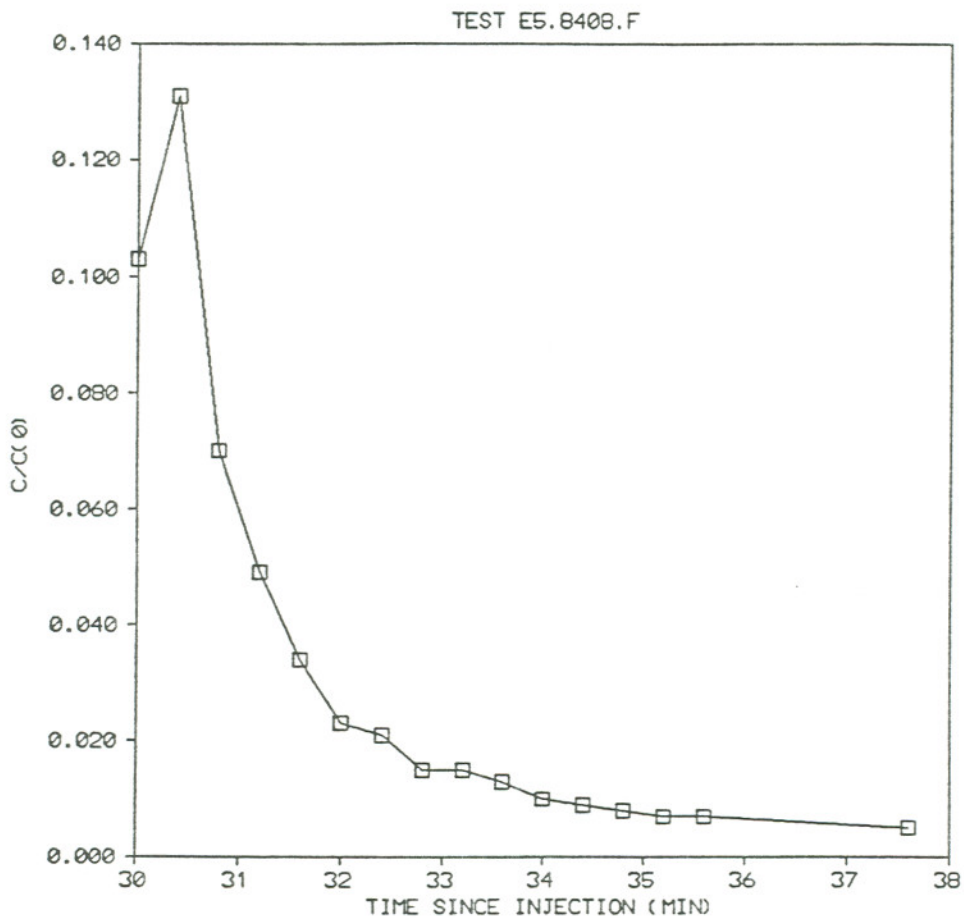


Figure IV.C.6 Fluorescein recovery curve for the "push-pull" test E5.8404.F with residence time = 0.5 hours. (Piezometer E, Figure II.E.2.)

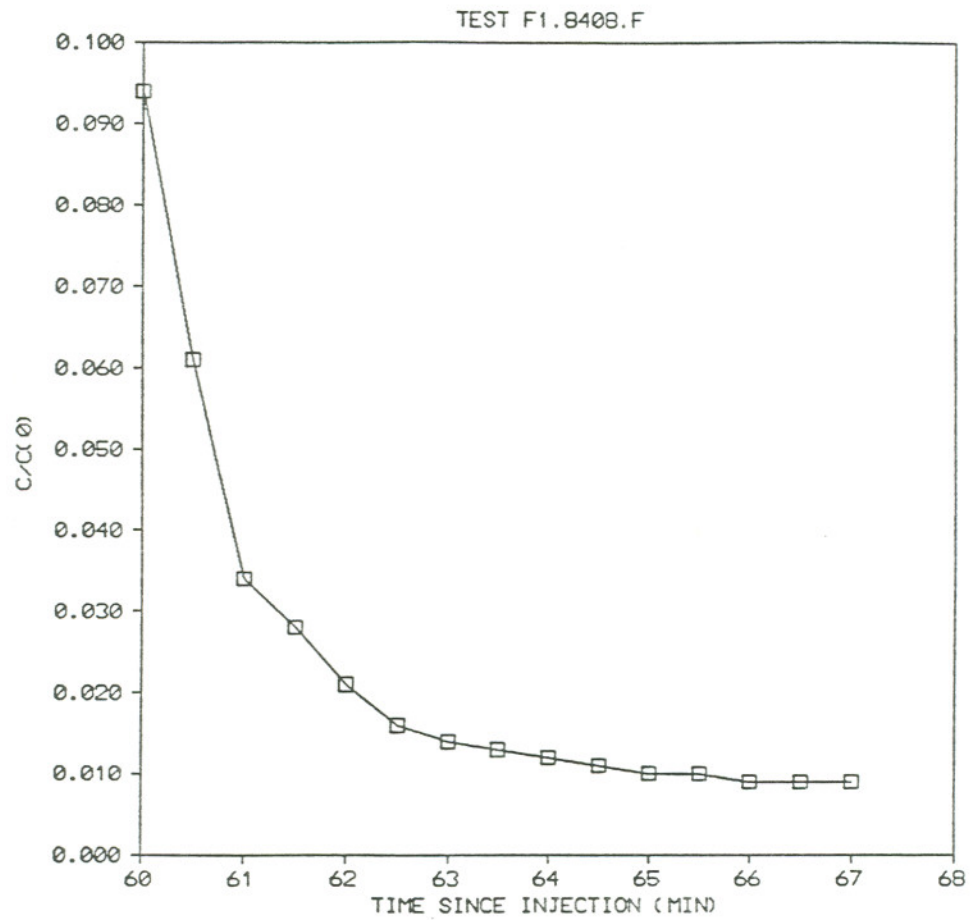


Figure IV.C.7 Fluorescein recovery curve for the "push-pull" test F1.8404.F with residence time = 1.0 hour. (Piezometer F, Figure II.E.2.)

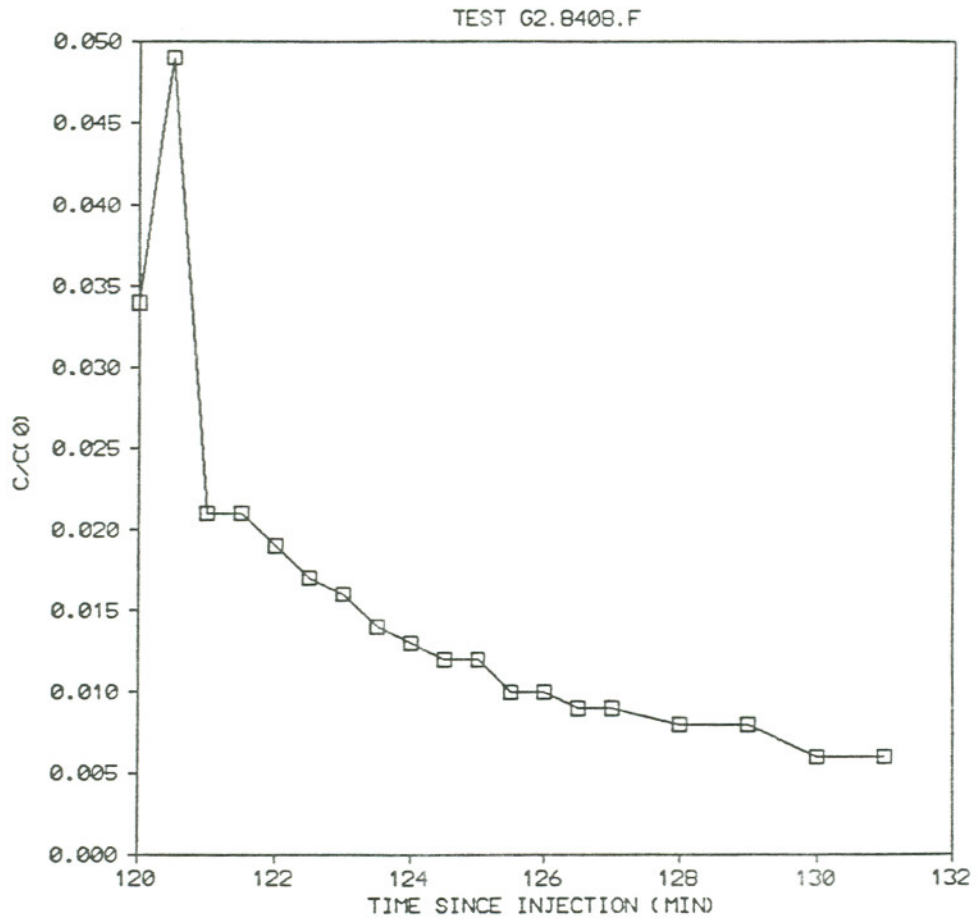


Figure IV.C.8 Fluorescein recovery curve for the "push-pull" test G2.8404.F with residence time = 2.0 hours. (Piezometer G, Figure II.E.2.)

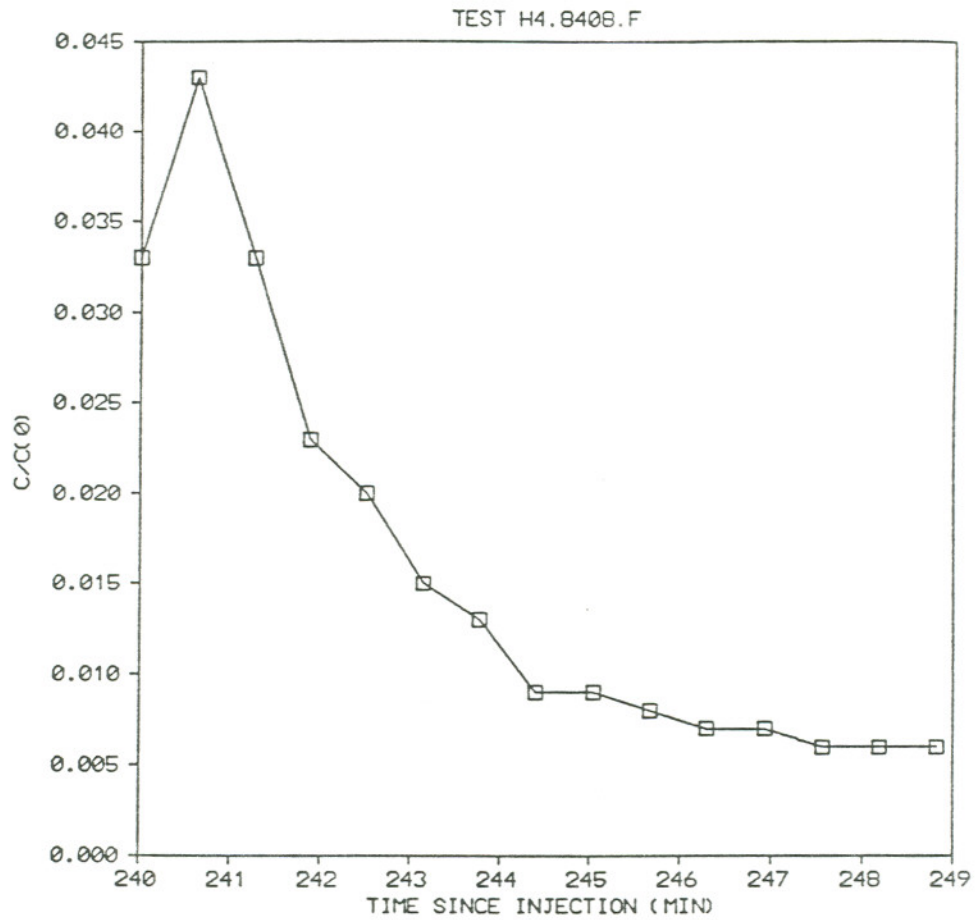


Figure IV.C.9 Fluorescein recovery curve for the "push-pull" test H4.8404.F with residence time = 4.0 hours. (Piezometer H, Figure II.E.2.)

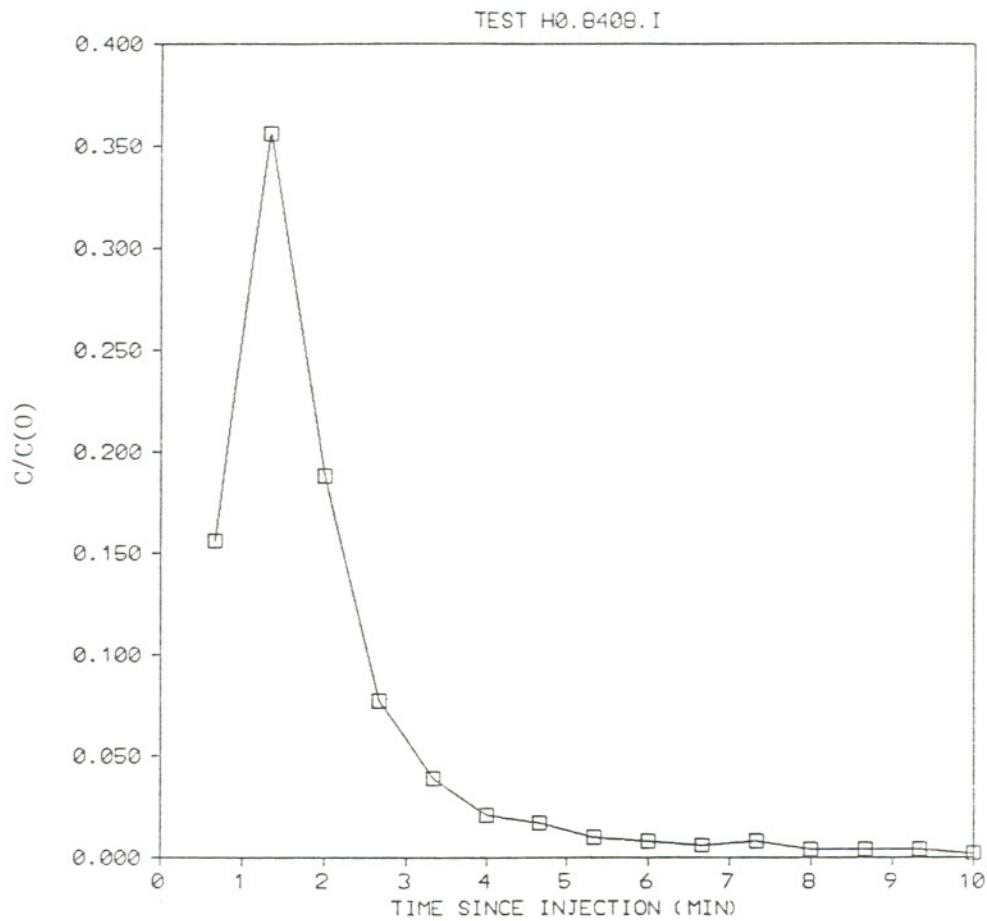


Figure IV.C.10 Iodide recovery curve for the "push-pull" test H0.8404.I with residence time = 0 hours. (Piezometer H, Figure 11.E.2.)

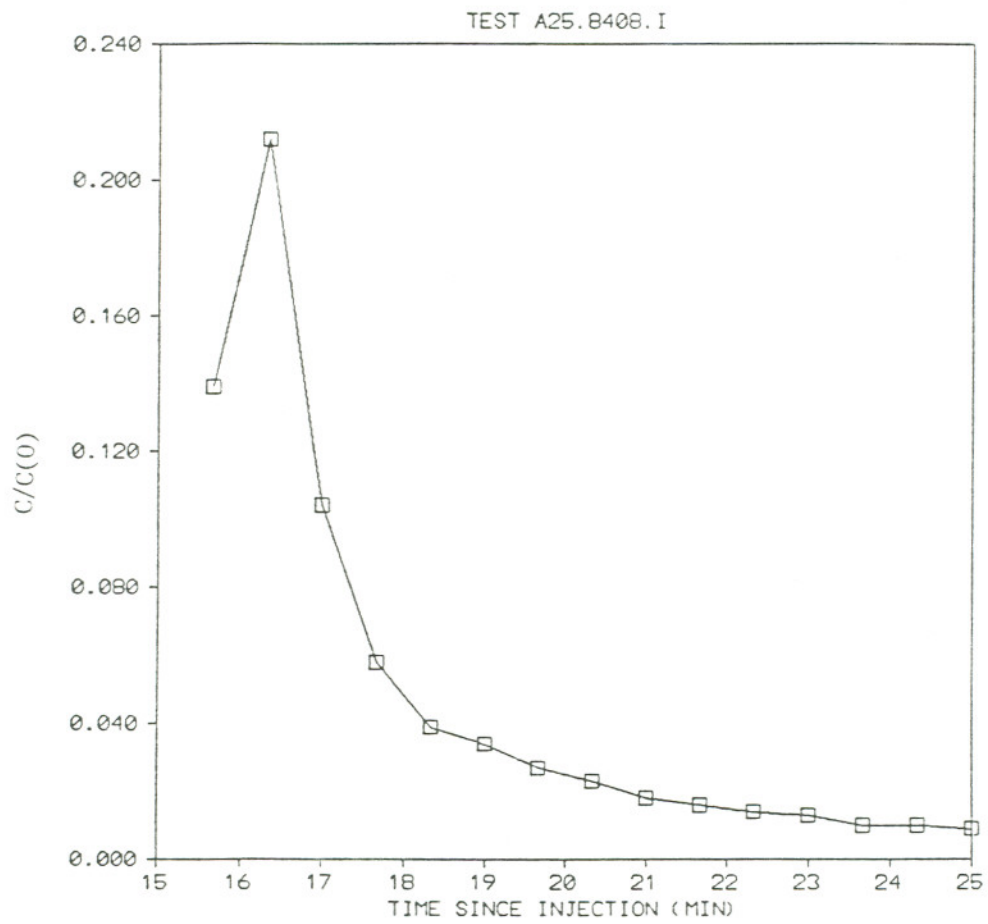


Figure IV.C.11 Iodide recovery curve for the "push-pull" test A25.8404.I with residence time = 0.25 hours. (Piezometer A, Figure II.E.2.)

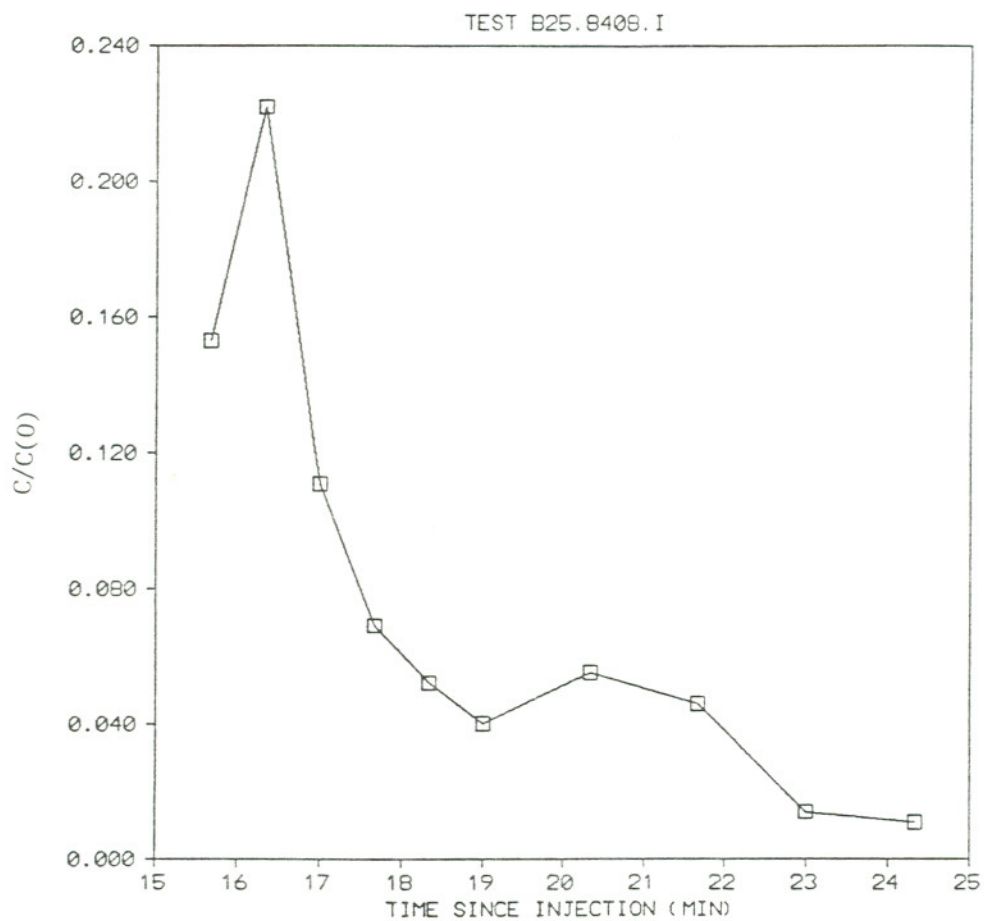


Figure IV.C.12 Iodide recovery curve for the "push-pull" test B25.8404.I with residence time = 0.25 hours. (Piezometer B, Figure II.E.2.)

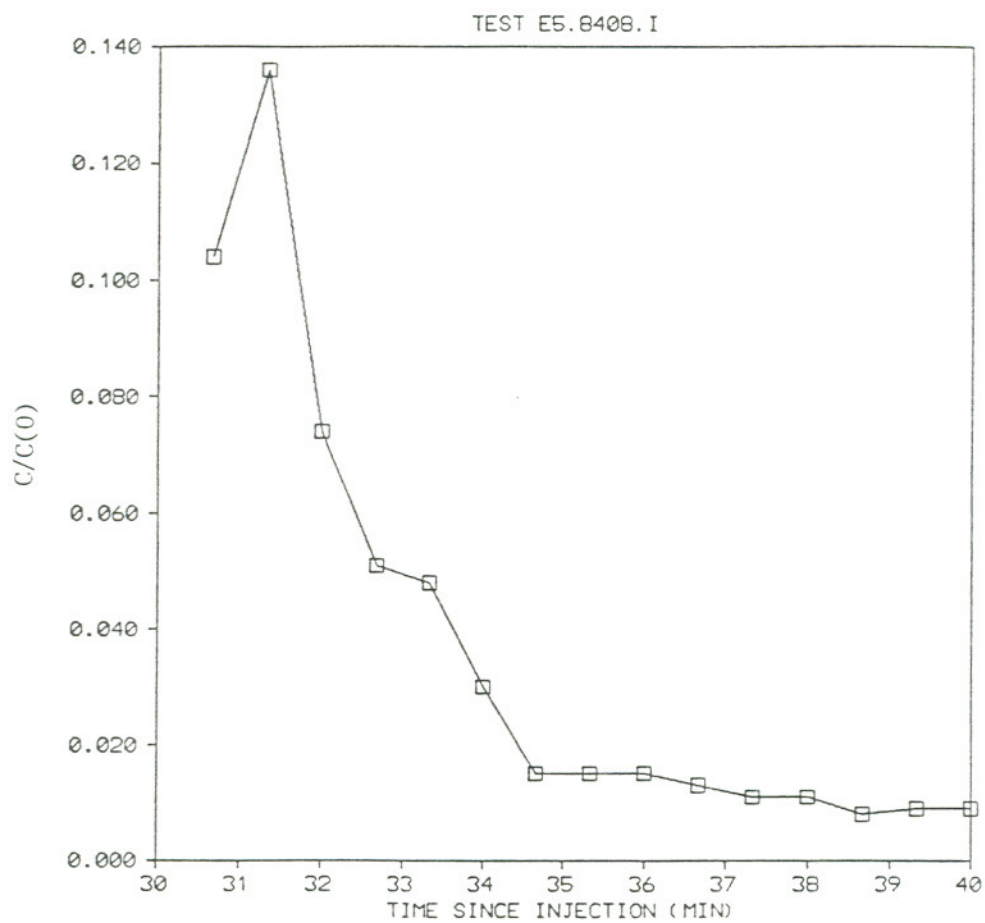


Figure IV.C.13 Iodide recovery curve for the "push-pull" test E5.8404.I with residence time = 0.5 hours. (Piezometer E, Figure II.E.2.)

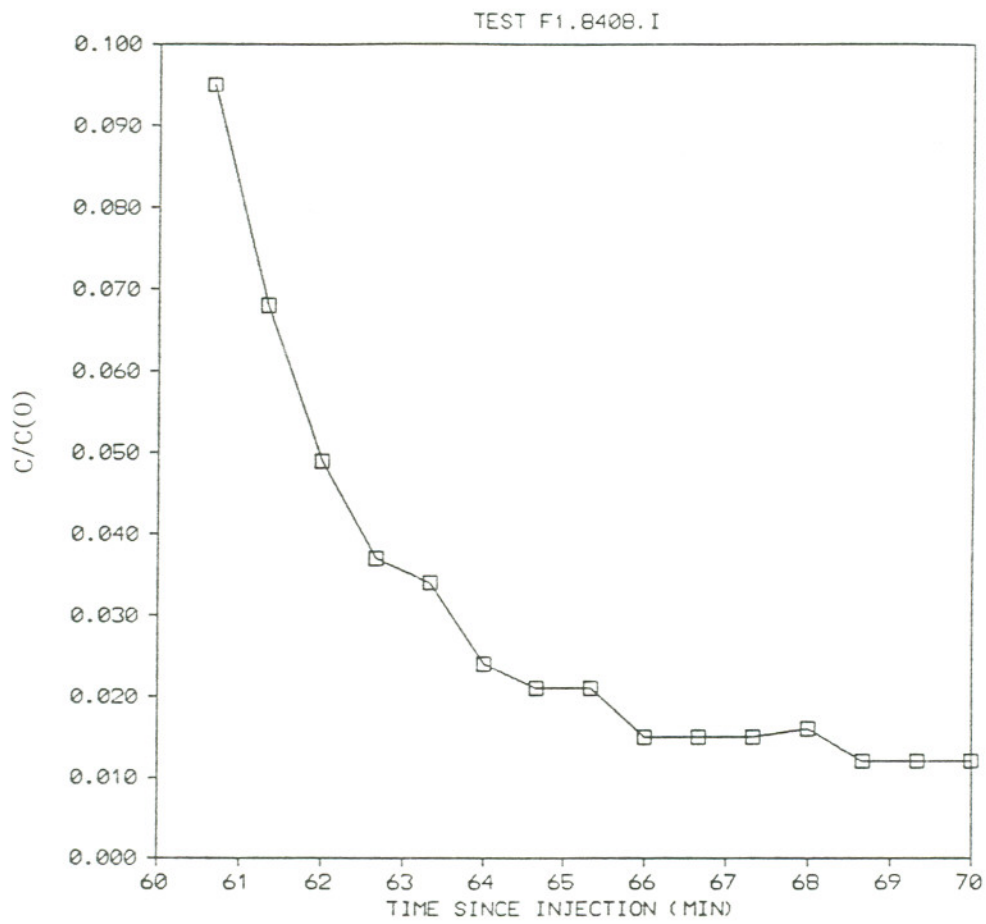


Figure IV.C.14 Iodide recovery curve for the "push-pull" test C1.8404.I with residence time = 1.0 hour. (Piezometer C, Figure II.E.2.)

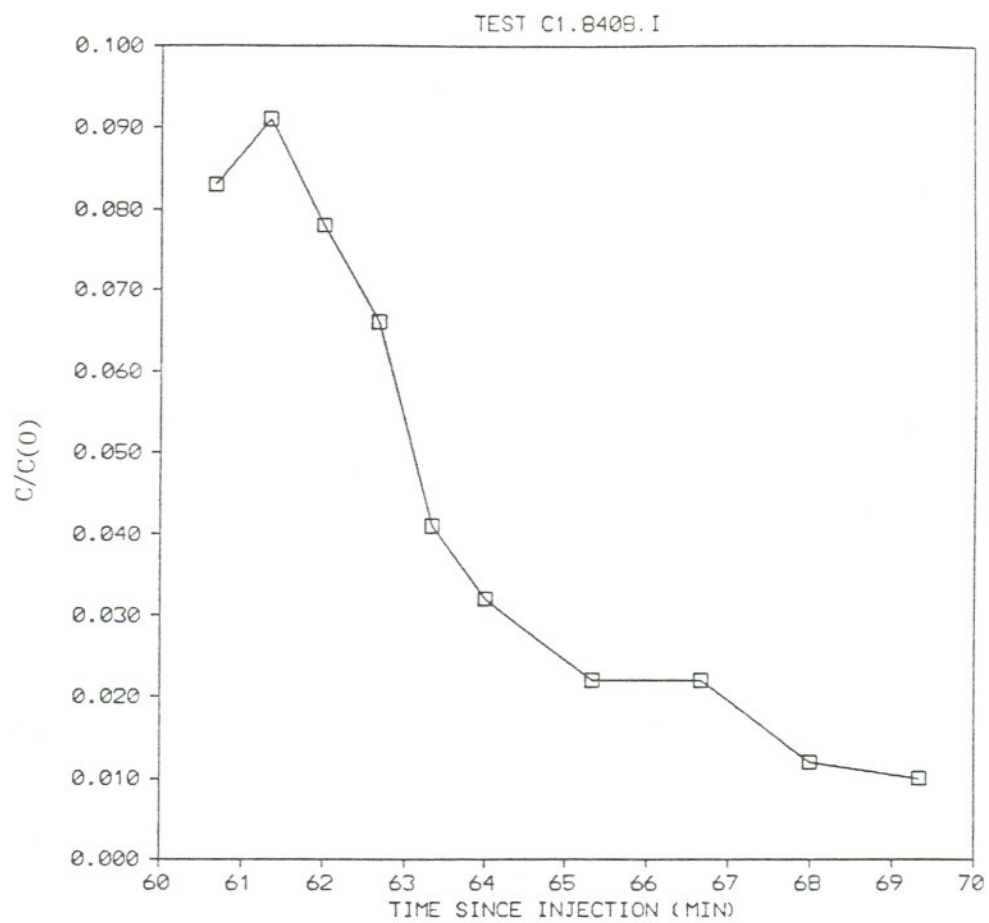


Figure IV.C.15 Iodide recovery curve for the "push-pull" test F1.8404.I with residence time = 1.0 hour. (Piezometer F, Figure II.E.2.)

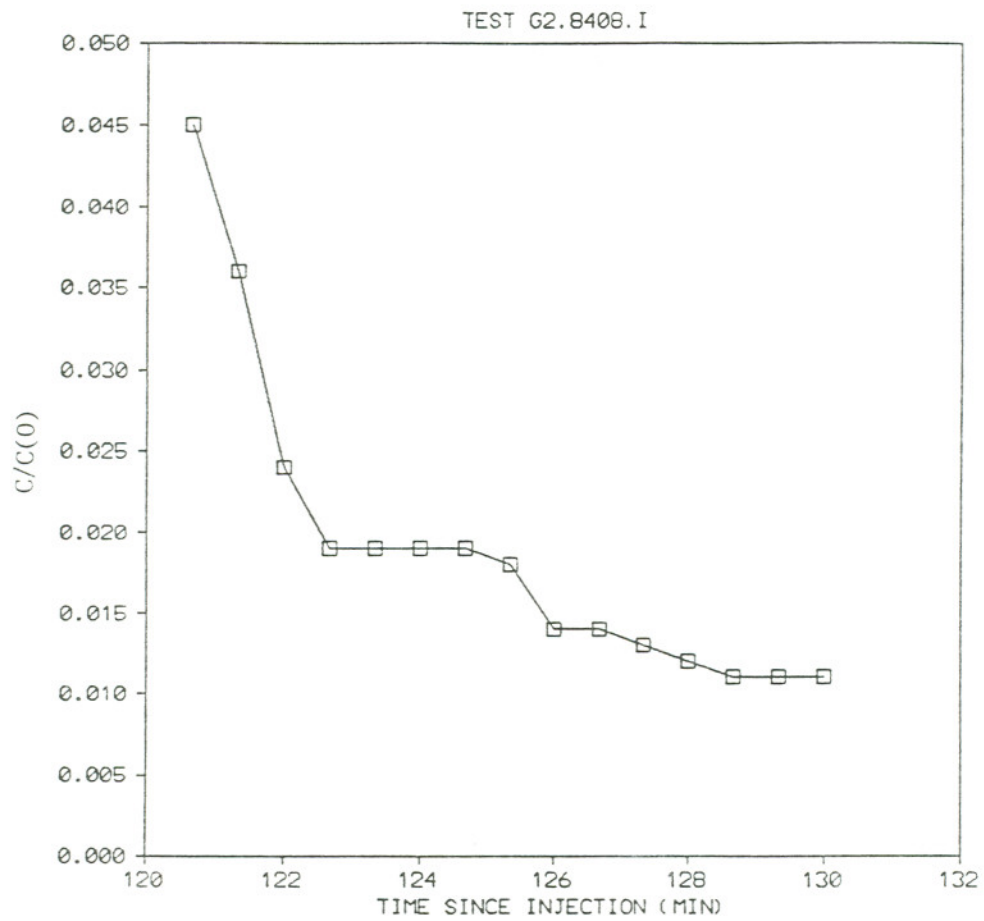


Figure IV.C.16 Iodide recovery curve for the "push-pull" test G2.8404.I with residence time = 2.0 hours. (Piezometer G, Figure II.E.2.)

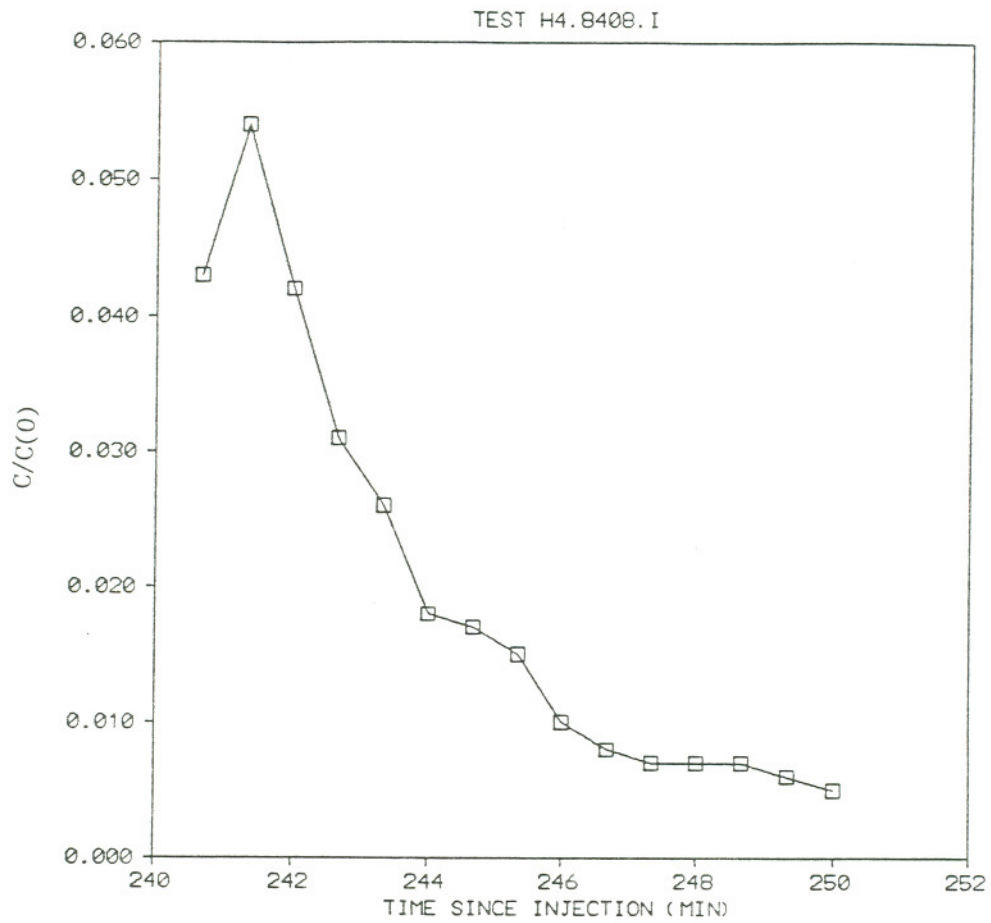


Figure IV.C.17 Iodide recovery curve for the "push-pull" test H4.8404.I with residence time = 4.0 hours. (Piezometer H, Figure II.E.2.)

"time = 0 " tests; and 3) for the longer residence time tests the "tail" became a major feature of the recovery curves. The first aliquot was not the highest because, at the initiation of pumping, both the well and pump were filled with tracer free water. This dead volume water diluted the first aliquot of pumped water. It was fairly straightforward to estimate the dead volume of the system and to correct for it. "Tailing" was the result of both matrix diffusion and non-plug flow during recovery of the tracer. The "time = 0" tests were used to evaluate the effect of non-plug flow on the recovery peak shape, for use in all of the longer-time tests (Section IV.C.1). As one moved to tests with longer and longer initial hold times, the concentration maximum decreased sharply and the long, flat "tail" became more pronounced. This is the result of matrix diffusion.

IV.C.3 MODELING OF THE "PUSH-PULL" TESTS

As previously stated, the goal of these tests was to quantitatively estimate values for the matrix diffusion coefficient and the average fracture aperture. A reasonable estimate of the matrix diffusion coefficient could be obtained based on known fracture spacings and the flux back into the fractures once pumping had begun (for the long-duration tests). It was more difficult, however, to estimate the fracture aperture because in the early phases of recovery there were several

processes going on simultaneously (e.g. diffusion, dispersion, dead-volume dilution, etc). To overcome these difficulties, a finite difference computer code was developed (Appendix E) which took into account all of these processes and gave an estimate of the mass remaining in the fracture at the end of the residence time.

The process of fitting the models to the field data involved the systematic variation of values for the unknown parameters (especially the matrix diffusion coefficient and fracture aperture) to obtain a best fit for all of the data. Because of the series of tests performed, advantage was taken of the fact that for tests with different residence times the relative importance of the various factors change. For example, for the "time = 0" test, diffusion had little effect on curve shape, and the primary effect was that of dispersion in recovering the tracer. At long times, the ratio of fracture aperture to fracture spacing was important in determining tracer concentrations remaining in the fracture. At intermediate times, fracture spacing was less important and the roles of fracture aperture and matrix diffusion coefficient dominated. These observations were used to sort out the various effects in order to arrive at accurate values for fracture aperture and the matrix diffusion coefficient for a given tracer. The parameter values found to provide the best fits to the fluorescein data are listed

in Table IV.C.2. Comparisons between field data and model simulation for fluorescein are presented in Figures IV.C.18-23.

The uncertainties associated with the values assigned to each of the parameters were evaluated by a sensitivity analysis. The simulation at one hour was used as a benchmark. Time, fracture aperture, fracture spacing, matrix diffusion coefficient, dispersion coefficient and matrix porosity were varied independently to observe the effect on recovery curve shape (Figures IV.C.24-29). The most important parameters in determining the shape of the early portion of the curves were, as expected, fracture aperture and matrix diffusion coefficient. The shape of the tail end of the recovery curves was determined primarily by the matrix thickness and the diffusion coefficient. Matrix thickness was important because, if it was large, the concentration gradient between the fracture and the center of the matrix block would have been maintained for a longer period of time. If pumping was initiated before the fracture and matrix had come to complete equilibrium, then diffusion would occur both towards the center of the matrix and back into the fractures. If fracture spacing was small, the matrix and fractures would be closer to attaining equilibrium, and the primary direction of diffusive flux would be back into the fracture.

To describe the effects of non-plug flow during tracer

TABLE IV.C.2 "BEST FIT" FRACTURE PARAMETERS FROM
"PUSH-PULL" TESTS

FRACTURE APERTURE = 150 μm

FRACTURE SPACING = 3 mm

MATRIX DIFFUSION = 0.05 cm^2/day
COEFFICIENT

MATRIX POROSITY = 0.65

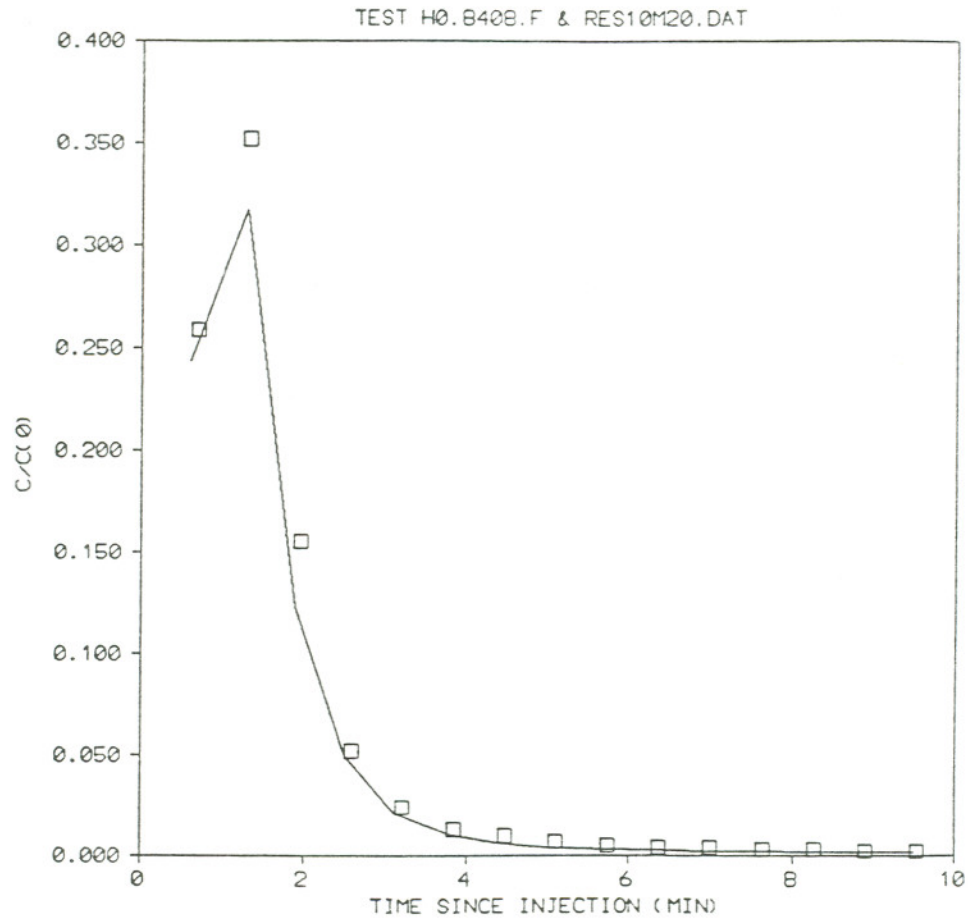


Figure IV.C.18 Fluorescein recovery curve and simulation results for the "push-pull" test H0.8408.F. (Piezometer H, Figure II.E.2.)

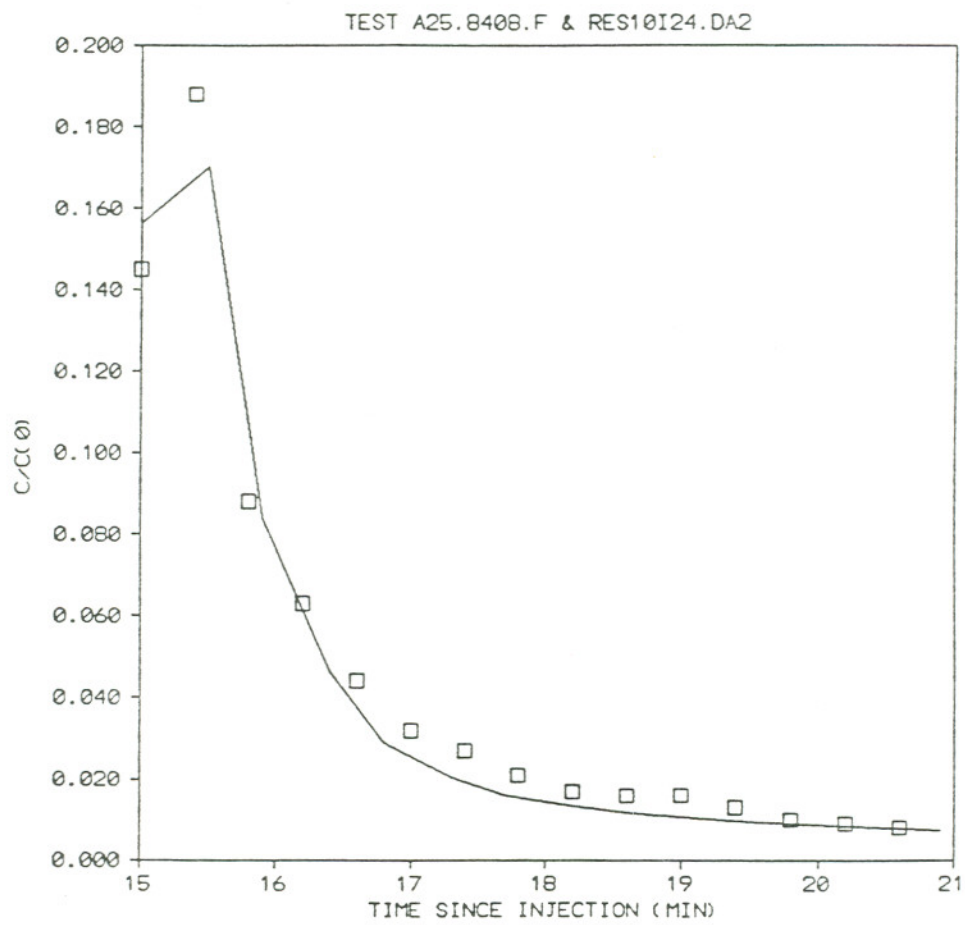


Figure IV.C.19 Fluorescein recovery curve and simulation results for the "push-pull" test A25.8408.F. (Piezometer A, Figure II.E.2.)

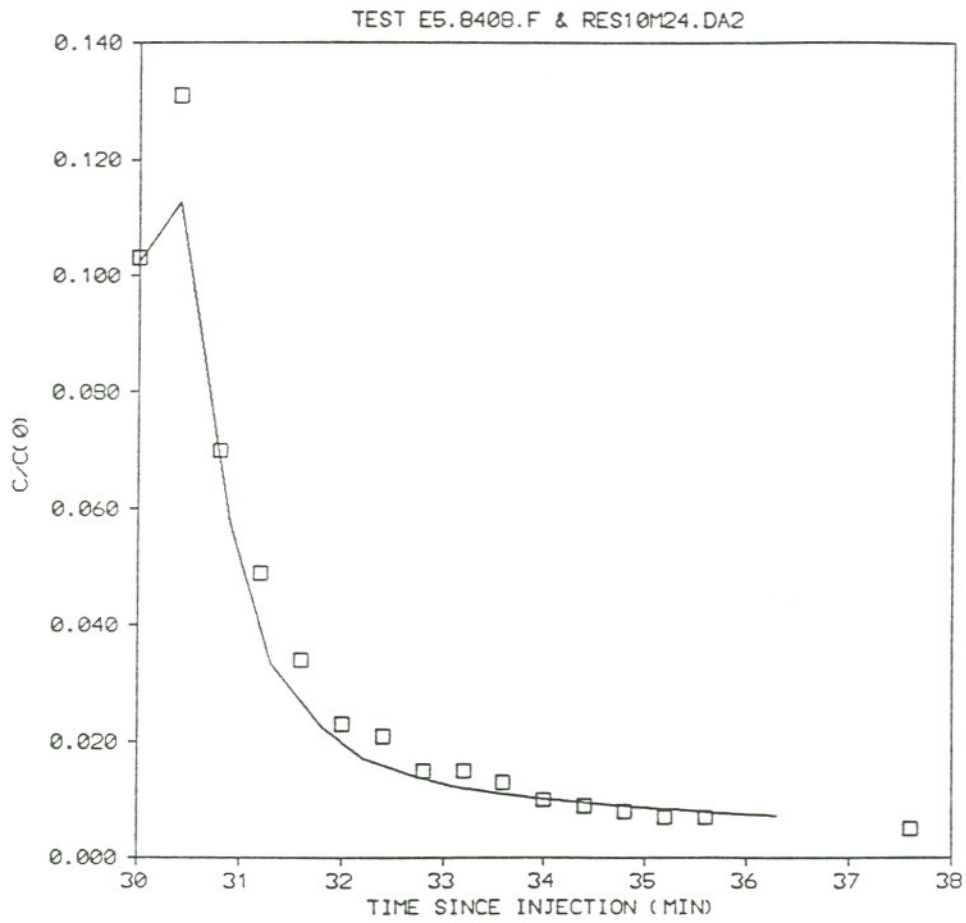


Figure IV.C.20 Fluorescein recovery curve and simulation results for the "push-pull" test E5.8408.F. (Piezometer E, Figure II.E.2.)

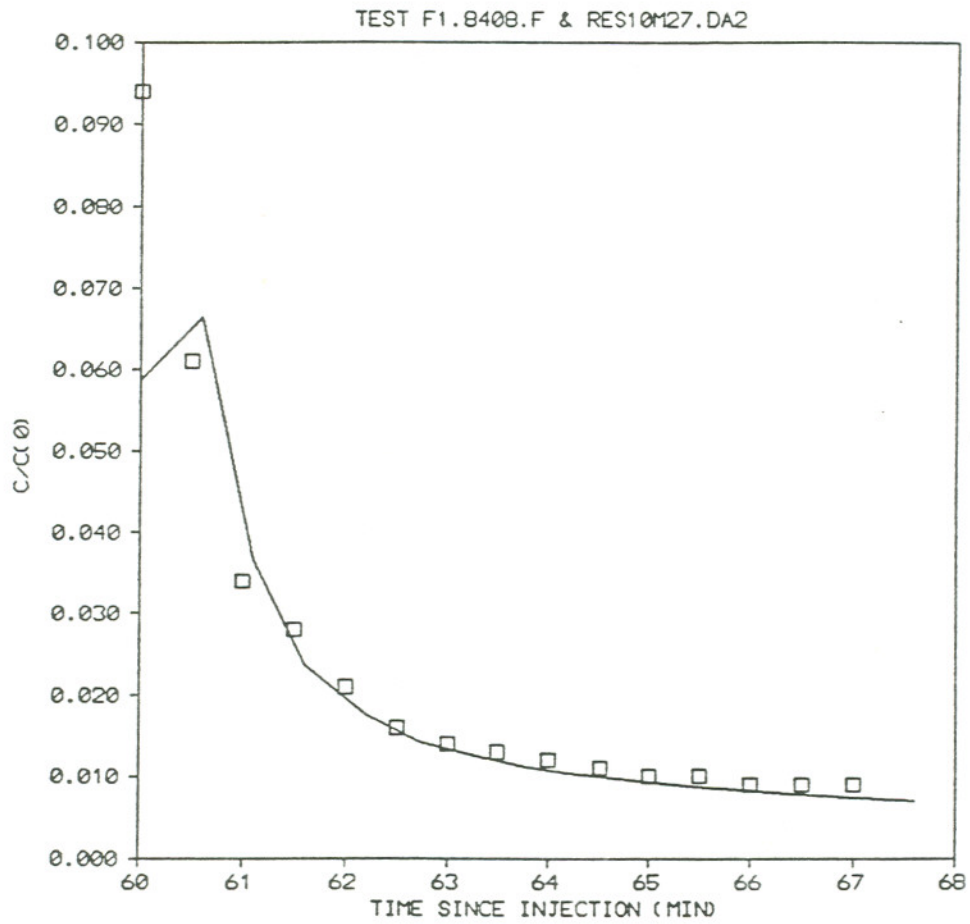


Figure IV.C.21 Fluorescein recovery curve and simulation results for the "push-pull" test F1.8408.F. (Piezometer F, Figure II.E.2.)

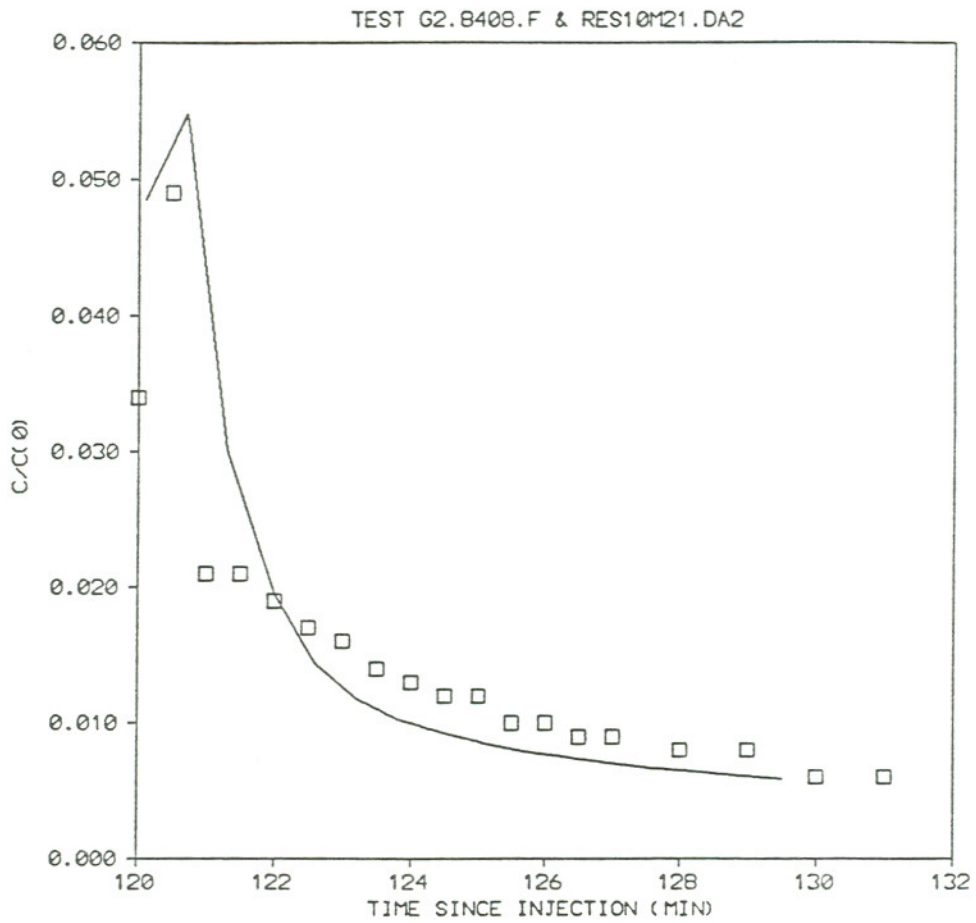


Figure IV.C.22 Fluorescein recovery curve and simulation results for the "push-pull" test G2.8408.F. (Piezometer G, Figure II.E.2.)

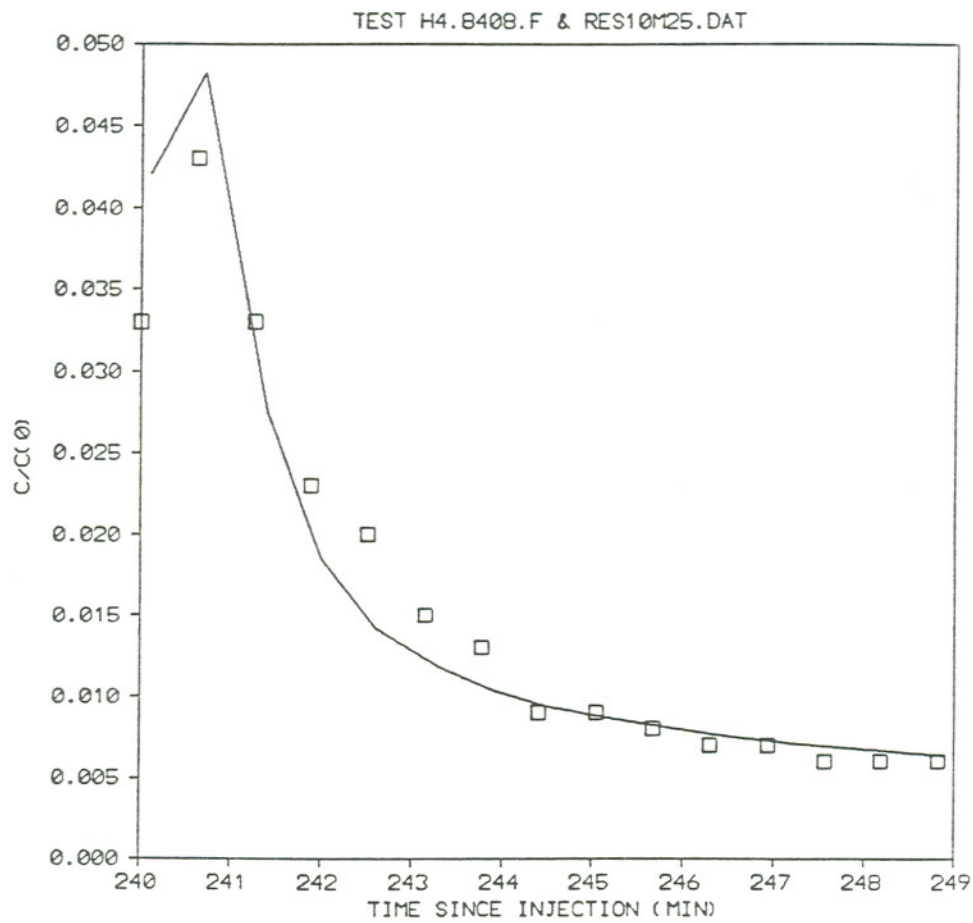


Figure IV.C.23 Fluorescein recovery curve and simulation results for the "push-pull" test H4.8408.F. (Piezometer H, Figure II.E.2.)

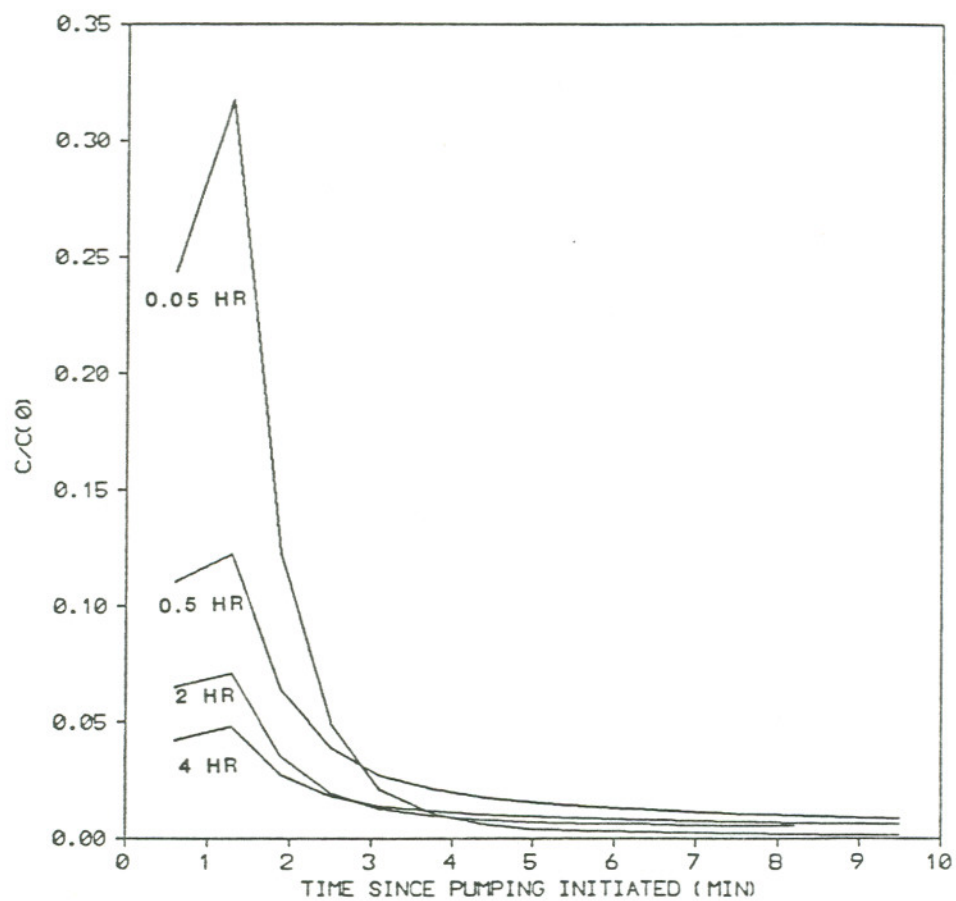


Figure IV.C.24 Sensitivity of the shape of the "push-pull" tracer recovery curve to residence time in the ground before pumping was initiated.

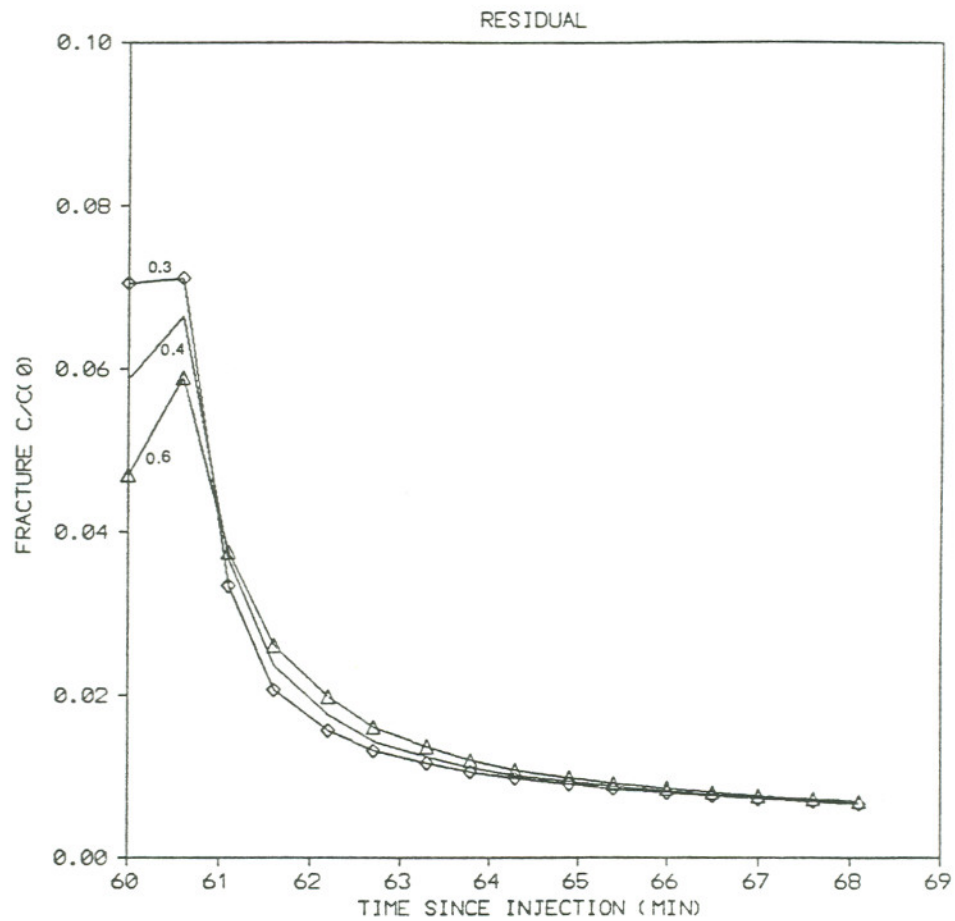


Figure IV.C.25 Sensitivity of the shape of the "push-pull" tracer recovery curve to dispersion caused by mixing in the fractures during recovery (called residual in the model).

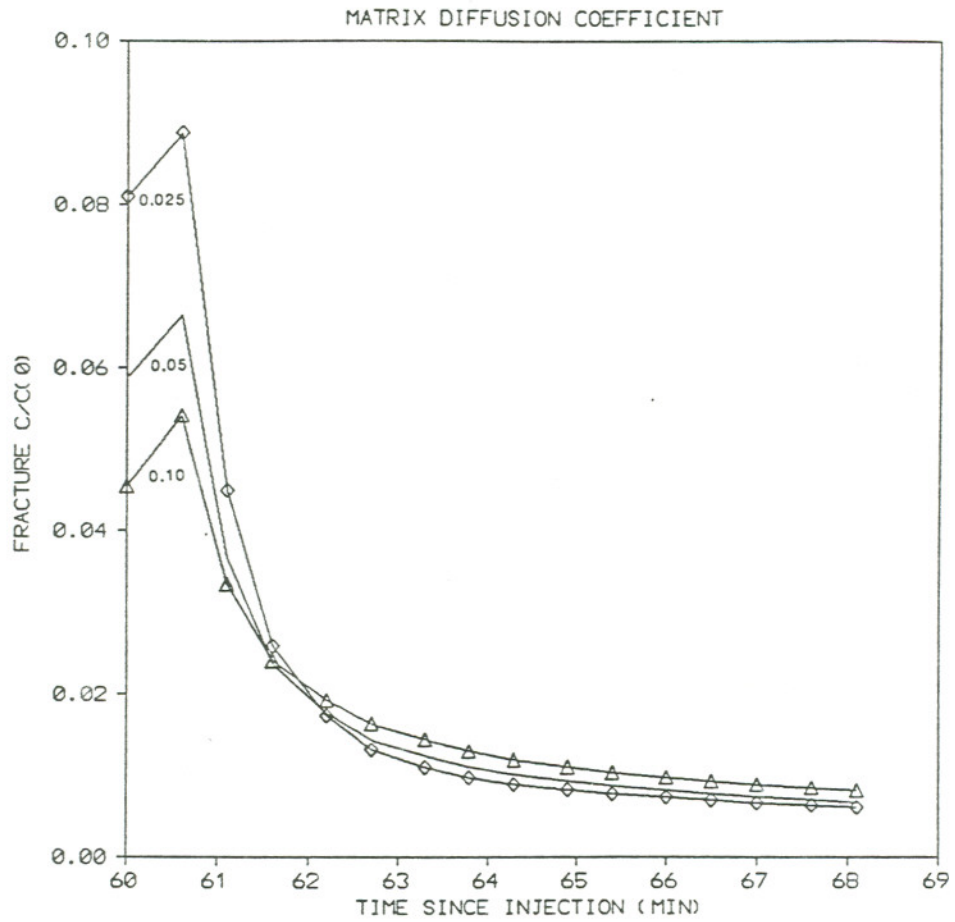


Figure IV.C.26 Sensitivity of the shape of the "push-pull" tracer recovery curve to the matrix diffusion coefficient.

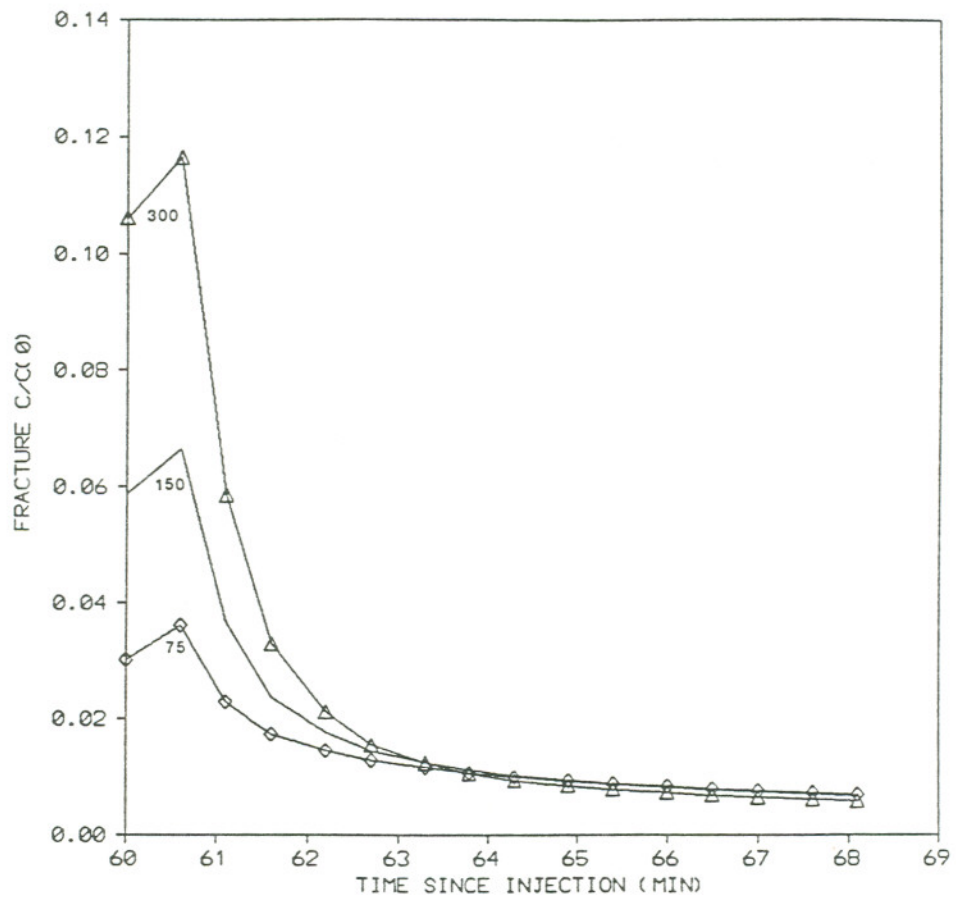


Figure IV.C.27 Sensitivity of the shape of the "push-pull" tracer recovery curve to fracture aperture. (μm)

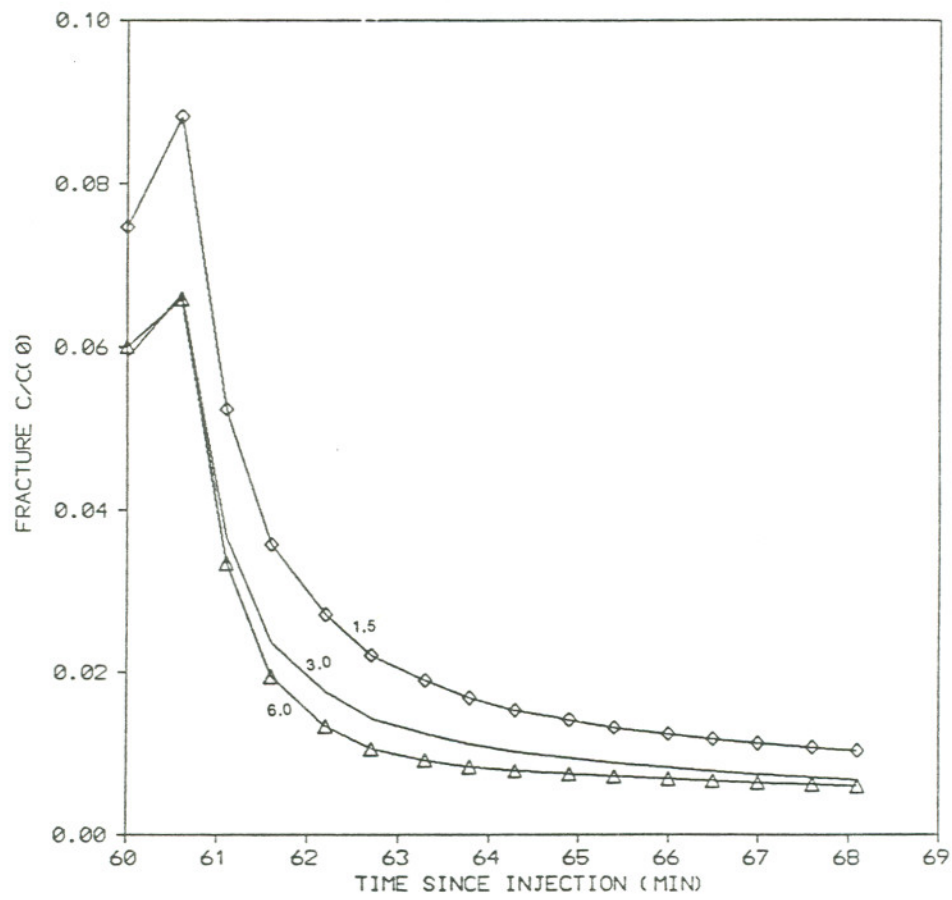


Figure IV.C.28 Sensitivity of the shape of the "push-pull" tracer recovery curve to fracture spacing. (mm)

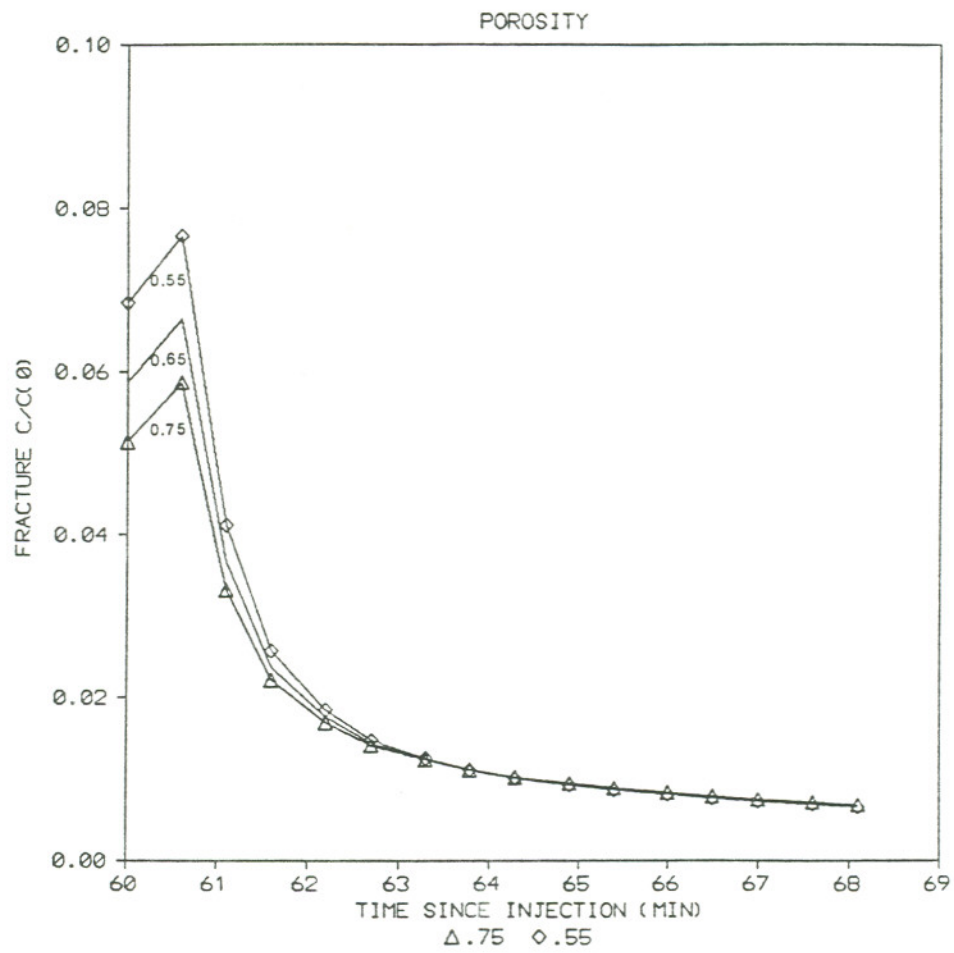


Figure IV.C.29 Sensitivity of the shape of the "push-pull" tracer recovery curve to matrix porosity.

recovery a dispersion term, "residual", was incorporated into the mathematical model. "Residual" has been defined as the fraction of the mass in the fractures at the beginning of pumping of an aliquot which remains in the fractures after that aliquot has been pumped. The "time = 0" tests were used to estimate a value for this parameter. A value of 0.4 was used in the mathematical simulations.

Although it is difficult to express quantitatively the uncertainties associated with each parameter, the values reported in Table IV.C.2 for fracture aperture and spacing and matrix diffusion coefficient are probably within a factor of two of the correct average values for the site. This level of uncertainty is of the same order as other measures of aquifer hydraulics (K_H , average velocity, etc.) and is therefore considered satisfactory.

Results of model calculations indicate that equilibration between the fractures and matrix is achieved fairly quickly at Alkali Lake. Figure IV.C.30 gives the mass remaining in the fractures as a function of time as estimated by the model. At 1 hour, more than 80% of the mass initially in the fractures should have diffused into the matrix and within approximately 6 hours the model predicts the system is essentially at equilibrium. This suggests that the equivalent porous medium model should work

MASS OF TRACER REMAINING IN FRACTURE

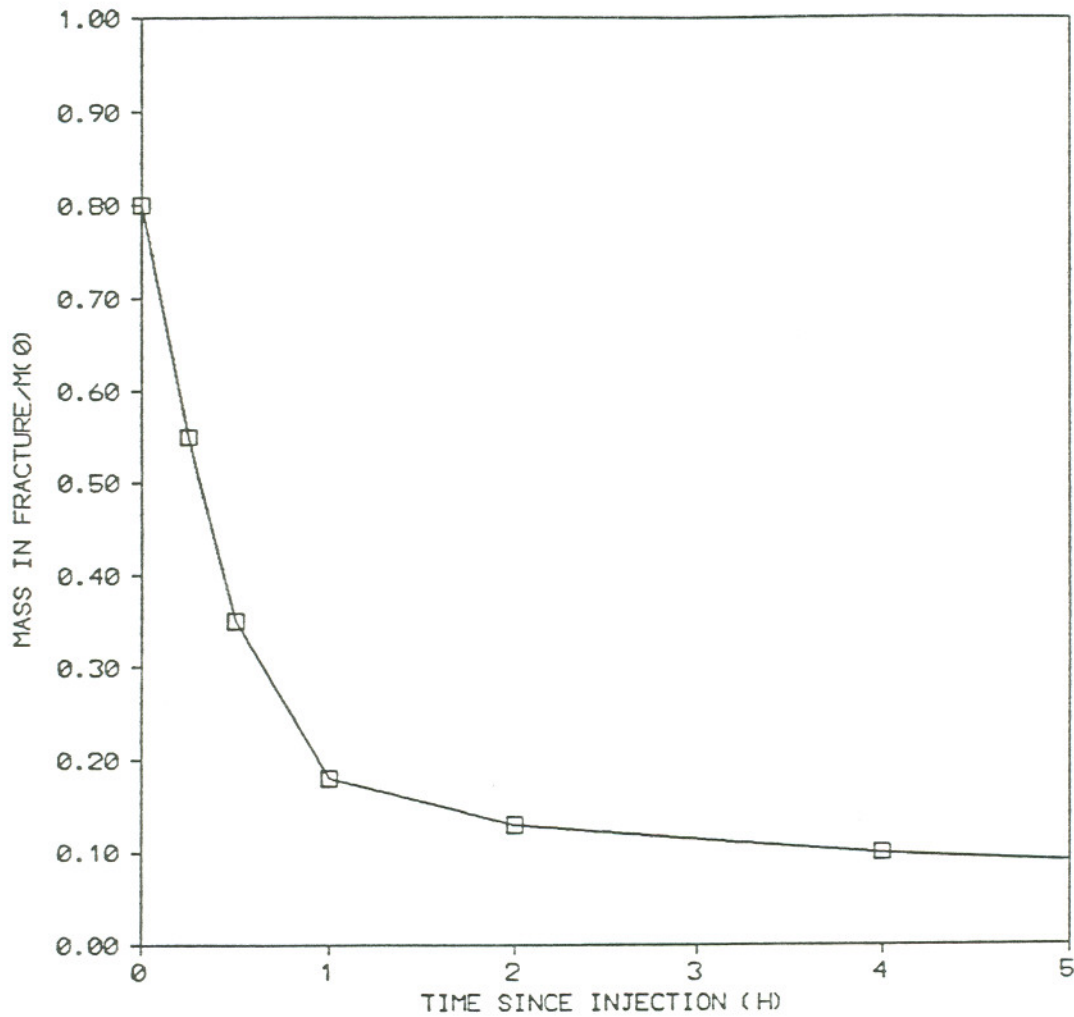


Figure IV.C.30 Mass of tracer remaining in the fractures versus residence time. Data are based on computer simulation of the "push-pull" tests.

well to predict contaminant transport at the Alkali Lake CDS.
(This will be discussed in greater detail in Section V.)

V. CONTAMINANT TRANSPORT AT THE ALKALI LAKE CDS

V.A INTRODUCTION

The purpose of the preceding sections has been to describe the processes which control the transport of the chlorophenolics at the Alkali Lake site. As has been demonstrated, solute transport in the groundwater is controlled by flow through fractures in the porous aquifer. During advective transport, the solutes were subject to dispersion as well as the retarding effects of diffusion and sorption. In this section, results of the preceding sections will be integrated into an explanation of the current distribution of contaminants at the site. The section is divided into four general parts: 1) an overview of retardation in porous and fractured media; 2) justification for describing the system as an equivalent porous medium; 3) a discussion of the current distribution of the chlorophenols and chlorophenoxyphenols; and 4) an explanation of the current distributions.

V.B RETARDATION IN POROUS AND FRACTURED MEDIA

Sorption has for some time been recognized as playing a fundamental role in retarding the movement of organic compounds in groundwater (Freeze and Cherry, 1979, Roberts et al., 1982). In porous systems, the extent to which a compound sorbs to the soil is described by the equilibrium partition coefficient (K_p). K_p is commonly determined by means of batch equilibrium experiments (as was reported here). The value of K_p depends on the nature of the soil, the solute, and to a lesser extent the nature of the aqueous phase. In practice, most modeling of the transport of sorbing organics has employed the Freundlich isotherm:

$$S = K_p C^{1/N} \quad (V.1)$$

where $S = (\text{g sorbed solute}) / (\text{g soil})$

$C = (\text{g dissolved solute}) / (\text{cm}^3 \text{ pore water})$

$N = \text{a constant greater than } 1.0.$

Linearity of the isotherm is often assumed ($N=1$), under which conditions the degree of retardation relative to the groundwater velocity for a homogeneous porous medium is given by:

$$R = 1 + \frac{\rho_b K_p}{n} \quad (V.2)$$

where R= the dimensionless retardation factor

ρ_b = soil bulk density

and n=soil porosity.

For a sorbed compound, the migration velocity will be less (by a factor of R) than the physical groundwater velocity.

The diffusion of solutes into zones of the aquifer matrix where there is no advective flow (immobile zones) has been much discussed recently as another mechanism for retardation. These zones can be either porous media between fractures (Freeze and Cherry, 1979; Grisak and Pickens, 1980,1981; Sudicky and Frind, 1982), or simply small volumes of aquifer of low hydraulic conductivity (van Genuchten, 1974). In such systems, even compounds which do not sorb will move more slowly than the physical velocity of the groundwater in the mobile regions since even non-sorbed compounds will diffuse into the immobile regions. A principle difference between the retardation effects of matrix diffusion and sorption is that the former is less compound specific. That is, for different species in a given molecular

weight range, the matrix diffusion coefficients (and therefore retardation due to matrix diffusion) will be of similar magnitude, while sorption can vary widely. In both porous and mobile/immobile (e.g. fractured) systems, the velocity of a non-sorbed compound is an obvious reference for considering the behavior of sorbed compounds. It is often of interest to compute the retardation of a sorbed compound relative to that of a non-sorbed compound. In the porous media case this relative retardation factor (R_r) will be the retardation factor calculated by Equation V.2, because in a porous medium a non-sorbed compound moves at the velocity of the groundwater. For sorbing compounds in a fractured system, however, the fraction of the solute sorbed to the soil will, in general, be less than predicted by Equation V.1. This is because the solute must diffuse from the fracture into the matrix in order to sorb. Competing with this process is advection in the fracture. The result is that, unless equilibrium between fracture and matrix is attained rapidly, sorption and hence retardation of the sorbing compound is reduced relative to a non-sorbed compound. (This is because more time is required for a sorbed compound to reach equilibrium with the matrix than for a non-sorbed compound.) If, however, equilibration between the matrix and fractures is rapid, the fracture system may, in time, approach the behavior of a porous medium.

V.C THE EQUIVALENT POROUS MEDIUM APPROACH

The presence at Alkali Lake of a very large number of small fractures and transport distances of several hundred meters has made it intractable to model the system as an assembly of discrete fractures. This is a problem of serious consequence and one which is frequently encountered in modeling contaminant transport in fractured systems. The most common method of overcoming this difficulty is to treat the system as an equivalent porous medium (EPM). The basic assumption underlying the EPM concept is that if at any given time nearly all of the solute is in equilibrium between the matrix and water, then the solute will effectively move as if all of the porous matrix (and not just the fractures) are available for advective transport. Though often used to describe such systems, this approach is seldom truly applicable, especially for sorbing compounds. Alkali Lake is a site at which the EPM approach appears to be appropriate. The reason for this lies in the nature of the fracture system. As discussed in Section II., the fractures probably had their origins as bedding planes in the lacustrine sediments. The bedding planes were opened into fractures by some physical process. As such the fractures are spaced at small and regular intervals and are spatially extensive, an ideal EPM

system.

An estimate of the time required for a system of regularly spaced fractures to develop the contaminant distribution profile predicted by the EPM model has been defined by Sudicky (1984) to be:

$$t = B^2/D' \quad (V.3)$$

where D' = matrix diffusion coefficient
and B = matrix half-width.

For the area down-gradient from the CDS, D' and B have been estimated as approximately $0.05 \text{ cm}^2/\text{day}$, and $.15 \text{ cm}$, respectively. This indicates that EPM behavior should be approached within one day. This is consistent with the results of the push-pull tests (Section IV.C). For sorbing compounds, the time needed to approach EPM behavior will be approximately the product of the time required for a non-sorbing compound to approach EPM behavior and the retardation factor due to sorption for that compound. (The meaning of retardation in a EPM system will be discussed shortly.) The largest retardation factor for the compounds of interest is 40, thus the roughly 2500 days since burial should have provided ample time to achieve EPM behavior.

For a system of parallel fractures, velocity in an EPM can be described in terms of the fracture velocity and geometry of the fracture system by the the equation:

$$V_{EPM} = V_{MF} \left\{ \frac{n_{MF} b}{n_{MF} b + n_{IM} B} \right\} \quad (V.4)$$

where n_{IM} =matrix porosity and n_{MF} =ratio of the open volume in the fractures to the total volume of the fractures. (Because fracture apertures are often calculated rather than measured, n_{MF} is generally taken as 1.0.) Equation V.2 can be rearranged to give an expression for the ratio of fracture velocity to EPM velocity:

$$R_D = \frac{V_{MF}}{V_{EPM}} = 1 + \frac{n_{IM} B}{n_{MF} b} \quad (V.5)$$

This equation is of very similar form to the classic porous media retardation factor (Equation V.2) and is the retardation factor due to matrix diffusion in an EPM system. For Equation V.5 to be satisfied, equilibrium must be established quickly between the mobile and immobile water, and essentially all of the solute mass must be in equilibrium at all times. Under these conditions, the solute will be transported as if all of the porosity were available for flow at a velocity of V_{MF}/R_D . If mass transport limitations prevent the rapid

establishment of an equilibrium partitioning (both physical and sorptive) between the mobile and immobile regions, then the transport velocity of the non-sorbing solute will be greater than predicted by Equation V.5.

If a compound sorbs in an ideal parallel fracture system which behaves like an EPM, the velocity of that compound can be estimated from the fracture geometry as:

$$V_{S-EPM} = V_{MF} \left(1 + \frac{\rho_t K_p}{n_t} \right) \left(1 + \frac{n_{IM} B}{n_{MF} b} \right) \quad (V.6)$$

where ρ_t and n_t are the bulk density and porosity of the total system of fractures plus matrix. More meaningful, perhaps, is the relative velocity (R_r) of a non-sorbed compound to a sorbed one. This is simply the ratio of Equations V.4 and V.6:

$$R_{r-EPM} = 1 + \frac{\rho_t K_p}{n_t} \quad (V.7)$$

which is equivalent to the retardation factor (Equation V.2) for the true porous medium case. Thus, in an equivalent porous medium, the relative retarded velocity (R_{r-EPM}) of a sorbed to a non-sorbed compound is the same as the porous medium retardation factor (R) predicted from the laboratory measurement

of the bulk physical properties ρ_t , K_p , and n_t . If mass transport limitations prevent equilibrium from being quickly established, the retardation of both non-sorbed and sorbed compounds will be reduced relative to the fracture water velocity. In addition, because sorbed compounds require more time to come into equilibrium with the matrix, the value of R_{r-EPM} will also be reduced.

The average groundwater velocity has been estimated from both the natural gradient tracer test and the current distributions of the chlorophenols. An additional estimate can be calculated from field data using Equation V.4 and a solution of the Navier-Stokes equation (Grisak and Pickens, 1980):

$$V_{MF} = \frac{r_L g (2b)^2}{12\mu} \frac{dh}{dx} \quad (V.8)$$

where V_{MF} = average velocity in the fracture

r_L = fluid density

g = gravitational constant

$2b$ = fracture aperture

dh/dx = hydraulic gradient, and

μ = dynamic viscosity of the fluid.

Using values of .0005 and 1.5×10^{-4} m for the gradient and fracture aperture, respectively, an average fracture velocity

of 0.7 m/day is calculated using Equation V.4. This is the expected fracture velocity in the vicinity of the natural gradient tracer site. Using the same aperture, and with fracture porosity, matrix porosity and fracture spacing values of 1.0, 0.65, and 0.003 m, respectively, a value of $V_{EPM}=0.05$ m/day is calculated. This value is nearly the same as the velocity estimated from the natural gradient test. The gradient at the tracer site is approximately half of the value of the gradient immediately west of the CDS, thus a more representative average velocity for the non-sorbed components of the contaminant plume is 0.1 m/day.

An effective longitudinal dispersion must also be estimated if a fractured system is to be modeled as an EPM. Again, the natural gradient tracer test can be used for this, or dispersion may be calculated from the physical properties of the fracture system. In Section IV.B D_{L-EPM} was estimated to be 0.15 m²/day. Sudicky (1983) has derived an equation for D_{L-EPM} for an ideal parallel fracture system as:

$$D_{L-EPM} = (b^2 B^3 (v_{MF})^2) / (3D'(B+b)^3) \quad (V.9)$$

Using $D' = 5 \times 10^{-6}$ m²/day and $v_{MF} = 1.4$ m/day a

value of $D_{L-EPM}=7.35 \times 10^{-4} \text{ m}^2/\text{day}$ is estimated.

This is much less than observed in the tracer study. Equation V.9 computes the effective dispersion caused by the process of matrix diffusion, it does not take into account dispersion processes which might be encountered in a non-ideal flow system (e.g. non-plug flow through the fractures due to wall roughness or variable aperture, mixing caused by discontinuities in the flow path, etc.). These are probably important at the site, and thus equation V.9 underestimates dispersion. The tracer study-derived value of $0.15 \text{ m}^2/\text{day}$ will be used in the EPM modeling in this dissertation.

V.D OBSERVED RETARDATION OF THE CHLOROPHENOLICS

If the di- and trichlorophenols are treated as non-sorbing compounds (especially 2,6-DCP), it should be possible to calculate relative retardation factors for the sorbing chlorophenolics using the 2% and 25% transport distances of the compounds with the relative retardation factors based on the bulk properties of the soil-water system. The success of this approach will be a measure of how well the site is described by the one-dimensional EPM. Values of $R_r(2\%)$ and $R_r(25\%)$ for the sorbed compounds as well as their retardation factors are summarized in Table V.D.1. The observed $R_r(2\%)$ and

TABLE V.D.1. RELATIVE RETARDATION FACTOR DATA

COMPOUND	$R_r(2\%)^a$	$R_r(25\%)^b$	R^c
2,4-DCP	1.0	1.0	1.0
2,6-DCP	1.0	1.0	1.0
2,4,6-TCP	1.0	1.0	1.0
TeCP	1.2	1.2	3.5
PCP	1.5	6.2	13.5
CL2D2	1.7	3.6	34.
CL3D3	1.4	1.7	20.
CL4D2	1.9	6.2	40.

^a $(X(2\%) \text{ for } 2,6\text{-DCP}) / (X(2\%) \text{ for compound of interest})$

^b $(X(25\%) \text{ for } 2,6\text{-DCP}) / (X(25\%) \text{ for compound of interest})$

^c porous media retardation factor

R_r (25%) are much smaller than the predicted R values. This indicates either that the EPM approach is not valid, or some other assumption has not been met.

As mentioned in Section III, the use of 2% and 25% concentration fronts instead of the 50% front leads to an artificial lowering of the R_r values. The amount of error introduced by using the 2% and 25% transport distances has been estimated using a one-dimensional porous medium model. Values for the longitudinal dispersion and velocity were taken from the natural gradient tracer test data (Section IV). Transport distances corresponding to the 2%, 25% and 50% concentration fronts for compounds which behave like 2,6-DCP, TeCP, CL3D3 and CL4D2 in groundwater flowing at 0.1 m/day for 2500 days are shown in Table V.D.2. From these data, relative retardation factors for the three concentration fronts were calculated (Table V.D.3). The observed R_r values decreased relative to the retardation factor used in the model with both increasing retardation factor and decreasing frontal concentration. For the compounds of interest at the Alkali Lake CDS, the errors resulting from using the 2% and 25% concentration fronts instead of the 50% front are shown in Table V.D.4. While these represent, in some cases, substantial discrepancies, the error introduced is small in comparison to the differences between the expected retardation and those observed at the site (Table V.D.1)

TABLE V.D.2. SIMULATED TRANSPORT DISTANCES FOR THE 2%,
25% AND 50% CONCENTRATION FRONTS

R ^a	X(50%)(m)	X(25%)	X(2%)
1.0	254	278	340
3.5	75	89	117
20.	15	21	33
40.	8	12.5	20

^aR = The retardation factor used in the porous media model.
Other model parameters included velocity = 0.1 m/day and
dispersivity = 3.0 m.

TABLE V.D.3. RELATIVE RETARDATION FACTORS CALCULATED
FROM THE DATA OF TABLE V.D.2

R^a	$R_r(50\%)$	$R_r(25\%)$	$R_r(2\%)$
3.5	3.4	3.1	2.9
20.	16.9	13.2	10.3
40.	31.8	22.2	17.0

^a R =the retardation factor used in the porous media model.

Other model parameters included velocity = 0.1 m/day and
dispersivity = 3.0 m.

TABLE V.D.4. ESTIMATIONS OF ERROR INTRODUCED BY USING 2%
AND 25% RELATIVE RETARDATION FACTORS
(BASED ON THE DATA OF TABLE V.D.3.)

R^a	$R_r(25\%)/R_r(50\%)$	$R_r(2\%)/R_r(50\%)$
3.5	0.91	0.85
20.	0.78	0.61
40.	0.70	0.55

^a R =the retardation factor used in the porous media model.

Other model parameters included velocity = 0.1 m/day and

dispersivity = 3.0 m.

The normalized concentrations from the source line down the center of the plume for the chlorophenolics are plotted in Figures V.D.1-2. For four of the chlorophenolics, concentration vs. distance from the site have been plotted in Figures V.D.3-6. along with the concentration predicted by the one-dimensional EPM model (using a velocity of 0.1 m/day and a longitudinal dispersion coefficient of $0.15 \text{ m}^2/\text{day}$). The differences between the two sets of curves are dramatic. The shape of the contaminant distribution curves, in particular 1) the rapid drop in observed concentration with distance from the site; and 2) the "leveling out" of the curves for all of the compounds at 100- 250 m from the source, cannot be explained by the EPM model. It is this leveling out which leads to the reduced values of R_r for the sorbed compounds.

V.E POSSIBLE EXPLANATIONS OF CONTAMINANT DISTRIBUTIONS

There are a number of possible explanations for why the observed contaminant distributions are not as predicted by the EPM model: 1) the basic EPM assumption of rapid equilibrium was not met; 2) the concentrations of contaminants moving from the site changed with time; 3) co-solvent effects led to decreased sorption of TeCP, PCP, and the CPPs; 4) the initial distribution

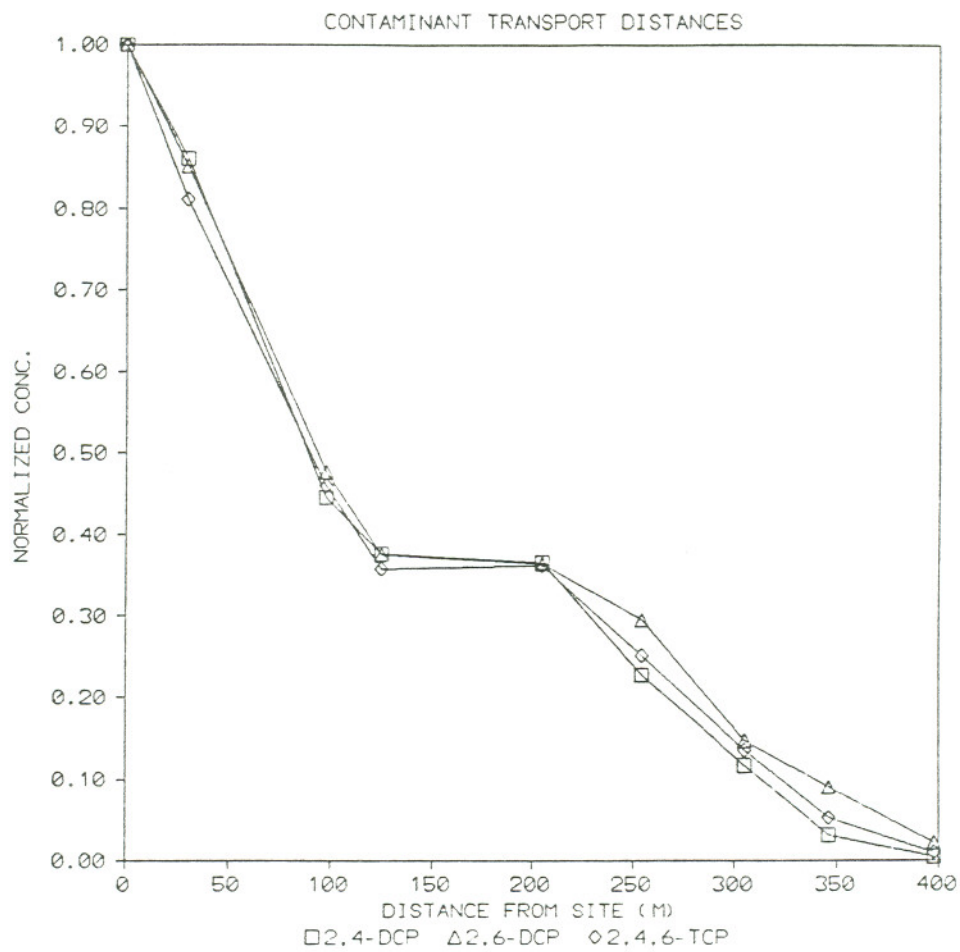


Figure V.D.1 Normalized concentration down the approximate contaminant plume center versus distance from the site for 2,4-DCP, 2,6-DCP and 2,4,6-TCP.

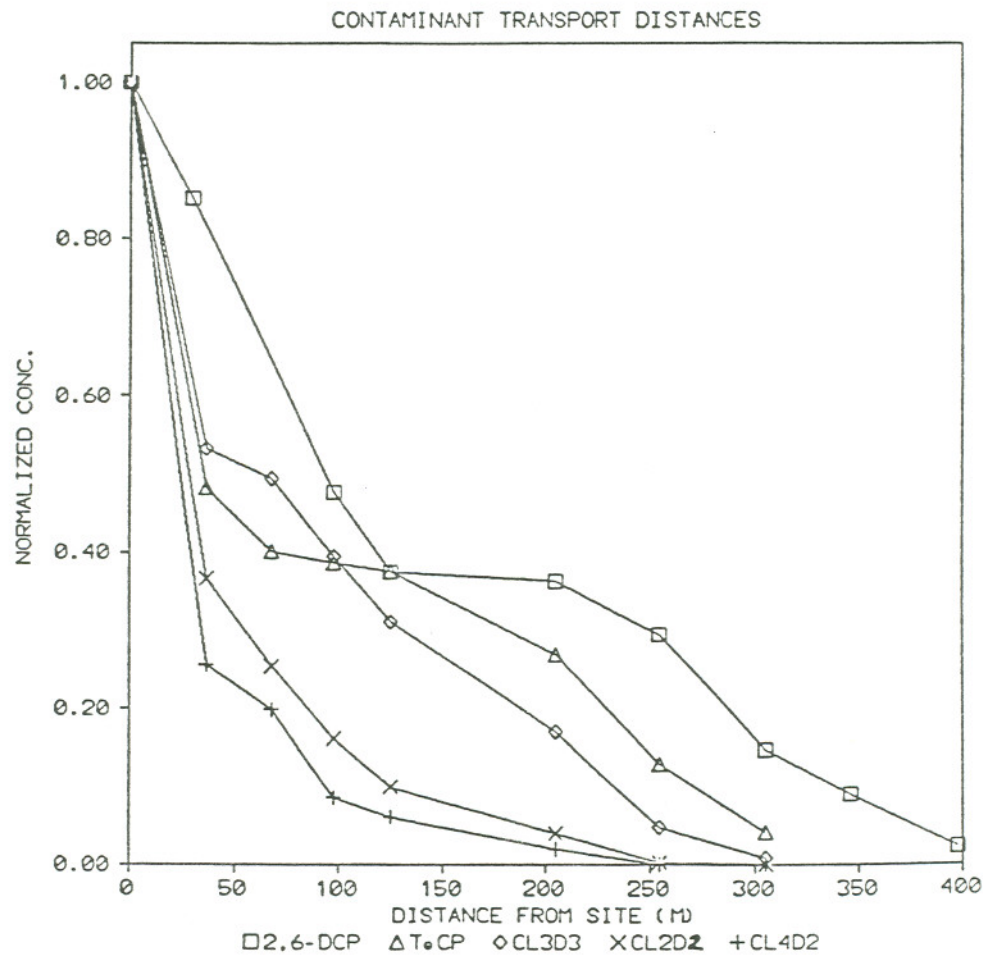


Figure V.D.2 Normalized concentration down the approximate contaminant plume center versus distance from the site for 2,6-TCP, TeCP, CL3D3, CL2D2, and CL4D2.

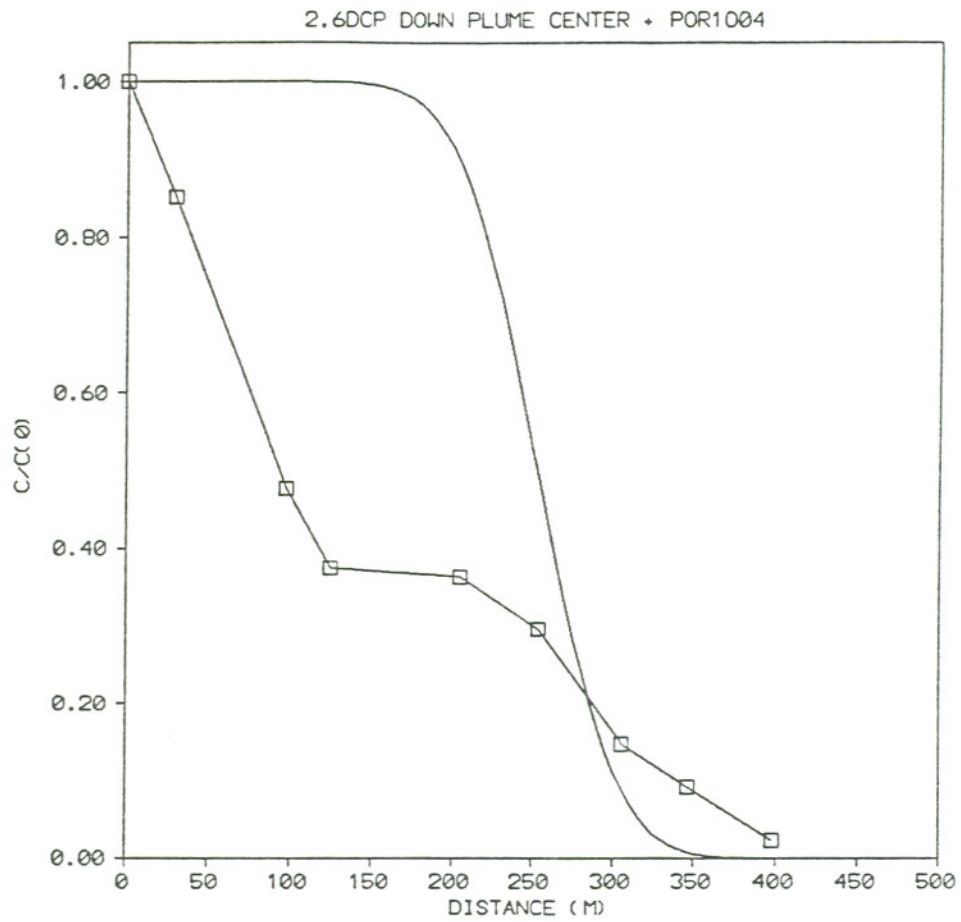


Figure V.D.3 Normalized concentration down the approximate contaminant plume center and one-dimensional EPM simulation of the contaminant distribution versus distance from the site for 2,6-DCP.

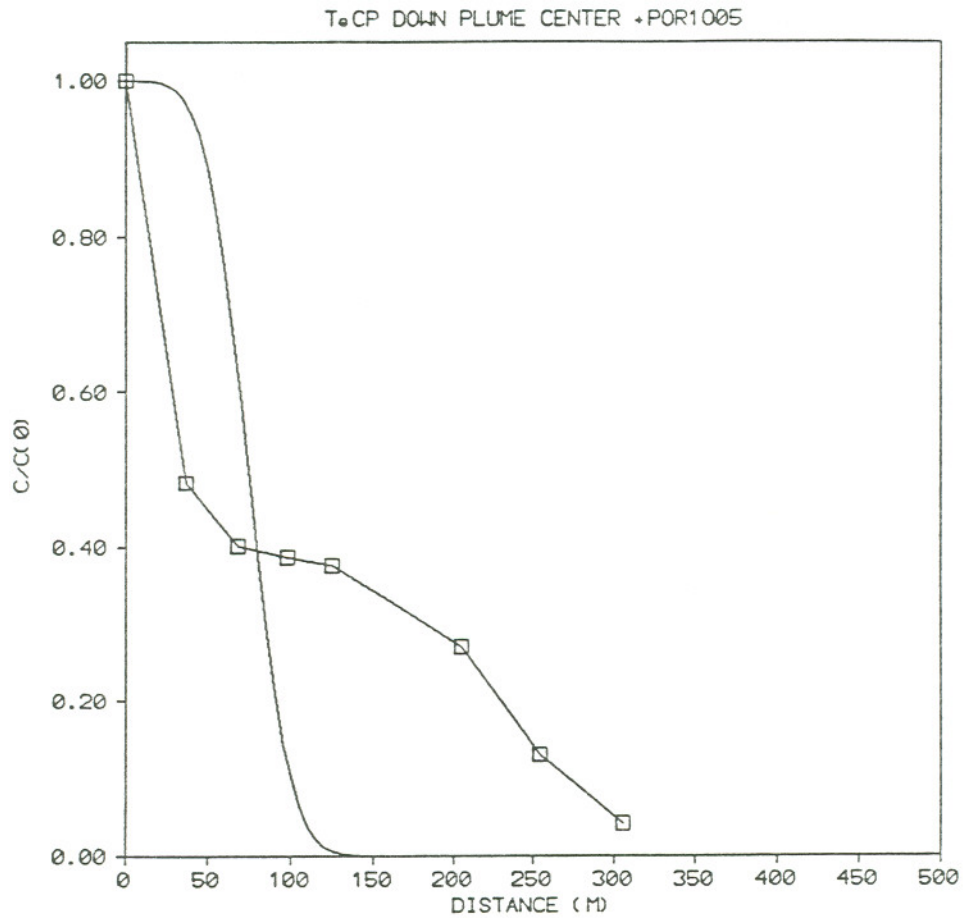


Figure V.D.4 Normalized concentration down the approximate contaminant plume center and one-dimensional EPM simulation of the contaminant distribution versus distance from the site for TeCP.

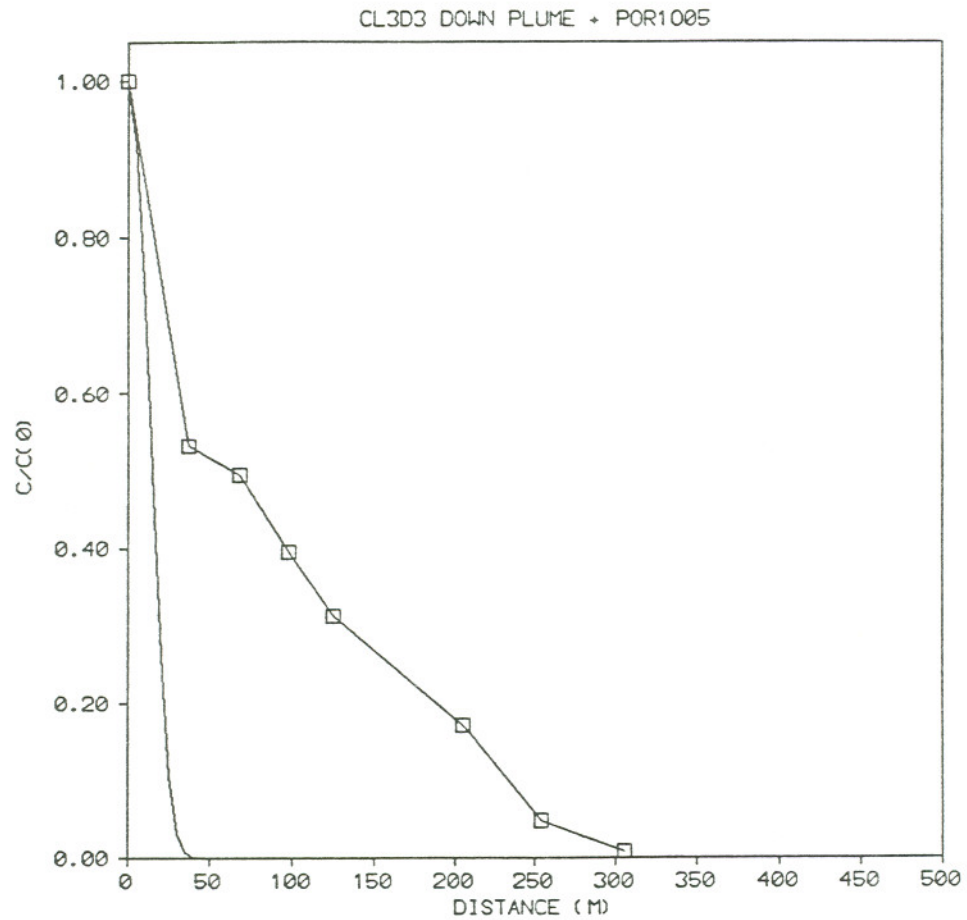


Figure V.D.5 Normalized concentration down the approximate contaminant plume center and one-dimensional EPM simulation of the contaminant distribution versus distance from the site for CL3D3.

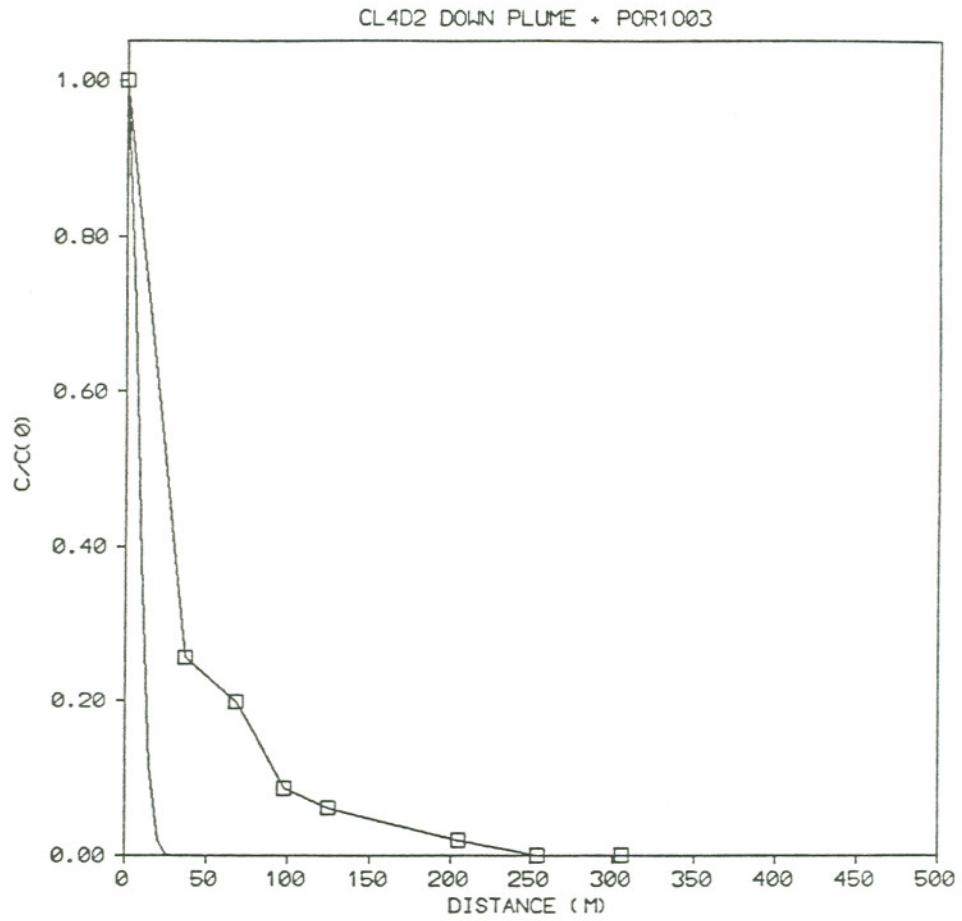


Figure V.D.6 Normalized concentration down the approximate contaminant plume center and one-dimensional EPM simulation of the contaminant distribution versus distance from the site for CL4D2.

of contaminants within the site was not uniform at the time of the original burial; 5) the groundwater velocity and direction were not uniform within the study area.

The EPM approach should be appropriate, if all of the other assumptions are valid. All of the field tracer data suggests that equilibrium between the fractures and matrix is rapid. The fact that the contaminant plume has had more than 2500 days to develop should result in a "typical" porous medium contaminant distribution curve.

Co-solvent effects could be due to either actual solvents in the contaminant plume and/or the high levels of di- and trichlorophenols. Since the bulk of the wastes buried at the site were in aqueous solution, large quantities of solvents are not believed to have been present in the waste, nor have any been detected at high concentrations. Since batch equilibrium experiments demonstrated no changes of the K_p values with overall phenol concentration nor with the addition of 500 mg/L of 2,4-DCP, co-solvent effects due to the high concentrations of chlorophenols in the plume itself also do not appear important.

The two most likely scenarios for changing source strength are a decrease or an increase with time. A source which decreases with time could explain the "leveling" of the tails of

the distributions, but not the sharp decrease in concentrations observed close to the site. An increasing source could show the rapid decrease with distance, but concentrations should fall even faster in the tails than for the simulated continuous source used in the Figures V.D.3-6. Therefore, a change in source strength does not seem an explanation of the observed distributions.

Figures III.D.1-8 provide evidence that the various compounds were not distributed uniformly in the site. It appears that the trenches of waste near the selected transport reference line have contributed most of the contamination of the compounds of interest since the concentrations of both the non-sorbed and sorbed compounds are highest in that area. The fact that the maximum concentrations for both sorbing and non-sorbing compounds occur roughly on the transport line also argues against movement of the centers of mass of the sources with time. If contaminants were distributed throughout the site and were all moving (e.g. if the contaminants were initially all in the groundwater below the site, rather than above the water table), the center of mass of the contaminants within the site would be shifting to the west. The rate of movement for the sorbed and non-sorbed compounds would be different. Since the high concentrations of each contaminant are all nearly on the same reference line, it seems unlikely that the original positioning of contaminants within the site could have occurred in such a manner as to generate the

current concentration maxima in the line observed.

Concentrations are also not uniform along the transport reference line (TRL). As a result, the source may act like one or more point sources, and transverse dispersion could cause a more rapid decrease in concentration with distance than predicted by the EPM model. If integrated transects of contamination rather than concentration are plotted vs. distance, the effect of transverse dispersion will be eliminated and the contaminant distribution should be the same as in a one-dimensional case. Integrated transects of contaminant distribution for all of the compounds are found in Figures V.E.1-2 and for four of the compounds have been plotted together with normalized concentrations (Figures V.D.1-2) vs. distance from the site (Figures V.E.3-6). Transects of TeCP, CL3D3, and CL4D2 all fall below, rather than above the normalized concentration line. For 2,6-DCP within 150 m of the site, the two normalized curves are essentially identical. This would not be the expected result if transverse dispersion is important.

The integrated transect data, combined with the patterns of contaminant distribution along the TRL suggest that water flow past the TRL is not uniform. These data suggest that the primary path of water flow is at the southern edge of the site. This conclusion is reached for two primary reasons. First, the

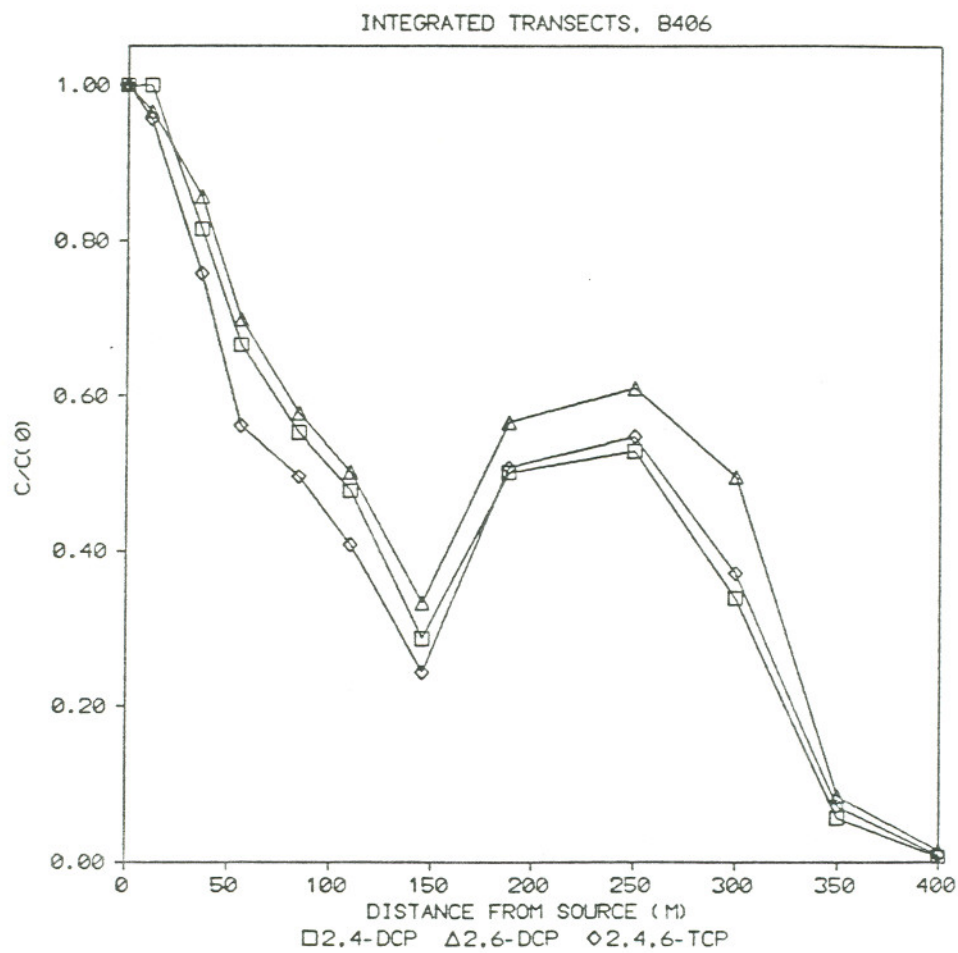


Figure V.E.1 Normalized integrated transects versus distance from the site for 2,4-DCP, 2,6-DCP and 2,4,6-TCP.

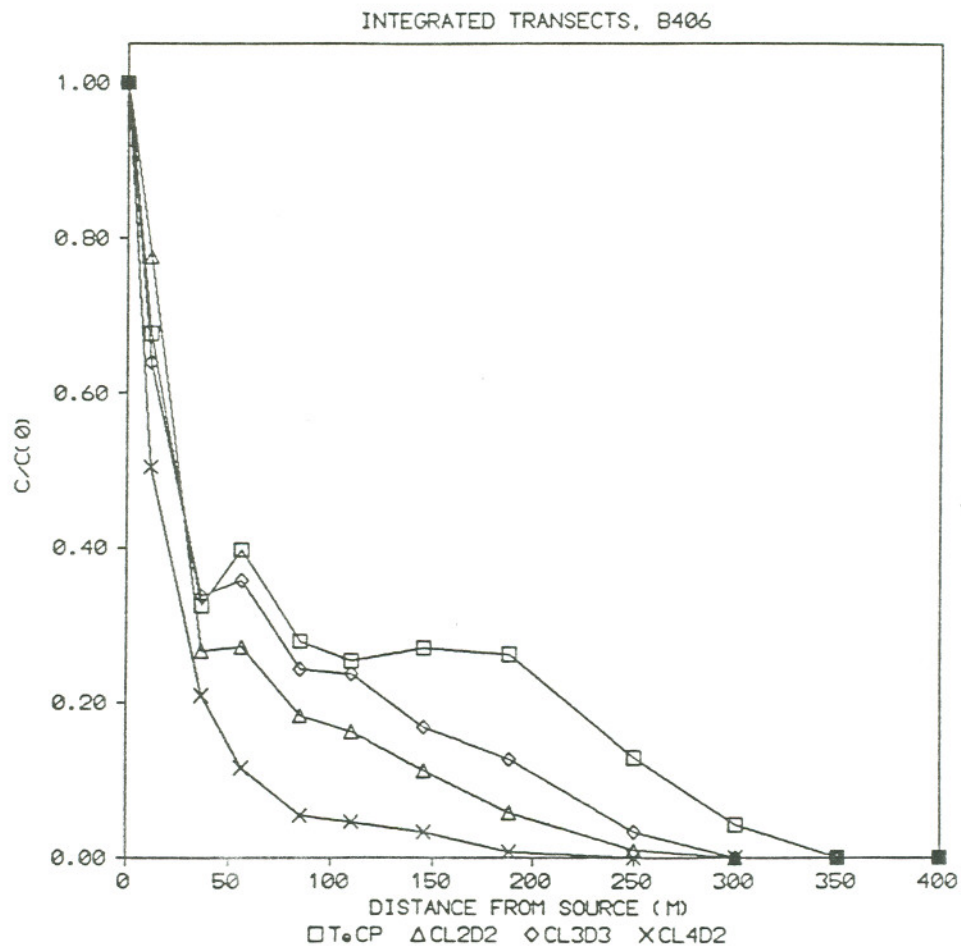


Figure V.E.2 Normalized integrated transects versus distance from the site for TeCP, CL2D2, CL3D3 and CL4D2.

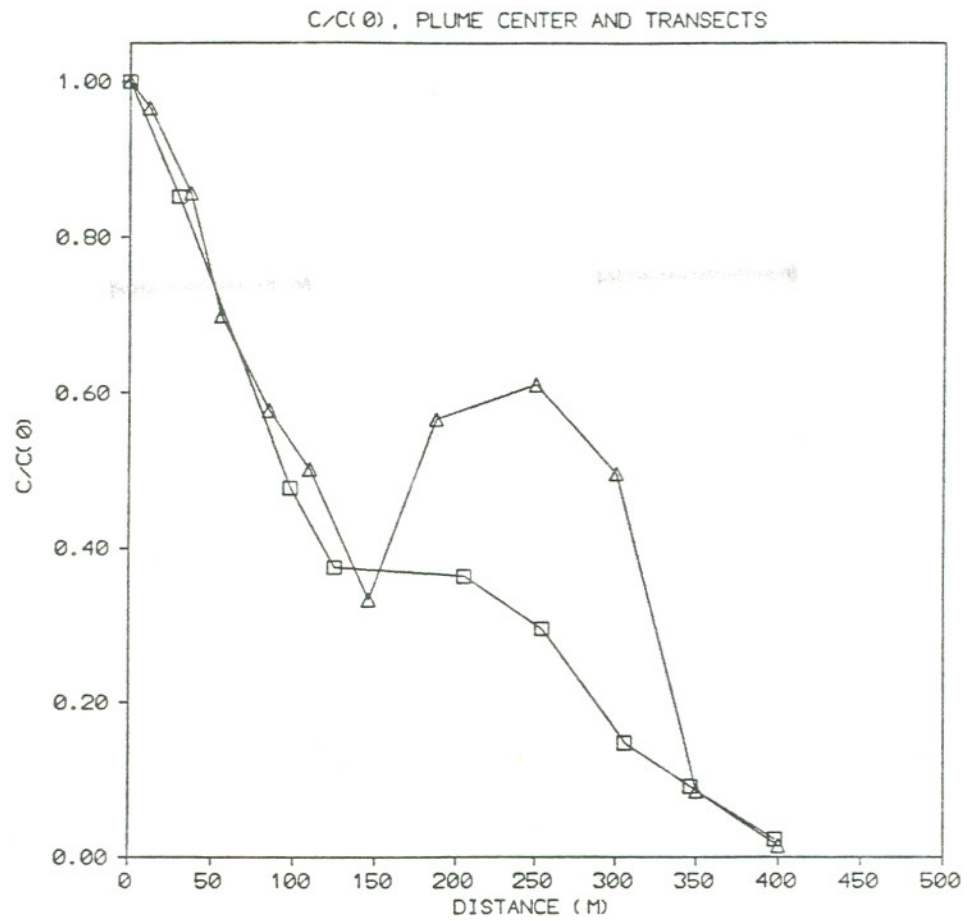


Figure V.E.3 Normalized concentration and normalized integrated transect versus distance from the site for 2,6-DCP.

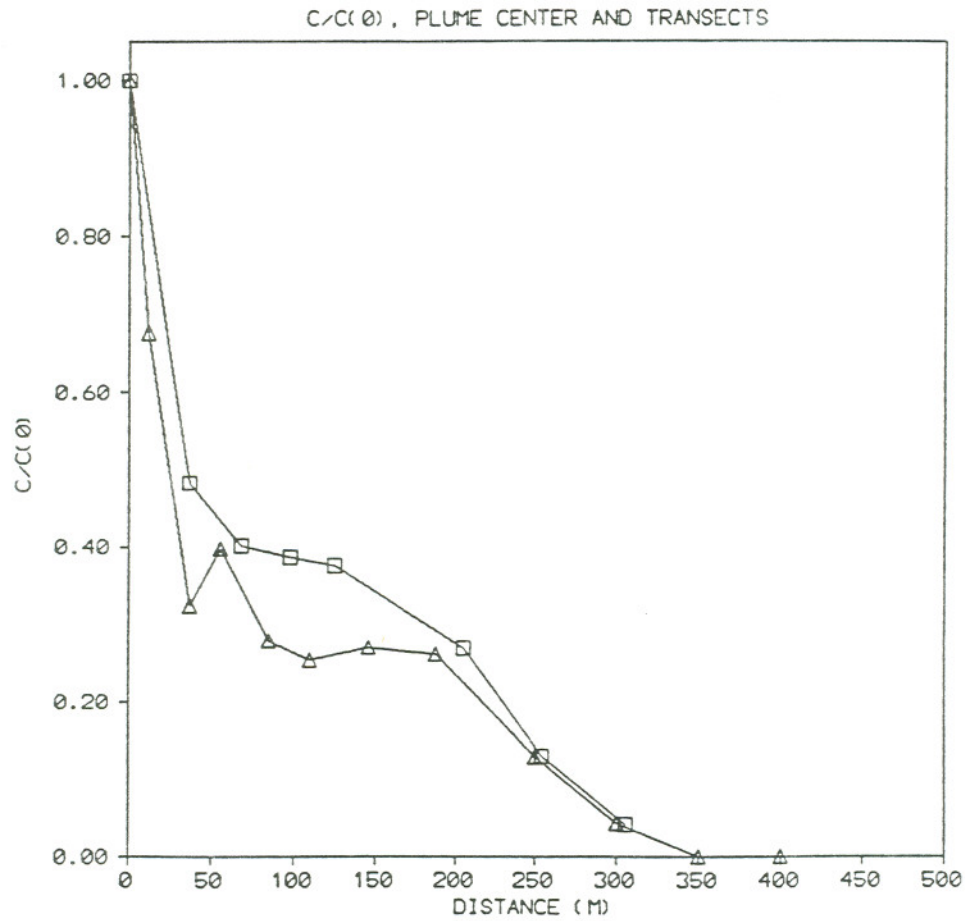


Figure V.E.4 Normalized concentration and normalized integrated transect versus distance from the site for TeCP.

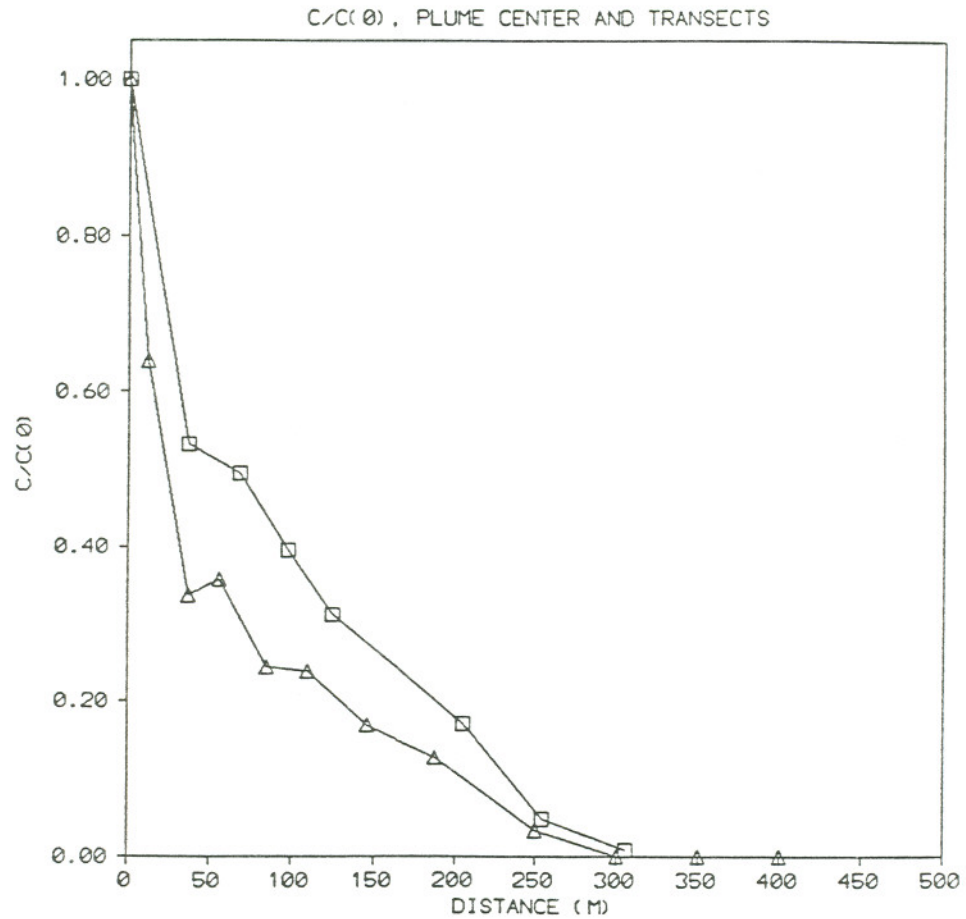


Figure V.E.5 Normalized concentration and normalized integrated transect versus distance from the site for CL3D3.

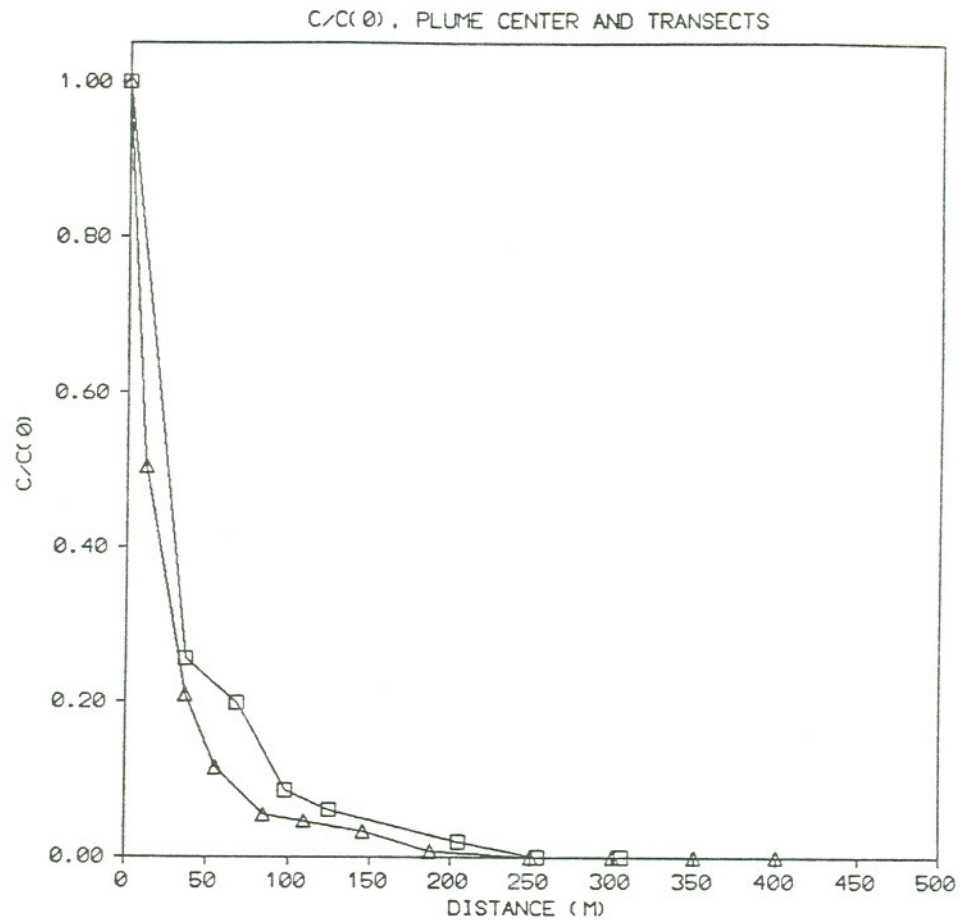


Figure V.E.6 Normalized concentration and normalized integrated transect versus distance from the site for CL4D2.

transect data for TeCP, CL3D3, and CL4D2 (as well as PCP and CL2D2) all fall below the "plume center" concentration values. The most probable explanation of this is that only part of the "line source" of contaminants is being exposed to the flow. Second, within 150 m of the site the shape of the 2,6-DCP (as well as 2,4-DCP and 2,4,6-TCP) transects are essentially the same as those of the normalized concentrations. For this to occur these compounds must have sources which behave somewhat like a "line source". For both of the above to be true the primary groundwater flow path must be near the point of high chlorophenol concentration at the southern edge of the site. This conclusion is consistent with the specific conductance survey (Figure II.C.9) which shows a path of low conductance water at the southern edge of the site.

Distributions of the sorbing compounds (all of which have areas of high concentration in the northwest portion of the site) suggest that there is also some groundwater flow moving west near the northern edge of the site, and that the northerly and southerly flows converge to the west of the site. This is supported by the detailed water table survey which suggests that K_H within the site is less than the surrounding area, and may cause much of the groundwater flow to divert around the site. The converging of groundwater flow 100-200 m west of the site is probably the result of a K_H -defined "constriction". This

constriction probably explains the narrowing of the di- and trichlorophenol contaminant plumes in that region.

The integrated transect for 2,6-DCP indicates an increase in mass of that compound beyond 150 m west of the site. This is the result of a slowing and lateral spreading of the contaminant plume as it moves closer to West Alkali Lake. This is consistent with the water table data of Figure II.C.6, which indicates a general decrease in hydraulic gradient beyond 150 m west of the site. It appears from the contaminant distributions that all of the compounds are currently being transported through the "constriction" 150+/-50 m west of the site. The leading edges of the plumes for the non-sorbed compounds have largely stagnated on the downgradient side of the constriction. The leading edges of the contaminant distributions of the sorbed compounds, however, are still moving. This is the primary reason why the $R_r(2\%)$ and $R_r(25\%)$ values estimated from the contaminant distributions are less than the calculated porous media retardation factors (R).

VI. CONCLUSIONS

The areal distributions of eight chlorinated phenolics have been used in discussions of the groundwater transport of organic compounds hydraulically downgradient from the Alkali Lake CDS. The primary features of this transport are as follows: 1) the CDS is located in a geographic conduit between Alkali Lake and West Alkali Lake; 2) springs to the east of the site create a water mound which provides the hydraulic gradient to move the contaminants; 3) groundwater moves westward around and through the site and passes through a "constriction" approximately 150+/-50 m west of the site, and 4) beyond the "constriction" contaminants spread out and slow down as West Alkali Lake is approached.

Groundwater transport near the CDS is facilitated by the presence of a very large number of fractures in the soil. These fractures probably had their origins as bedding planes in the lacustrine sediments which were opened by the processes of dehydration and rehydration or by dissolution of carbonates. Groundwater velocities within these fractures may exceed 1 m/day, even under the mild gradients (~ 0.001) present at the site.

The most important factors controlling the shape of the contaminant distributions downgradient of the CDS are matrix diffusion, sorption and areal variations in groundwater flow within the study area. Sorption and matrix diffusion are important in controlling the distances to which the contaminants have been transported, while variations in groundwater flow are responsible for the overall shape of the contaminant plume.

Concentrations of the contaminants drop off rapidly with distance immediately downgradient of the CDS primarily because of the non-uniform flow past the transport reference line (TRL). At a distance of ~150-200 m west of the CDS the contaminant transport slows and begins to spread. Concentrations in this region change more slowly than near the site. In fact, the integrated transects of the non-sorbed compounds increase with distance in this region. The non-sorbed compounds are affected by this stagnation to a much larger extent than the sorbed compounds. The result is a decrease in the observed R_r values.

The variation in the local groundwater velocity and direction are the principle reasons why the one-dimensional equivalent porous medium model has not been successful in predicting contaminant distributions. A two-dimensional model has not been employed, however, because a sufficiently detailed study of variations in groundwater velocity within the study area has not

been carried out to date.

Contaminant transport distances, as well as results of the tracer tests, and fluid mechanical calculations based on aquifer properties all suggest that transport velocities from the CDS are much less than the groundwater velocity in the fractures. This is due to the retarding effects of matrix diffusion and sorption. The average velocity of a non-sorbed conservative tracer is probably 0.1 m/day or less.

The ultimate destination of the materials transported from the CDS is probably West Alkali Lake. There is a high probability that contaminants will be carried to ground surface at that point. There is also a possibility that the water table may rise above ground surface in the area 200-400 m west of the site. This is an area where the groundwater is already contaminated at high levels. If the chlorophenolic materials are brought to the surface, the environmental hazard posed by the CDS area could increase significantly.

The role of the fractures and diffusion from the fractures in transport was successfully characterized in this thesis by a series of tracer tests. Specifically, the natural gradient tracer test provided estimates of the average transport velocity and dispersion coefficient for a non-sorbing tracer. The

two-hole pumping test gave an estimate of the fraction of the total soil volume through which advection is occurring. The one-hole "push-pull" tests provided direct evidence of the role of matrix diffusion, and allowed further estimates of fracture aperture and matrix diffusion coefficient to be made. These tests, coupled with field observations and laboratory measurement of bulk soil/water properties, allowed a fairly complete picture of the fracture system to be deduced. This work represents the first time that "push-pull" tracer tests have been used to understand the aquifer properties of a fractured porous system. The tests represent a potentially important new methodology for the characterization of fractured porous systems such as the Alkali Lake CDS.

APPENDIX A

This appendix contains a copy of the referenced paper
Pankow et al., 1984.

- Hvorslev, M. J. 1951. Time Lag and Soil Permeability in Groundwater Observations. U.S. Army Corps of Engrs. Waterways Exp. Sta. Bull. 36, Vicksburg, MS.
- Johnson, R. L. 1981. Design and Evaluation of a Thermal-Optical Method for the Analysis of Carbonaceous Aerosols. M.S. Thesis. Oregon Graduate Center, Beaverton, OR.
- Johnson, R. L., S. M. Brillante, J. E. Houck, L. M. Isabelle, and J. F. Pankow. 1985. Migration of Chlorophenolic Compounds at the Chemical Waste Disposal Site at Alkali Lake, Oregon-2. Contaminant Distributions. Ground Water, v23, July-August
- Karickhoff, S. W. 1981. Semi-Empirical Estimation of Sorption of Hydrophobic Pollutants on Natural Sediments and Soils. Chemosphere, v.10, 833-846.
- Karickhoff, S. W. 1983. Sorption Kinetics of Hydrophobic Pollutants in Natural Sediments. Extended Abstracts, Div. of Environ. Science, 186th National American Chemical Society Meeting, Washington, D.C.
- Mundorff, N. L. 1947. The Geology of Alkali Lake Basin, Oregon. Master's Thesis, Oregon State University.
- National Oceanic and Atmospheric Administration. 1984. Climatological Data, Oregon, 1961-1984. Environmental Data Service, Ashville, MD.
- Newton, V. C., Jr., and D. Baggs. 1971. Geologic Evaluation of the Alkali Lake Disposal Site. State of Oregon Department of Geology and Mineral Industries. Open File Report. July 1.
- Oregon Department of Environmental Quality. 1977a. Alkali Lake Disposal Project Monitoring Report No.1. June 14, 1977. 8pp.
- Oregon Department of Environmental Quality. 1977b. Alkali Lake Disposal Project Monitoring Report No.2. November 17, 1977. 5pp.
- Oregon Department of Environmental Quality. 1978. Alkali Lake Disposal Project Monitoring Report No.3. December 22, 1978. 8pp.

- Oregon Department of Environmental Quality. 1979. Alkali Lake Disposal Project Monitoring Report No.4. October 1, 1979. 6pp.
- Oregon Department of Environmental Quality. 1981. Alkali Lake Disposal Project Monitoring Report No.5. January 5, 1981. 7pp.
- Oregon Department of Environmental Quality. 1982. Alkali Lake Disposal Project Monitoring Report No.6. February 12, 1982. 9pp.
- Pankow, J. F., L. M. Isabelle, and D. F. Barofsky. 1981. The identification of chlorophenoxyphenols in soil and water samples by solvent extraction and field desorption mass spectrometry. *Anal. Chim. Acta.*, v.124, 357-364.
- Pankow, J. F., R. L. Johnson, J. E. Houck, S. M. Brillante, and W. J. Bryan. 1984. Migration of Chlorophenolic Compounds Stored at the Chemical Waste Disposal Site at Alkali Lake, Oregon-1. Site Description and Ground-Water Flow. *Ground Water*, v.22, 593-601.
- Pankow, J. F. and L. M. Isabelle. Interface for the Direct Coupling of a Second Gas Chromatograph to a Gas Chromatograph/Mass Spectrometer for use with a Fused Silica Capillary Column. *Analytical Chemistry*, v.56, in press.
- Research Triangle Institute. 1982. Master Analytical Scheme for the Analysis of Organic Compounds in Water, v.III.
- Roberts, P. V., M. Reinhard, and A. J. Valocchi. 1982. Movement of Organic Contaminants in Groundwater: Implications for Water Supply. *J. American Water Works Assoc.*, v.14, 408-413.
- Schellenberg, K., C. Leuenberger, and R. P. Schwarzenbach. 1984. Sorption of Chlorinated Phenols by Natural Sediments and Aquifer Materials. *Environ. Sci. Tech.*, v.18, 652-7.
- Schwarzenbach, R. P. and K. Westall. 1981. Transport of Nonpolar Organic Compounds from Surface Water to Groundwater. *Laboratory Sorption Studies. Environ. Sci. Tech.* v.15, 1360-7.

- Sudicky, E. and E. O. Frind. 1982. Contaminant Transport in Fractured Porous Media: Analytical Solutions for a System of Parallel Fractures. *Water Res. Research*, v.18, 1634-1642.
- Sudicky, E. A. 1983. An Advection-Diffusion Theory of Contaminant Transport for Stratified Porous Media. Ph.D. Thesis. University of Waterloo, Waterloo, Ontario, Canada.
- Sudicky, E.A. 1984. Personal Communication.
- van Genuchten, M. T. 1974. Mass Transfer Studies in Sorbing Porous Media. Ph.D. Thesis, New Mexico State Univeristy, Las Cruces, NM.
- Young, A. L., J. A. Calcagni, C. E. Thalken, and J. W. Tremblay. 1978. The Toxicology, Environmental Fate, and Human Risk of Herbicide Orange and its Associated Dioxin. USAF OEHL Technical Report OEHL TR-78-92.

CURRICULUM VITAE

Richard L. Johnson
304 S. W. Hamilton St.
Portland, Oregon 97601
(503) 224-9047

Personal

Born: 5 September 1951
Married: May 1973
Health: Excellent
Citizenship: USA

Education

1973 University of Washington, B.S., Chemistry
1981 Oregon Graduate Center, M.S., Environmental Science
1984 Oregon Graduate Center, Ph.D., Environmental Science

Employment History

1984- University of Waterloo, Groundwater Research Institute,
Waterloo, Ontario, Canada, and
Oregon Graduate Center, 19600 N.W. Walker Road, Beaverton,
Oregon. Joint Postdoctoral Research Associate
1981-1984 Oregon Graduate Center, 19600 N.W. Walker Road, Beaverton,
Oregon. Graduate Student Research Assistant.
1974-1981 Oregon Graduate Center, 19600 N.W. Walker Road, Beaverton,
Oregon. Research Associate.

Research Interests

The transport and fate of pollutants in aqueous and atmospheric systems; instrumentation and methods development for the analysis of trace organic compounds in the environment; tracer techniques for characterization of solute transport in groundwater; impact of fine particle emissions on air quality; carbonaceous aerosols in urban and rural areas.